SOCIETY OF ECOLOGICAL CHEMISTRY AND ENGINEERING

Proceedings of ECOpole

Vol. 10 **No. 1**

2016

Editorial Office
University of Opole
ul. kard. B. Kominka 6, 45-032 Opole
phone +48 77 455 91 49
fax +48 77 401 60 51
email: maria.waclawek@uni.opole.pl

Secretary Office
phone +48 77 401 60 42
email: mrajfur@o2.pl

The primary version of the journal is the online one

Proceedings of ECOpole
were partly financed by
Ministry of Science and Higher Education, Warszawa

ISSN 1898-617X

Dear ECOpole Participants
we invite you to publish in the journal
your contributions presented during the Conference

Editors

CONTENTS / SPIS TREŚCI

Papers

Artykuły

DOI: 10.2429/proc.2016.10(1)001 2016;10(1)

Dariusz BARAN[1], Stanisław FAMIELEC[2], Małgorzata KONCEWICZ-BARAN[3]
Mateusz MALINOWSKI[2] and Zygmunt SOBOL[1]

THE CHANGES IN EXHAUST GAS AND SELECTED WASTE PROPERTIES DURING BIOSTABILIZATION PROCESS

ZMIANY SKŁADU GAZÓW PROCESOWYCH ORAZ WYBRANYCH WŁAŚCIWOŚCI FIZYKOCHEMICZNYCH ODPADÓW PODCZAS STABILIZACJI TLENOWEJ

Abstract: In recent years mechanical-biological waste treatment facilities increasingly apply the biostabilization process to treat the undersize fraction (most frequently less than 80 mm in diameter) obtained from municipal solid waste. The process lasts at least 14 days in closed but aerated chambers. The process gas exiting the chamber is transferred to biofilters filled with biomass, which ensure odours elimination. The aim of the study was to analyze the aerobic biostabilization process of selected waste groups using a laboratory BKB 100 reactor, especially in the aspect of exhaust gas composition changes. The bioreactor was equipped with a 116-liter, thermally insulated chamber, controlled air flow and a system of gases and temperature analyzers. The analyzed parameters were: CO_2 and O_2 concentration in the emitted gases, the temperature changes during the process, waste density, C:N ratio, organic matter content as well as moisture content. As a result of the research it was stated that the temperature changes in the processed waste vary in different seasons and might depend on the share of fine and biodegradable fractions in waste. In the case of waste collected in summer or autumn the thermophilic phase began during the 2nd or 3rd day of the process and lasted about 5-6 days, causing a considerable CO_2 emission (with the maximum between the 1st and 4th day). The changes in O_2 and CO_2 concentration were directly connected with the process intensity. Waste collected during winter or spring and subjected to the process didn't reach the temperature which would ensure waste stabilization and hygienization.

Keywords: municipal solid waste, undersize fraction, aerobic biostabilization

Introduction

Mechanical-biological treatment (MBT) facilities integrate mechanical processes, (such as comminution, separation, sieving, classification) and biological processes, which occur in aerobic and/or anaerobic conditions [1-3]. As a result of the mechanical processes, which in most cases include waste separation in drum screens (with 80 mm square-shaped meshes), two fractions are obtained: undersize and oversize. The undersize fraction contains the considerable share of organic substances and is subjected to biological treatment [2]. Among most commonly used biological processes applied at this stage are aerobic biostabilization and biodrying process [2]. These processes consist in autothermic self-heating of treated material, which results from the heat released during organic matter decomposition [2]. Thus, they seem to be an interesting alternative of waste treatment from the economical point of view. Biological treatment methods for biodegradable municipal

[1] Institute of Machinery Management, Ergonomics and Production Processes, University of Agriculture in Krakow, ul. Balicka 116b, 30-149 Kraków, Poland, phone +48 12 662 46 66, email: rtbarand@cyf-kr.edu.pl
[2] Institute of Agricultural Engineering and Informatics, University of Agriculture in Krakow, ul. Balicka 116b, 30-149 Kraków, Poland, phone +48 12 662 46 60, email: mateusz.malinowski@ur.krakow.pl
[3] Department of Agricultural and Environmental Chemistry, University of Agriculture in Krakow, al. A. Mickiewicza 21, 31-120 Kraków, Poland, phone +48 12 662 43 49, email: m.koncewicz-baran@ur.krakow.pl
[*] Contribution was presented during ECOpole'15 Conference, Jarnoltowek, 14-16.10.2015

waste bring about decrease in microbial activity as well as reduction of gaseous emission (CO_2, SO_2, NO_x and CH_4) in case of subsequent landfilling of processed waste [1-7]. Regulation of the Polish Minister of the Environment concerning MBT determines that biological treatment of waste can be executed at the initial stage in a closed bioreactor with an aeration system and post-process gas ventilation to biofilters, for the period of 2 weeks at minimum in the processes of aerobic biostabilization [8].

The main aim of the research was to analyze the aerobic biostabilization process of the undersize fraction (particle size less than 80 mm) separated from municipal solid waste, especially in the aspect of exhaust gas composition changes. The process was carried out in the laboratory bioreactor (type: BKB 100). Analyses were repeated four times. The analyzed undersize fraction was collected at the Regional Installation for Municipal Solid Waste Treatment.

Materials and methods

This study was conducted at the Faculty of Production and Power Engineering (University of Agriculture in Krakow, Poland). The bioreactor (type: BKB 100) with the chamber volume of 116 dm^3 was used for the experiments (Fig. 1). Tests were carried out using aerobic biostabilization process of organic matter. The waste for research (the undersize fraction separated from municipal solid waste (Ø < 80 mm)) was obtained from a mechanical and biological waste treatment plant (MIKI Recycling Ltd.), located in Krakow (southern Poland). To determine temperature changes during the process, which lasted for approx. 14 days, a PT1000 temperature sensor was used. Analyses were carried out for the period of 14 days (or more, in some cases), which is required by the Regulation on the MBT for biological processes of waste treatment [8]. In spring and summer the experiments were conducted for 14 days. In case of waste collected in autumn and winter the process time was longer - 16 and 22 days, respectively. It was possible to regulate the air flow into the investigated waste, to display the recorded temperature changes occurring in stabilized material, as well as to analyze emitted gases (oxygen content, carbon dioxide content, methane content and hydrogen sulphide content in exhaust gas). The air supply was maintained at 0.5-1.5 $m^3 \cdot (kg\ d.m. \cdot d)^{-1}$. The aeration intensity was regulated according to the Schultz rule, which states that the oxygen demand depends on process temperature as follows [9]:

$$W = 0.1 \cdot 1.067^t$$

where: W - oxygen demand [mg $O_2 \cdot (g\ d.m. \cdot h)^{-1}$], t - temperature in a range 20-70ºC.

The average temperatures of air supplied to the bioreactor differed in each season and were as follows: 15ºC in winter, 17ºC in spring, 26ºC in summer and 19ºC in autumn.

The analyzed waste originated from rural outskirts of Krakow agglomeration. The samples were collected once a quarter (in January, April, July and October), the mass of each sample was 60 kg at minimum. The laboratory samples were prepared according to the standard [10]. For each sample following characteristics were determined: morphological composition [2], moisture content [11], dry organic mass content [12], C:N ratio, waste density (at the beginning and at the end of the process) as well as Kjeldahl nitrogen content. The latter analysis was conducted in presence of selenium mixture using Kjeltec 1026

System II analyzer (producer: Tecator) and was preceded by the sample mineralisation in concentrated H_2SO_4. Total organic carbon content was determined by oxidative titration.

Fig. 1. The BKB 100 bioreactor used in the research

Results

Table 1 shows the morphological composition of the undersize fraction from waste processed at MIKI Recycling Ltd in Krakow between January and October 2015. As the results reveal, the fraction of fine material (particle size less than 10 mm) constitutes a predominant share in analyzed waste, independent on the season. In waste collected in July (summer) there are considerable shares of organic waste and glass, as well. In Table 1 a sum of biodegradable waste, calculated according to NWMP and [2, 13], is also given. The least shares of such waste were noticed in case of samples collected in January (winter) and April (spring), the highest - for samples taken in October (autumn).

Table 1

Morphological composition of undersize fraction in different seasons

No.	Waste group	Winter ±*SD**	Spring ±*SD**	Summer ±*SD**	Autumn ±*SD**
		[%]	[%]	[%]	[%]
1.	Fine fraction	43.1 ±5.1	34.7 ±1.0	22.4 ±2.7	30.4 ±2.1
2.	Organic waste	14.8 ±4.4	5.9 ±4.4	20.8 ±0.8	15.8 ±3.6
3.	Wood	0.2 ±0.1	0.9 ±0.3	1.2 ±0.7	2.2 ±0.4
4.	Paper	8.1 ±4.4	14.2 ±4.1	9.9 ±2.7	16.1 ±3.3
5.	Textiles	3.8 ±2.0	2.9 ±1.6	2.8 ±2.0	3.3 ±1.1
6.	Plastics	8.8 ±2.4	14.7 ±4.7	7.4 ±2.3	8.6 ±4.5
7.	Glass	12.5 ±0.5	17.8 ±2.9	18.0 ±3.4	13.1 ±6.0
8.	Metal	1.1 ±0.6	3.6 ±2.0	1.1 ±0.5	0.4 ±0.1
9.	Composite waste	0.2 ±0.1	1.4 ±1.2	3.8 ±0.9	2.7 ±0.3
10.	Hazardous waste	0.4 ±0.1	0.6 ±0.2	1.1 ±0.6	0.2 ±0.1
11.	Personal hygiene product	0.3 ±0.1	0.4 ±0.1	1.8 ±0.8	0.8 ±0.3
12.	Inert waste	6.7 ±5.0	2.9 ±0.3	9.7 ±1.3	6.4 ±2.2
	Total share of biodegradable waste	**38.0 ±4.2**	**33.6 ±5.1**	**41.9 ±2.9**	**46.2 ±3.3**

**SD* - standard deviation

The changes in temperature values during biological waste treatment processes indicate the occurrence of three subsequent phases [14]. The most important is the second one - the thermophilic phase [15], in which a sudden temperature increase is observed. It ensures stabilization and hygienization of waste [16, 17]. Figure 1 presents the changes in temperature measured inside the bioreactor (in its central area) during the analyzed processes. The thermophilic phase for waste collected in summer or autumn was observed already in the 2nd or 3rd day of the process and lasted approx. 5-6 days. The increase in temperature to the level of 60 or more degrees Celsius is supposed to ensure proper stabilization and hygienization of the processed material. For waste collected in winter or spring the thermophilic phase occurred much later (after 13 and 6 days of the process, respectively), which might have been caused by high fine fraction content and low share of biodegradable waste in the processed material. The rate of temperature changes during the process and temperature values measured in summer and autumn tests resembled the results presented in [2].

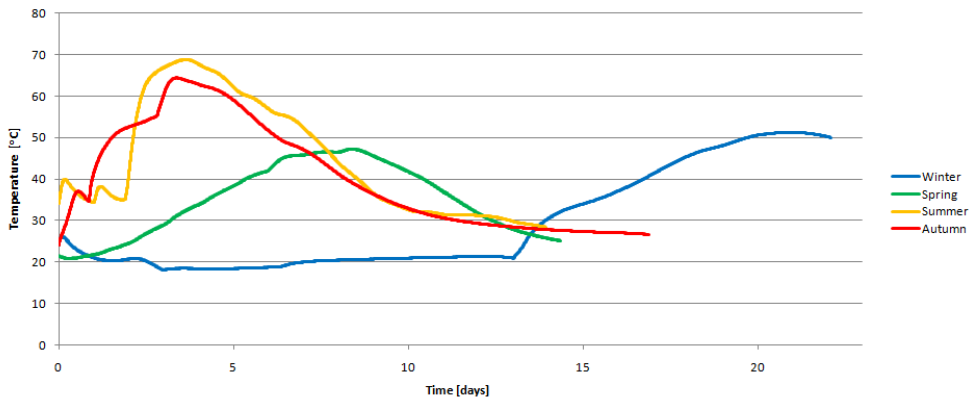

Fig. 2. Temperature changes during biostabilization of undersize fraction

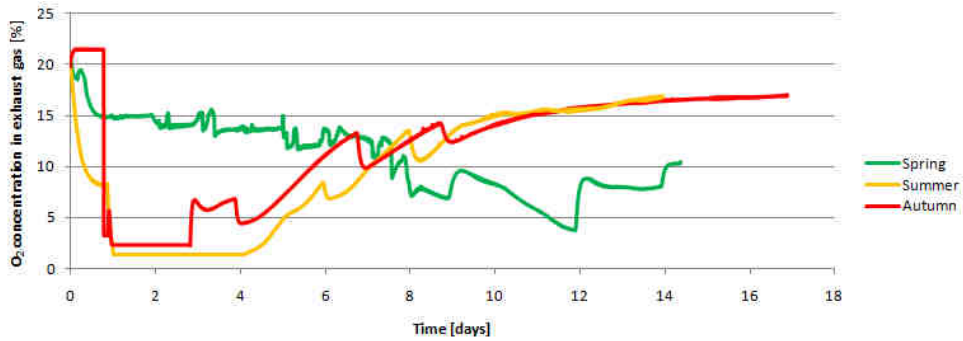

Fig. 3. Changes in O_2 concentration in exhaust gas during biostabilization of undersize fraction

To ensure that the process is carried out properly the analyzed waste has to be supplied with a sufficient amount of air. It is necessary for organic matter decomposition, which results from intense growth of aerobic microorganisms [18]. CO_2 content in exhaust gas is the best indicator for assessing the intensity of biological processes in waste. Figures 3 and 4 present the changes in O_2 and CO_2 concentration in emitted gases. For samples collected in summer and autumn the changes in gaseous emission were observed in first days of the process, which resembles the temperature curves in Figure 2. In spring the changes were less intense and O_2 concentration did not lower to less than 4%. Due to technical issues it was not possible to measure exhaust gas composition in winter. The presented curves (Figures 3 and 4) do not include CH_4 and H_2S measurements - concentrations of these gases were below 0.2%, which is less than inaccuracy rate of the analyzing instrument (BIOTEX-XL).

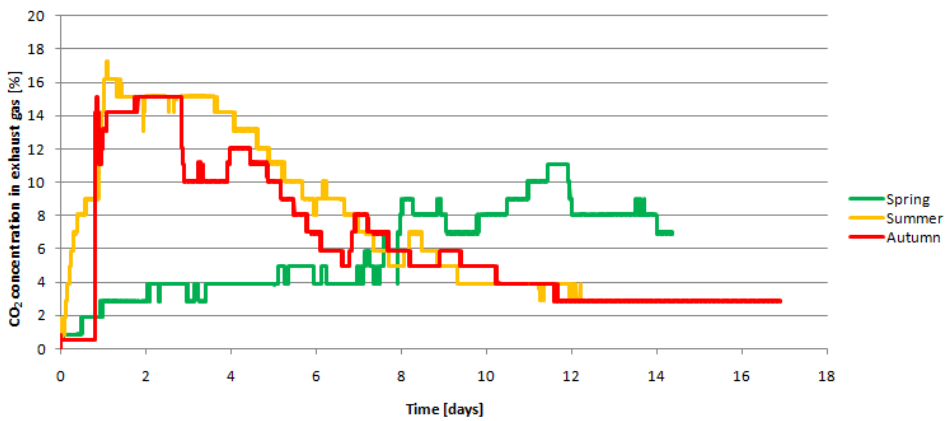

Fig. 4. Changes in CO_2 concentration in exhaust gas during biostabilization of undersize fraction

Table 2

Changes in selected properties of stabilized waste

No.	Property	Unit	Season	Before the process	After the process
1.	Waste density	[kg·m^{-3}]	Winter	539.7	611.9
			Spring	520.9	551.3
			Summer	490.0	530.7
			Autumn	466.9	475.9
2.	Moisture content	[% w.w]	Winter	38.3 ±1.4	26.9 ±6.8
			Spring	29.0 ±6.2	26.5 ±4.1
			Summer	35.6 ±2.3	30.9 ±2.1
			Autumn	27.6 ±4.8	24.2 ±3.8
3.	Organic matter content	[% d.m.]	Winter	47.6 ±0.9	44.5 ±0.6
			Spring	52.8 ±1.9	42.3 ±2.1
			Summer	53.6 ±1.4	44.5 ±0.9
			Autumn	55.0 ±0.9	42.3 ±7.0

As a result of the biostabilization process, some considerable changes in waste properties were observed (Table 2). In each cycle of tests waste density increased - the

values varied from 466.9 $kg \cdot m^{-3}$ (the minimal density of processed material) to 611.9 $kg \cdot m^{-3}$ (the maximal density), while waste volume and mass decreased about 11 ±3% and 2.3 ±0.4%, respectively. Apart from winter tests, in all experiments the occurrence of leachate from the bioreactor was observed. Average carbon content in waste dry mass varied from 19.8 to 25.1% before the process and from 17.9 to 22.3% after the process. Average nitrogen content in waste dry mass also changed - from the range 0.6-0.94% before the process to 0.8-0.82% after the process. C:N ratio in analyzed waste decreased during biostabilization from approx. 30 to 25. Moisture and organic matter content in the processed waste decreased slightly, while ash content increased. In each test minor changes in pH occurred - the average values rose from 7.3 (close to neutral) before the process to 7.9 (more basic conditions) after the process.

Conclusions

The main conclusions drawn on the results presented above are:

1. The morphological composition of waste, especially fine fraction (particle size less than 10 mm) and biodegradable waste content, can influence the intensity of aerobic biostabilization.
2. Temperature changes in processed waste during biostabilization are not the same in each season. The thermophilic phase, which corresponds to the highest CO_2 emission, for waste collected in summer and autumn occurred already in the 2nd or 3rd day of the process and lasted approx. 5-6 days.
3. The changes in O_2 and CO_2 concentration in exhaust gas were directly connected to the intensity of the process. In case of tests carried out in summer and autumn the highest CO_2 emission was measured between the 1st and 4th day of the process.
4. In case of waste collected in winter and spring it was not possible to reach the process temperature which would ensure proper stabilization and hygienization of the material.

Acknowledgments

This Research was financed by the Ministry of Science and Higher Education of the Republic of Poland - project BM 4627/WIPIE/2015.

References

[1] Dębicka M, Żygadło M, Latosińska J. Investigations of bio-drying process of municipal solid waste. Ecol Chem Eng A. 2013;20(12):1461-1470. DOI: 10.2428/ecea.2013.20(12)132.

[2] Dziedzic K, Łapczyńska-Kordon B, Malinowski M, Niemiec M, Sikora J. Impact of aerobic biostabilization and biodrying process of municipal solid waste on minimization of waste deposited in landfills. Chemical and Process Engineering. 2015;36(4):381-394. DOI: 10.1515/cpe-2015-0027.

[3] Hurka M, Malinowski M. Assessment of the use of EWA bioreactor in the process of bio-drying of undersize fraction manufactured from mixed municipal solid waste. Infrastructure and Ecology of Rural Areas. 2014;IV(1):1127-1136. DOI: 10.14597/infraeco.2014.4.1.083.

[4] Adani F, Tambone F, Gotti A. Biostabilization of municipal solid waste. Waste Management. 2004;24:775-783. DOI: 10.1016/j.wasman.2004.03.007.

[5] Adani F, Baido D, Calcaterra E, Genevini P. The influence of biomass temperature on biostabilization-biodrying of municipal solid waste. Bioresour Technol. 2002;83:173-179. DOI: 10.1016/S0960-8524(01)00231-0.

[6] Sugni M, Calcaterra E, Adani F. Biostabilization-biodrying of municipal solid waste by inverting air-flow. Bioresour Technol. 2005;96:1331-1337. DOI: 10.1016/j.biortech.2004.11.016.

[7] Domińczyk A, Krzystek L, Ledakowicz S. Biologiczne suszenie mieszaniny stałych odpadów przemysłu papierniczego oraz organicznej frakcji stałych odpadów komunalnych. Inż Ap Chem. 2012;51(4):115-116. http://inzynieria-aparatura-chemiczna.pl/pdf/2012/2012-4/InzApChem_2012_4_115-116.pdf.
[8] Rozporządzenie Ministra Środowiska z dnia 11 września 2012 roku w sprawie mechaniczno-biologicznego przetwarzania zmieszanych odpadów komunalnych (DzU 2012, poz. 1052). http://isap.sejm.gov.pl/DetailsServlet?id=WDU20120001052.
[9] Jędrczak A. Biologiczne przetwarzanie odpadów. Warszawa: Wyd Nauk PWN; 2008.
[10] PN-EN 15443-2011 Stałe paliwa wtórne - Metody przygotowania próbki laboratoryjnej. http://sklep.pkn.pl/pn-en-15443-2011e.html.
[11] PN-EN 15414-3-2011 Stałe paliwa wtórne - Oznaczanie zawartości wilgoci metodą suszarkową - część 3: wilgoć w ogólnej próbce analitycznej. http://sklep.pkn.pl/pn-en-15414-3-2011e.html.
[12] PN-EN 15403-2011 Stałe paliwa wtórne - Oznaczanie zawartości popiołu. http://sklep.pkn.pl/pn-en-15403-2011e.html.
[13] KPGO 2014. Krajowy Plan Gospodarki Odpadami na lata 2010-2014 (MP Nr 101. poz. 1183). isap.sejm.gov.pl/Download?id=WMP20101011183&type=2.
[14] Niżewski P, Dach J, Jędruś A. Zagospodarowanie zużytego podłoża z pieczarkarni metodą kompostowania. J Res Appl Agric Engin. 2006;51(1):24-27. http://www.pimr.poznan.pl/biul/2006_1_5NDJ.pdf.
[15] Piotrowska-Cyplik A, Chrzanowski Ł, Cyplik P, Dach J, Olejnik A, Staninska J, et al. Composting of oiled bleaching earth: Fatty acids degradation, phytotoxicity and mutagenicity changes. Int Biodeter Biodegr. 2013;78:49-57. DOI: 10.1016/j.ibiod.2012.12.007.
[16] Sidełko R, Seweryn K, Walendzik B. Optymalizacja procesu kompostowania w warunkach rzeczywistych. Roczn Ochr Sr. 2011;41(13):681-692. http://old.ros.edu.pl/text/pp_2011_041.pdf.
[17] Szpadt R, Jędrczak A. Wytycznie dotyczące wymagań dla procesów kompostowania, fermentacji i mechaniczno-biologicznego przetwarzania odpadów. Warszawa. 2008. https://www.mos.gov.pl/fileadmin/user_upload/odpady/Wytyczne_dotyczce_wymagan_dla_procesow_kompostowania__fermentacji_i_przetwarzania.pdf.
[18] Wolna-Maruwka A, Schroeter-Zakrzewska A, Dach J. Analysis of the growth and metabolic activity of microorganisms in substrates prepared on the base of sewage sludges and their impact on growth and flowering of garden verbena. Fresen Environ Bull. 2012;21(2):325-336. https://www.researchgate.net/publication/285837803_Analysis_of_the_growth_and_metabolic_activity_of_microorganisms_in_substrates_prepared_on_the_base_of_sewage_sludges_and_their_impact_on_growth_and_flowering_of_garden_verbena.

ZMIANY SKŁADU GAZÓW PROCESOWYCH ORAZ WYBRANYCH WŁAŚCIWOŚCI FIZYKOCHEMICZNYCH ODPADÓW PODCZAS STABILIZACJI TLENOWEJ

[1] Instytut Eksploatacji Maszyn, Ergonomii i Procesów Produkcyjnych
[2] Instytut Inżynierii Rolniczej i Informatyki
[3] Katedra Chemii Rolnej i Środowiskowej
Uniwersytet Rolniczy w Krakowie

Abstrakt: W zakładach mechaniczno-biologicznego przetwarzania odpadów komunalnych do przetwarzania biologicznego frakcji podsitowej (najczęściej o uziarnieniu poniżej 80 mm), wydzielonej ze strumienia zmieszanych odpadów komunalnych, coraz częściej wykorzystuje się proces stabilizacji tlenowej. Proces ten przebiega przez okres co najmniej 2 tygodni w zamkniętych i napowietrzanych kontenerach. Powietrze procesowe odprowadzane jest do biofiltra wypełnionego biomasą, która ma zapewnić redukcję uciążliwych zapachów. Celem badań była analiza przebiegu procesu stabilizacji tlenowej w laboratoryjnym bioreaktorze BKB 100 ze szczególnym uwzględnieniem zmian w składzie emitowanego powietrza procesowego. Bioreaktor był wyposażony w termicznie izolowaną komorę o pojemności 116 dm^3, system pozwalający na kontrolowane wprowadzanie powietrza do procesu, system czujników temperatury oraz analizator gazów poprocesowych. Analizom podlegał udział CO_2 i O_2 w objętości emitowanych gazów procesowych, zmiana temperatury w czasie trwania procesu, a także gęstość odpadów, stosunek C:N, zawartość substancji organicznej i wilgotność. W wyniku przeprowadzonych analiz stwierdzono, że przebieg zmian temperatury w stabilizowanej masie

wsadowej nie jest jednakowy w poszczególnych porach roku i może ona zależeć od udziału frakcji drobnej oraz zawartości odpadów ulegających biodegradacji. Faza termofilna dla odpadów pobranych w okresie lata i jesieni nastąpiła już w 2-3 dniu procesu, trwała około 5-6 dni i spowodowała dużą emisję CO_2. Zmiana zawartości O_2 oraz CO_2 była bezpośrednio powiązana z intensywnością procesu. Odpady pobrane w okresie zimy i wiosny nie osiągnęły temperatury, która mogłaby wskazywać na stabilizację i higienizację materiału. Odpady pobrane latem i jesienią charakteryzowały się największą emisją CO_2 pomiędzy 1 a 4 dniem procesu.

Słowa kluczowe: odpady komunalne, frakcja podsitowa, stabilizacja tlenowa

DOI: 10.2429/proc.2016.10(1)002 2016;10(1)

Tomasz BERGIER[1] and Agnieszka WŁODYKA-BERGIER[1]

THE INFLUENCE OF REED *Phragmites australis* ON AN EFFICIENCY OF OIL-DERIVATIVES REMOVAL

WPŁYW TRZCINY POSPOLITEJ *Phragmites australis* NA SKUTECZNOŚĆ USUWANIA ZANIECZYSZCZEŃ ROPOPOCHODNYCH

Abstract: Constructed wetlands are the effective mean of stormwater management, also in a case of runoff from highways, parking lots and other surfaces contaminated with oil-derivatives, which are potential risk for environment, human health and biological wastewater treatment units. The mechanisms of oil-derivatives removal on wetland beds are complex and not fully understood, however the most important role seem to be played by adsorption on mineral filling, the activities of microorganisms and higher plants. The goal of the presented research is to evaluate the role of macrophytes in oil-derivatives removal processes, as well as to assess the plants' resistance to the high concentrations of these pollutants. The research was conducted as pot experiments, with the usage of reed *Phragmites australis* and model solutions, simulating runoff from surfaces contaminated with oil-derivatives, in three concentrations (0.01, 0.02 and 0.05% of diesel fuel) and three detection times (24, 48 and 96 h). Both in raw and treated solutions, following parameters were measured: pH, conductivity, the sum of aliphatic hydrocarbons C7-C40 and their individual concentration. The research results were used to define the removal efficiency of the studied contaminates, especially oil-derivatives, on constructed wetlands beds, as well as to assess the macrophytes' influence on these processes. The state and conditions of plants were also observed to assess their reaction on the examined concentrations of oil substances.

Keywords: stormwater treatment, constructed wetlands, oil-derivatives, aliphatic hydrocarbons, reed *Phragmites australis*

Introduction

One of the most urgent challenges of the sustainable water management, both in Poland [1, 2] and world-wide [3, 4], is to develop the rational methods of stormwater treatment and management. In recent years, as a result of urbanization processes, changes in the patterns of land-use and land-cover, and especially sealing of the municipal surfaces, a significant increase of stormwater amount has been observed [5]. The problem of proper management of stormwater is especially complex and important in case of run-off from roads, parking lots and other kinds of road transport infrastructure [6, 7]. Due to the presence of specific contaminants, especially oil-derivatives and other petroleum products, it is necessary to pre-treat stormwater from such areas, before it is discharged to the municipal wastewater system or into the environment.

In case of countries with a developed network of roads and motorways, constructed wetlands and other natural based solutions are applied increasingly more often to treat and manage stormwater coming from the road infrastructure [8, 9]. They guarantee the effective stormwater treatment in-situ, therefore minimizing the costs and negative environmental effects.

[1] Department of Environmental Management and Protection, Faculty of Mining Surveying and Environmental Engineering, AGH University of Science and Technology, al. A. Mickiewicza 30, paw. C-4, 30-059 Krakow, Poland, phone +48 12 617 47 57, email: tbergier@agh.edu.pl
[*] Contribution was presented during ECOpole'15 Conference, Jarnoltowek, 14-16.10.2015

Despite the simplicity of these objects, the mechanisms and dynamics of pollutants' removal by constructed wetlands are complicated and complex, and not fully understood and studied [10]. It is particularly difficult to comprehend and describe these mechanisms in a case of oil-derivatives, however the main paths of removing, which are reported for these compounds, are volatilization, biological or microbial degradation with the activity of macrophytes and microorganisms, sorption and sedimentation in mineral filling [11]. However there is a limited number of articles and research reports, which would allow us to predict the effectiveness and role of these mechanisms for different oil-derivatives and constructed wetlands technical parameters, thereby to accurately plan and design such the facilities.

The goal of the pot experiments presented in this paper was to evaluate (and isolate) the influence of plants on effectiveness of the oil-derivatives removal, and also to determine the plants resistance towards high concentrations of these compounds. They were complementary studies to the research project on semi-technical objects, treating stormwater from the gas filling station and car service [12].

Materials and methods

The experiments, mentioned in the previous paragraph, were carried out in pots in a form of glass vessels, with volume of 3 dm^3. The studies were conducted on model solutions, which were produced with Ekodiesel by Orlen. The whole quantity of diesel fuel was purchased once, thus the identical fuel was used for all experiments. Three types of model solutions were prepared with following concentrations of oil-derivatives: 0.01 (by adding 0.1 cm^3 of diesel fuel per one liter of water), 0.02 and 0.05%. The experiments were performed with common reed (*Phragmites australis*) and were performed for three values of retention time: 24, 48 and 96 h.

The following parameters were measured both in raw and treated solutions: pH, conductivity, the concentration of all individual aliphatic hydrocarbons C7-C40, the total concentration of sum of aliphatic hydrocarbons C7-C40 (Σn-alkanes). The extraction of aliphatic hydrocarbons was conducted with liquid-liquid method with n-pentane used as solvent. Then they were analyzed with gas chromatograph with mass spectrometer (GC-MS) - Trace Ultra DSQ-II by Thermo. The capillary column Rxi^{TM}-5ms by Restek company was used (film thickness 0.5 µm; column length 30 m; diameter 0.25 mm) and helium as carrier gas (flow rate 0.6 cm^3/min). The analysis of each sample lasted 90 minutes and the following temperature programme was used: from 35ºC (6 min) to 130ºC (0 min) with temperature increase 8ºC/min, and then from 130ºC (0 min) to 250ºC (0 min) with temperature increase 5ºC/min and from 250ºC (0 min) to 335ºC (10 min) with temperature increase 1ºC/min. The detection limit for each individual analyzed alkane was 0.02 µg/dm^3.

Results and discussion

Total concentration of aliphatic hydrocarbons

Figure 1 presents the total concentration of all aliphatic hydrocarbons in a function of retention time. The values of Σn-alkanes for model solutions with the initial concentrations

of 0.01, 0.02 and 0.05%, were respectively 28.69, 52.12 and 121.32 mg/dm^3. As a result of treatment in experimental pots, the decrease in hydrocarbons concentrations was observed. For the solution with the initial concentration of 0.01%, the concentration of aliphatic hydrocarbons dropped to the level of 17.08 mg/dm^3 in the pots without plants, and to 5.48 mg/dm^3 in the pots with plants, which is respectively 40 and 81% lower than for the raw model solution (28.69 mg/ dm^3). The higher decrease in the concentration of n-alkanes was observed after 48 h. For the pots without plants, the hydrocarbons concentration was 12.48 mg/dm^3 (a decrease by 56% in compare with the initial concentration), and 2.77 mg/dm^3 for the pots with plants (90%). After the longest studied retention time (96 h) the lowest concentrations of the aliphatic hydrocarbons were observed - in case of pots without plant, this concentration decreased to 3.42 mg/dm^3 (88%), and in case of pots with plants to 0.68 mg/dm^3. Generally the higher values of Σn-alkanes removal efficiency were observed for the longer retention times.

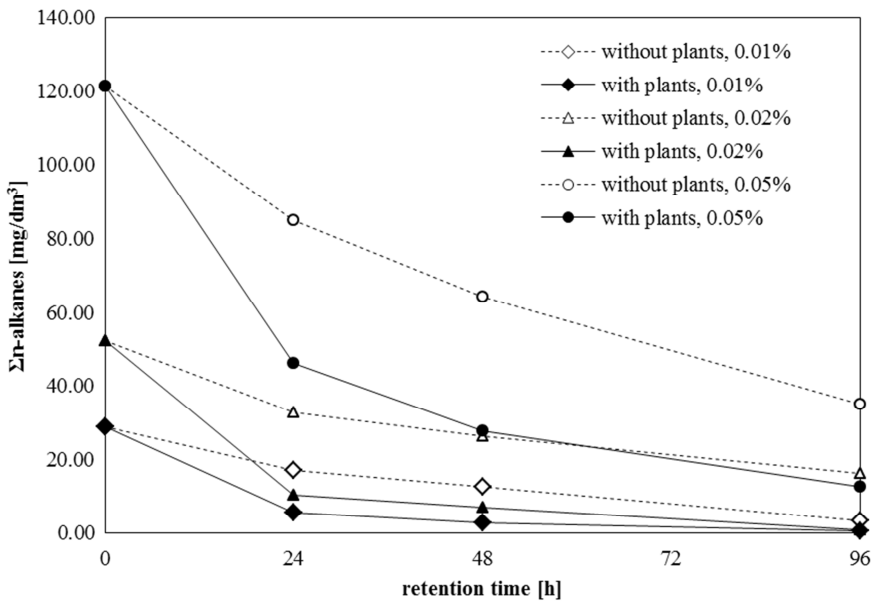

Fig. 1. The total aliphatic hydrocarbons concentration (Σn-alkanes) in a function of retention time, for solutions with the initial concentrations of diesel fuel: 0.01, 0.02 and 0.05%

The similar relationships were observed for the model solution 0.02%, in which the initial concentration of Σn-alkanes was 52.12 mg/dm^3. In case of the pots without plants, Σn-alkanes concentration for 24 h retention time was 32.59 mg/dm^3 (increased by 37%), for 48 hours - 26.39 mg/dm^3 (49%), and for 96 h - 16.12 mg/dm^3 (69%). In case of samples collected from the pots with plants, greater levels of effectiveness in hydrocarbons removal were observed. For 24 h retention time the concentration of Σn-alkanes decreased to

10.31 mg/dm^3, for 48 h - 7.09 mg/dm^3, for 96 h - 0.98 mg/dm^3, what correspond to the effectiveness of 80, 86 and 98%, respectively.

For the model solution with the highest initial concentration 0.05% (Σn-alkanes 121.32 mg/dm^3), the significant decrease in the oil-derivatives concentration was also observed. In a case of samples without plants, for retention time of 24 h Σn-alkanes concentration decreased to the level of 84.96 mg/dm^3 (30% lower than the initial concentration), for 48 h to 64.37 mg/dm^3 (47%), and for 96 h to 34.99 mg/dm^3 (71%). In a case of samples with plants, these values were respectively: 46.01 mg/dm^3 (62%), 27.58 mg/dm^3 (77%) and 12.67 mg/dm^3 (90%).

It is clearly visible from the above results, that plants caused the more efficient removal of oil-derivatives. To evaluate and isolate their role in these processes, the percentage share of their influence was calculated, as the effectiveness of hydrocarbons removal in a pot with plants minus this effectiveness in a pot without plants. For the model solution of 0.01%, the plant isolated influence was the highest for 24 h (40%), and it was decreasing along with the longer values of retention time, reaching 34% for 48 h and 10% for 96 h. The similar patterns were observed for the higher initial concentrations, thus for the initial concentration of 0.02% the isolated plants influence on n-alkanes removal was 32% for 24 h, 30% for 48 h, 18% for 96 h. While for the initial concentration of 0.05% they were respectively: 43, 37 and 29%. These results have verified the thesis that plants have important role in n-alkanes removal, especially for short retention times this effect was very clear and strong. However the plants influence on the hydrocarbons removal depends not only on retention time, but also on the initial n-alkanes concentration.

Sensitivity of plants towards the presence of petroleum products

During and upon completion of the studies presented above, there were also observations over the plants condition carried out. They were realized for 8 pots, subjected to regular inspections: two pots for each diesel fuel concentration in the model solutions (0.01, 0.02, 0.05%), and two control pots, which were planted with macrophytes, but only watered (without model diesel).

Table 1 presents the results of these observations the plants upon completion of the studies. In majority of cases, presence of mold and discoloring of the plants tissues were observed. Conditions of the experiment were handled with the worst by the plants from one of the pots with the highest initial diesel concentration (0.05%) - it dried out, mildewed, its leaves and stems became yellow-brown, its rhizome was brown-green, with only one new sprout. No significant differences were observed in case of conditions of the plants from the control pots (without the petroleum products), and from the pots with the lowest studied concentration (0.01%) - they handled the experimental conditions in a similar good way. First signs of yellowing became visible in both groups, but just the leaves' tips were dried out. The mold appeared on the plants regardless the initial diesel concentration. It may be generally stated that the laboratory conditions were not advantageous for the plants, and they were the main factor shaping the plants conditions, although negative influence of the petroleum products was observable in case of the initial concentration of 0.02%, and even more observable for 0.05% concentration.

Within the course of the studies discussed above, the evaluated plants were also weighted in order to determine their loss in weight, as a result of exposure to toxic petroleum products. However, no unambiguous relationships were observed, and the loss of weight resulted rather from the conditions, which the pot studies were carried out in, or it was accidental, it did not depend on the oil-derivatives concentration in a pot, which is why it was decided not to present or discuss those results.

Table 1

Plants condition upon completion of the pot studies over removal of the petroleum products

Pot; Initial concentration	Condition
Control sample 1, 0.00%	• no new sprouts • the rhizome started to get moldy • new roots
Reference sample 2, 0.00%	• leaves tips started to dry out, their other parts remained green • no mold on the plant • no new sprouts • the rhizome started to get moldy
Pot 1, 0.01%	• the rhizome started to get moldy • no new sprouts
Pot 2, 0.01%	• leaves tips started to dry out, their other parts remained green • no mold on the rhizome, however it is dry, yellow-brown in color • no mold on the plant • no new sprouts • new roots
Pot 1, 0.02%	• leaves tips started to dry out, their other parts remain green • the rhizome is green-brown • no mold • new roots
Pot 2, 0.02%	• yellowish leaves and the stem • the rhizome is green-brown • 3 new sprouts, on covered with mold
Pot 1, 0.05%	• the plant dried out • mold on the stem, leaves and the rhizome • the leaves and stem are yellow-brown • the rhizome is brown and greenish • a new sprout at the greenish rhizome
Pot 2, 0.05%	• no mold • brown-green rhizome • now new sprouts • from the old sprouts: 2 dried out, 1 started do dry out, 1 remained green

Conclusions

Results of experiments on assessment of the influence of reed *Phragmites australis* on an efficiency of aliphatic hydrocarbons removal from the model solution with oil-derivatives allow to draw the following conclusions:

- The high values of removal effectiveness was observed for the experimental pots. The macrophytes play the important role in these processes of n-alkanes' removal. They were responsible for removing 10-43% of alkanes, which were originally in treated

solutions. The stronger plants influence were observed for higher values of retention times, however it also depends on the initial concentration of hydrocarbons in a solution.

- The higher initial hydrocarbons concentrations and longer retention time caused an decrease in plants influence on alkanes removal - in these cases the process of hydrocarbons vaporing to the atmosphere are probably more intensive than their biological degradation processes driven by the plants.
- While analyzing the removal effectiveness of individual aliphatic hydrocarbons, it may be observed than an increase of retention time causes more effective removal of a wider range of hydrocarbons; for short retention times C14-35 hydrocarbons were effectively removed, and elongation of this time allowed highly effective removal of even the heaviest C39 and C40 hydrocarbons.
- The relatively low sensitivity of plants on the influence of oil-derivatives, they survived the experiments in a relatively good conditions for all analyzed initial diesel concentrations. However some negative changes were observable for the initial concentration of 0.02%, and even more observable for 0.05%.

These results have positively verified the thesis that plants play an important role in n-alkanes removal, especially for short retention times (24 h) this effect was very clear and strong. It is of great utilitarian importance, because in case of difficult weather conditions (high flow rates and short treatment time) it guarantees the effective removal of oil-derivatives.

References

[1] Wagner I, Krauze K, Zalewski M. Blue aspects of green infrastructure. Sust Develop Appl. 2013;4:144-155. http://sendzimir.org.pl/en/series4.

[2] Bergier T. Municipal management. In: Kronenberg J, Bergier T, editors. Challenges of Sustainable Development in Poland. Kraków: The Sendzimir Foundation; 2010. http://sendzimir.org.pl/en/textbook.

[3] Li C. Ecohydrology and good urban design for urban storm water-logging in Beijing, China. Ecohydrol Hydrobiol. 2012;12:287-300. DOI: 10.2478/v10104-012-0029-8.

[4] Vymazal J, Kröpfelová L. Wastewater Treatment in Constructed Wetlands with Horizontal Sub-Surface Flow. Dordrecht: Springer; 2008.

[5] Januchta-Szostak A. Ecosystems services in cities. Sust Develop Appl. 2012;3:89-110. http://sendzimir.org.pl/en/series3.

[6] Göbel P, Dierkes C, Coldewey WG. Storm water runoff concentration matrix for urban areas. J Contaminant Hydrol. 2007;91:26-42. DOI: 10.1016/j.jconhyd.2006.08.008.

[7] Shutes RBE, Ellis JB, Revitt DM, Forshaw M, Winter B. Urban and highway runoff treatment by constructed wetlands. In: Wong MH, editor. Wetlands Ecosystems in Asia - Function and Management. Amsterdam - Boston - Heidelberg - London - New York - Oxford - Paris - San Diego - San Francisco - Singapore - Sydney - Tokyo: Elsevier; 2004.

[8] Terzakis S, Fountoulakis MS, Georgaki I, Al-Bantakis D, Sabathianakis I, Karathanasis AD, at al. Constructed wetlands treating highway runoff in the central Mediterranean region. Chemosphere. 2008;72:141-149. DOI: 10.1016/j.chemosphere.2008.02.044.

[9] A Handbook of Constructed Wetlands. Stormwater. Philadelphia: U.S. EPA; 2000. http://nepis.epa.gov/Exe/ZyPURL.cgi?Dockey=200053P9.txt.

[10] Vymazal J. Constructed wetlands for treatment of industrial wastewaters: A review. Ecol Eng. 2014;73:724-751. DOI: 10.1016/j.ecoleng.2014.09.034.

[11] Xuelu G, Shaoyong C. Petroleum pollution in surface sediments of Daya Bay, South China, revealed by chemical fingerprinting of aliphatic and alicyclic hydrocarbons. Estuarine, Coastal Shelf Sci. 2008;80:95-102. DOI: 10.1016/j.ecss.2008.07.010.

[12] Bergier T, Włodyka-Bergier A. Semi-technical scale research on constructed wetland removal of aliphatic hydrocarbons C7-C40 from wastewater from a car service station. Desal Water Treat. 2016;57:1534-1542. DOI: 10.1080/19443994.2015.1030122.

WPŁYW TRZCINY POSPOLITEJ *Phragmites australis* NA SKUTECZNOŚĆ USUWANIA ZANIECZYSZCZEŃ ROPOPOCHODNYCH

Katedra Kształtowania i Ochrony Środowiska, AGH Akademia Górniczo-Hutnicza w Krakowie

Abstrakt: Oczyszczalnie hydrofitowe są efektywnym sposobem zagospodarowania wód deszczowych, w tym również spływów powierzchniowych z dróg, parkingów i innych powierzchni zanieczyszczonych związkami ropopochodnymi, które stanowią zagrożenie dla środowiska naturalnego, zdrowia ludzi, a także systemów biologicznego oczyszczania ścieków. Mechanizmy usuwania związków ropopochodnych przez złoża hydrofitowe są złożone i nie w pełni poznane, jednak najważniejszą rolę wydaje się pełnić adsorpcja na wypełnieniu mineralnym złoża, działanie mikroorganizmów w nim bytujących oraz aktywność roślin wyższych. Celem prezentowanych badań jest określenie wpływu roślinności na skuteczność usuwania zanieczyszczeń ropopochodnych, a także ocena odporności roślin na wysokie stężenia tych związków. Badania przeprowadzono w formie doświadczeń wazonowych z wykorzystaniem trzciny pospolitej (*Phragmites australis*) oraz ścieków modelowych, symulujących spływy powierzchniowe z powierzchni zanieczyszczonych ropopochodnymi, o trzech stężeniach (0,01, 0,02 i 0,05% oleju napędowego), dla trzech czasów retencji ścieków (24, 48 i 96 h). W ściekach surowych oraz w ściekach po odpowiednim czasie zatrzymania oznaczano następujące parametry: odczyn pH, przewodność elektryczną właściwą, sumę węglowodorów alifatycznych C7-C40 oraz stężenia pojedynczych węglowodorów z tej grupy. Wyniki tych badań posłużyły do określenia efektywności usuwania badanych zanieczyszczeń, w szczególności ropopochodnych, przez złoża hydrofitowe i do określenia wpływu roślinności w tym zakresie. Poza tym prowadzono obserwacje stanu i kondycji roślin, co pozwoliło określić ich odporność na badane stężenia związków ropopochodnych.

Słowa kluczowe: hydrofitowe oczyszczanie wód deszczowych, ropopochodne, węglowodory alifatyczne, trzcina pospolita *Phragmites australis*

DOI: 10.2429/proc.2016.10(1)003 2016;10(1)

Katarzyna GRATA[1]

BIOCONTROL ACTIVITIES OF *Pseudomonas fluorescens* AGAINST ASPARAGUS PATHOGEN

AKTYWNOŚĆ BIOLOGICZNA *Pseudomonas fluorescens* WOBEC PATOGENA PORAŻAJĄCEGO SZPARAGI

Abstract: *Pseudomonas* spp. and their metabolites present environmentally friendly alternative to chemical products to improve plant growth in many different applications. Extensive studies have shown that these microorganisms and their metabolites could have an important role in agriculture and horticulture in improving crop productivity. The aim of the research was to assess a potential biological activity of *Pseudomonas fluorescens* against *Fusarium oxysporum* isolated from the spears of asparagus. The antagonistic properties of metabolites were assayed with a dual culture plate method on PDA and Czapek media for supernatants obtained from 6, 12, 24 and 48-hour culture of *P. fluorescens.* The culturing process was conducted at 26ºC for 8 days and the fungal linear growth was measured every 1-2 days and compared to control. The fungistatic activity of *P. fluorescens* was estimate on the basis the growth rate index. The highest inhibition of the linear growth of mycelium, reaching 61%, has been found for 48-hour supernatants at OD = 2.0 and lowest for 12-hour supernatants on Czapek medium compared with the control trial. Significantly weaker linear growth of mycelium within the range of 4.0-33.0% was observed on PDA medium with a maximum inhibition for 48-hour supernatants at OD = 2.0 (33.0%). Promising method to asparagus protection against *Fusarium* sp. may be the use of *P. fluorescens* as the biocontrol agents.

Keywords: asparagus, *Fusarium oxysporum*, antifungal activity, *Pseudomonas fluorescens*

Introduction

Asparagus *(Asparagus officinalis* L.) is a vegetable (spears) grown worldwide, with well documented knowledge on its nutritional value. They are known as a source of vitamins, microelements, protein. It is essential for consumers to have asparagus spears free of pathogenic fungi and toxins produced by them. Fungi of *Fusarium* genus are one of the most significant pathogens of asparagus [1-3]. Some of the pathogens are able to form mycotoxins - secondary metabolites (*eg* fumonisin, moniliformin, trichothecenes) with possible health hazards and significant influence on food safety [1, 4, 5].

Fusarium oxysporum, F. proliferatum occurring and occasionally occured *F. culmorum and F. solani* in asparagus are known as the most important fungal pathogens worldwide causing crown and root rot of asparagus [1, 3, 6]. Asparagus plant protection is particularly difficult. Currently there are no safe chemicals for protection of asparagus against agrophages. Promising method to control of *Fusarium* spp. may be the biological resources of the group of bacterial antagonists. Therefore, *Pseudomonas* spp. and their metabolites may be an ecofriendly alternative to chemicals for plant growth enhancement. Many research has demonstrated that these microorganisms and their metabolites could have an important role in agriculture and horticulture in enhanced crop productivity. They may be useful as potential antagonist towards phytopathogenic fungi *eg*

[1] Chair of Biotechnology and Molecular Biology, University of Opole, ul. kard. B. Kominka 6a, 45-035 Opole, Poland, phone +48 77 401 60 56, email: kgrata@uni.opole.pl
[*] Contribution was presented during ECOpole'15 Conference, Jarnoltowek, 14-16.10.2015

Rhizoctonia solani, *Verticillium* spp., *Aspergillus niger*, *Fusarium* spp. [7-12]. *Pseudomonas* species have been demonstrated to show antifungal activity with varying degrees of antagonism. The production of lytic enzymes (chitinase, glucanase, pectinase), salicylic acid, iron (Fe)-chelating siderophores, indole-3-acetic acid (IAA), HCN and secondary metabolites including antibiotics is probably one of the most important mechanisms of *Pseudomonas* antifungal properties. Many effective antibiotics synthesized by *Psudomonas* spp. has been detect, such as pyoluteorin (Plt), pyrrolnitrin (Prn) and phenazine-1-carboxylic acid (PCA) [11, 13-16]. In many instances the production of these compounds has been directly correlated with biocontrol activity [11]. Therefore, it is presently believed that *Pseudomonas* can play a significant role in biological control.

The purpose of this study was to evaluate the antifungal of *Pseudomonas fluorescens* against *Fusarium oxysporum* isolated from the asparagus.

Materials and methods

Due to the fact that many of the factors determine the activity of the microorganisms in the carried out tests taken into consideration three: the bacterial cell density, the composition of the medium and the cell-free supernatant. In this study the fungistatic properties of the *P. fluorescens* supernatants were determined against the growth rate index and the rate of mycelial growth inhibition of *Fusarium oxysporum.* The strain of tested fungus was isolated from the white spears of asparagus.

Mycelium growth. Fungistatic activity of *P. fluorescens* was determined with the culture-plate method on PDA and Czapek media. Fungal mycelial-discs (diameter of 7.0 mm) obtained from growing cultures of tested fungal isolates were placed in the centre of this media containing 0.5 cm^3 supernatants (inoculum) obtained from 6, 12, 24 and 48-hour culture of *P. fluorescens* at different optical density (OD = 1.0 and OD = 2.0). The control plate contained only *F. oxysporum* cultures and aseptic broth medium in place of the supernatant. All plates were incubated at 25 ±2°C for 8 days and the fungal linear growth was measured every 1-2 days until the mycelium of *F. oxysporum* in the control plate, reached the edge of the plate and compared to the control. The experiment was conducted in four replicates, where one repeat was represented by a one plate containing the growth medium with one mycelia disc. The influence of metabolites secreted by *P. fluorescens* on the growth of *F. oxysporum* was estimated as the growth rate index [17]. The inhibition of fungal growth was described as the percentage reduction of the growth rate index in the treated plate versus the growth rate index in the control plate.

Results and discussion

The involvement of antifungal activity compounds produced by *Pseudomonas fluorescens* in the inhibition of fungal growth was confirmed by the ability of cell-free culture filtrate of this strain to inhibit the hyphal growth of *F. oxysporum.* Conducted tests revealed the direct influence of *P. fluorescens* on the growth rate of the tested fungus under study. Studies shows that prolonging the bacterial culturing time and at the same time increasing the amount of secondary metabolites affect the inhibition the growth of the fungus.

On the PDA medium the reduction of the growth rate index increases as the culturing time of bacteria is longer. The measured values of the indexes for the control ranged between 56.6-59.9. However, in the trials tested the value of the growth rate index for the bacterial inoculum at initial optical density equal 1.0 amounted 38.4-57.5 and 38.4-46.9 (for OD equal 2.0) (Fig. 1).

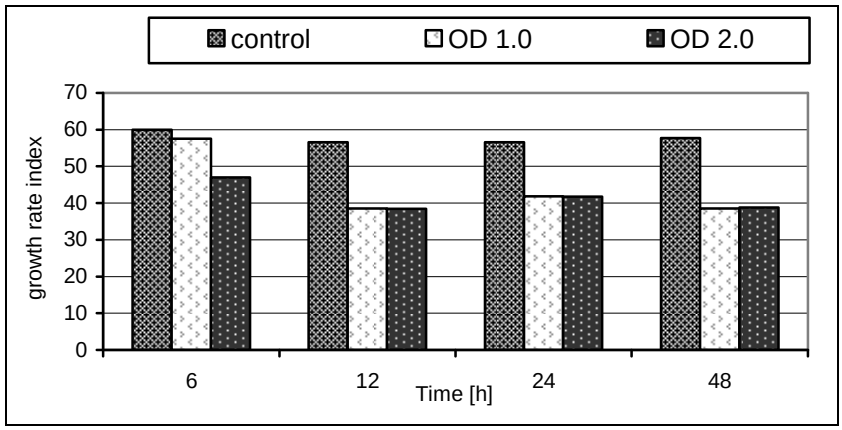

Fig. 1. Influence of *P. fluorescens* on the growth rate index of *F. oxysporum* on PDA medium

The highest inhibition of the growth rate index of *F. oxysporum* was noted in case of 48-hour culture of *P. fluorescens* at OD equal 2.0 (33.2%), while the lowest in case of metabolites obtained after 6-hours culture of this strain at OD equal 1.0 (3.98%) (Fig. 2).

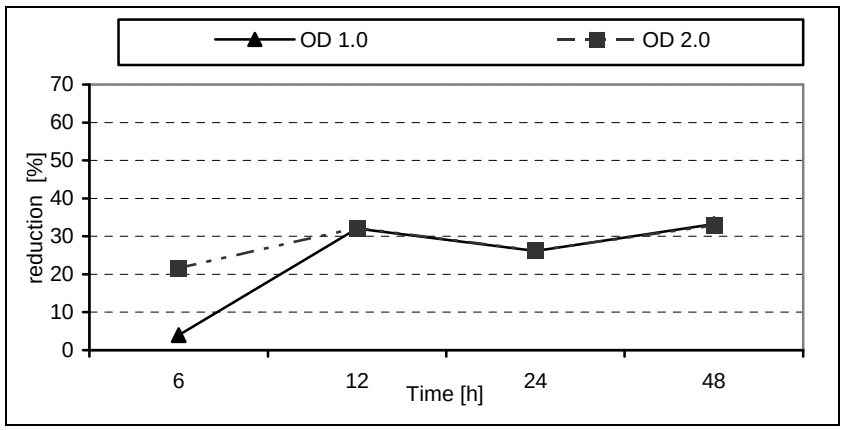

Fig. 2. Reduction of the growth rate index of *F. oxysporum* on PDA medium

The highest measured value of the growth inhibition indexes were noted on the medium with sucrose (Czapek medium). The value of the growth rate index amounted

21.8-27.6 (for OD equal 1.0) and 20.5-26.9 (for OD equal 2.0) compared to the control (54.8-63.2) (Fig. 3).

The most effective was the 48-hour culture of *P. fluorescens* at OD equal 2.0, while the lowest in case of 12-hour culture at OD equal 1.0. The decrease in the growth rate index amounted 61.4 and 51.4%, respectively. Despite everything they were the best results the influence of *P. fluorescens* on the *F. oxysporum* obtained during these tests (Fig. 4).

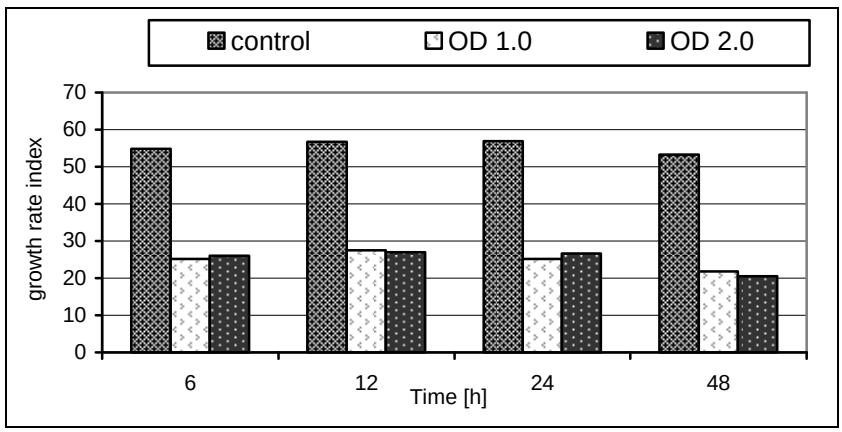

Fig. 3. Influence of *P. fluorescens* on the growth rate index of *F. oxysporum* on Czapek medium

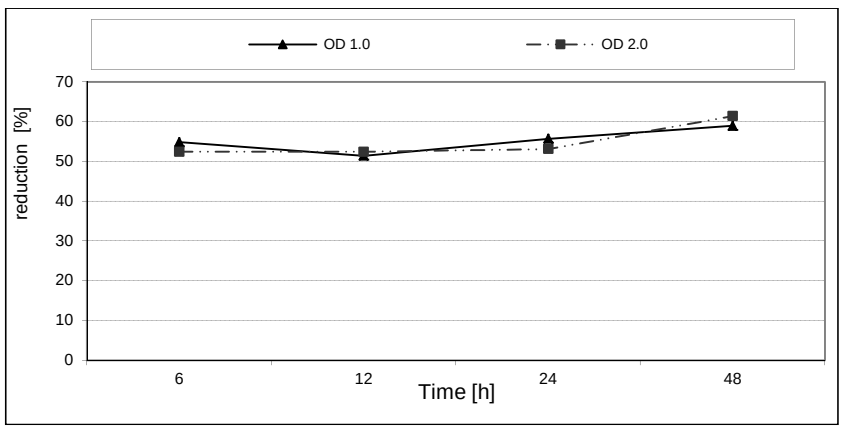

Fig. 4. Reduction of the growth rate index of *F. oxysporum* on Czapek medium

Selective activity of *P. fluorescens* against of phytopathogens has been described in many research papers. The researchers report that the antifungal properties of Pseudomonas largely depend on the capability of secretion of secondary metabolites, notably lytic enzymes and antibiotics [15, 18]. Koche et al [7] found that *P. fluorescens* isolate Pf_{20} was most efficient in inhibiting the mycelial growth up to 38.88%. Whereas, research by Toua

et al [8] demonstrated restricting the growth of the two formae speciales of *F.oxysporum* from 8.33 to 49.33% by five strains of *P. fluorescens.* Moreover conidial germinartion and germ tube elongation were inhibited and reduced. The results of the experiments by Jankiewicz et al [15] indicate the importance synthesized by *P. fluorescens* of salicylic acid in reducing of fungal phytopathogens. The least sensitive to salicylic acid proved to *F. graminearum*, and growth inhibition was found for *F. culmorum*. The inhibition of mycelial growth amounted to successively from 50% for *F. greaminarum*, next between 80-90% for *F. avenaceum* and *F. solani* and in the range 80-100%, depending on the tested *Pseudomonas* strain [15]. The inhibitory properties of *P. fluorescens* obtained in our research could be probably due to the production by own strain of secondary metabolites and/or lytic enzymes that can degrade cell wall. Although Jankiewicz [19] reported that fungal lysis need not necessarily be caused by lytic enzymes capable of decomposition of glycosidic bonds - chitinase and β 1,3 glucanase but also by other substances which are manufactured by bacteria from the *Pseudomonas* genus which include intensively secreted siderophores, hydrogen cyanide as well as exogenous proteases.

Conclusions

Conducted research confirmed fungistatic properties of *P. fluorescens* against *F. oxysporum* strains and prove that growth inhibition of the fungi depends not only on the biological properties and age of the bacterial culture and also susceptibility of the fungus to bacterial metabolites. Based on the data obtained in the these studies it can be concluded that the highest inhibition of the linear growth of mycelium, reaching 61%, has been observed for 48-hour supernatants on Czapek medium. A slightly weaker linear growth of mycelium have been observed on PDA medium with a maximal inhibition of 48-hour supernatants (33.0%). Therefore, promising method to asparagus protection against *Fusarium* sp. may be the application of *P. fluorescens* as the biocontrol agents. However, antagonist Pseudomonas with the antagonistic activity in vitro may not act in vivo due to environmental conditions and competition with other microorganisms. Therefore, it is important that biocontrol potential under field conditions should be further evaluated.

References

[1] Elmer WH, Johnson DA, Mink GI. Plant Dis. 1996;80:117-125.
[2] Korolewski Z, Waskiewicz A, Irzykowska L, Bocianowski J, Kostecki M, Goliński P, et al. Polish J Environ Stud. 2011;20(4):911-918 http://www.pjoes.com/pdf/20.4/Pol.J.Environ.Stud.Vol.20.No.4.911-918.pdf.
[3] Weber Z, Karolewski L, Irzykowska L, Knaflewski M, Kosiada T. Phytopathol Pol. 2007;45:9-15. http://www.up.poznan.pl/~ptfit1/pdf/PP45/PP_45_02.pdf.
[4] Suchorzyńska M, Misiewicz A. Post Mikrobiol. 2009;48(3):221-230. http://www.pm.microbiology.pl/web/archiwum/vol4832009221.pdf.
[5] Wolny-Koładka K. Kosmos. Ser A, Biologia. 2014;63(4):623-633. http://kosmos.icm.edu.pl/PDF/2014/623.pdf.
[6] Andrzejak R, Werner M. Progress in Plant Protection. 2006;46(2):700-703. http://www.researchgate.net/publication/242516602_WPYW_WYBRANYCH_PREPARATW_NA_WZROST_IN_VITRO_GRZYBW_RODZAJU_FUSARIUM_USZKADZAJCYCH_WYPUSTKI_SZPARAGW.
[7] Koche MD, Gade M, Deshmukh AG. The Bioscan. 2013;8(2):723-726. http://thebioscan.in/Journal%20Supplement/82Sup25%20MINA%20D.%20KOCHE.pdf.

[8] Toua D, Benchabane M, Bnsaid F, Bakour R. Glob J Microbiol Res. 2013;1(1):075-084. http://globalscienceresearchjournals.org/full-articles/evaluation-of-pseudomonas-fluorescens-for-the-biocontrol-of-fusarium-wilt-in-tomato-and-flax.pdf?view=inline.
[9] Manwar AV, Khandelwal SR, Chaudhari BL, Meyer JM, Chincholkar SB. Appl Biochem Biotechnol. 2004;118:243-251. DOI: 10.1385/ABAB:118:1-3:243.
[10] Wu M, Zhang X, Zhang H, Zhang Y, Li X, Zhou Q, et al. Bull Environ Contam Toxicol. 2009;88:313-317. DOI: 10.1007/s00128-009-9731-7.
[11] Ligon JM, Hill DS, Hammer PE, Torkewitz NR, Hofmann D, Kempf HJ, et al. Pest Manage Sci. 2000;56(8):688-695. DOI: 10.1002/1526-4998(200008)56:8<688::AID-PS186>3.0.CO;2-V.
[12] Hass D, Defago G. Nat Rev Microbiol. 2005;3(4):307-319. DOI: 10.1038/nrmicro1129.
[13] Kumar RS, Ayyadurai N, Pandiaraja P, Reddy AV, Venkateswarlu Y, Prakash O, et al. J Appl Microbiol. 2005;98:145-154. DOI: 10.1111/j.1365-2672.2004.02435.x.
[14] Vanitha S, Ramjegathwsh R. J Plant Pathol Microb. 2004;5(1):216. DOI: 10.4172/2157-7471.1000216.
[15] Jankiewcz U, Gołąb D, Frąk M. Polish J Agronomy. 2013;15:65-68. http://www.iung.pulawy.pl/PJA/wydane/15/PJA15str65_68.pdf.
[16] Arora NK, Kim MJ, kang SC, Maheshwari DK. Can J Microbiol. 2007;53:207-2012. DOI: 10.1139/W06-119.
[17] Burgieł Z, Acta Agraris et Silvestria. 1984;XXIII:187-195.
[18] Sallam NA, Raid SN, Mohamed MS, El-eslam AS. J Plant Protect Res. 2013;53(3):295-300. DOI: 10.2478/jppr-2013-0044.
[19] Jankiewicz U. Woda Środ Obsz Wiejskie. 2010;10(2):83-92. http://www.itp.edu.pl/wydawnictwo/woda/zeszyt_30_2010/artykuly/Jankiewicz%20i%20 in.pdf.

AKTYWNOŚĆ BIOLOGICZNA *Pseudomonas fluorescens* WOBEC PATOGENA PORAŻAJĄCEGO SZPARAGI

Samodzielna Katedra Biotechnologii i Biologii Molekularnej, Uniwersytet Opolski

Abstrakt: *Pseudomonas* spp. oraz ich metabolity mogą stanowić alternatywę dla związków chemicznych w celu poprawy wzrostu roślin. Mogą one odegrać istotną rolę w rolnictwie i ogrodnictwie w poprawie wydajności upraw. Celem przeprowadzonych badań była ocena właściwości przeciwgrzybowych *Pseudomonas fluorescens* wobec *F. oxysporum*, wyizolowanego z podstawy pędów szparaga. Ocenę właściwości antagonistycznych metabolitów bakteryjnych (6-, 12-, 24- i 48-godzinnych) przeprowadzono metodą hodowlano-płytkową z zastosowaniem podłoży Czapka i PDA. Hodowlę prowadzono w temp. 26ºC przez 8 dni, dokonując pomiarów co 1-2 dni i porównywano w stosunku do kontroli. Na podstawie indeksu tempa wzrostu określono aktywność fungistatyczną *P. fluorescens.* Największą inhibicję wzrostu liniowego grzybni wynoszącą 61% obserwowano na podłożu Czapka po zastosowaniu supernatantów z 48-godzinnej hodowli bakterii o gęstości 2.0, a najmniejszą dla 12-godzinnej hodowli. Znacznie słabszą inhibicję wzrostu grzybni, w zakresie od 3,98 do 33,2%, obserwowano na podłożu PDA. Maksimum aktywności (33,0%) stwierdzono dla supernatantów pozyskanych z 48-godzinnej hodowli bakterii o gęstości 2.0. Efektywną metodą zmniejszenia porażenia szparagów przez *Fusarium* sp. może być zastosowanie bakterii *P. fluorescens* jako czynnika biologicznej ochrony.

Słowa kluczowe: szparagi, *Fusarium oxysporum*, aktywność przeciwgrzybowa, *Pseudomonas fluorescens*

DOI: 10.2429/proc.2016.10(1)004 2016;10(1)

Michał KOZIOŁ[1]

SELECTED ECOLOGICAL ASPECTS OF CO-INCINERATION OF GLYCERIN PHASE WITH COAL IN GRATE FURNACES

WYBRANE ASPEKTY EKOLOGICZNE WSPÓŁSPALANIA FAZY GLICERYNOWEJ Z WĘGLEM W PALENISKACH RUSZTOWYCH

Abstract: The prospect of depletion of reserves of fossil fuels and concerns about the environment have significantly increased the interest in renewable energy sources and have consequently led to a large increase in their use, both in Poland and in other EU countries. One of the important sources of renewable energy is biomass, which can be used, inter alia, for the production of biofuels and bioliquid, including esters. The applicable rules impose increasing consumption of such substances and, as a result, increase in their production. Ester production is accompanied by the production of glycerol phase whose management in an efficient manner poses a number of problems. The problems arise from the large variability in the glycerol phase depending on the technology and materials used in the production of esters, as well as the relatively large mass of glycerol phase waste produced in the country. The paper presents the results of research on selected environmental aspects of co-incineration of glycerin phase with coal in grate furnaces. The specificity of national power utilities is the existence of a relatively large number of boilers with travelling grates. The research which was done includes the study of the incineration of compounds with the mass fraction of the glycerol phase ranging from 5 to 20%. The paper presents the methodology of the study and the outcomes of the resulting emissions of CO and NO.

Keywords: glycerin phase, co-incineration, grate furnaces, emission

Introduction

The prospects of the depletion of fossil fuel resources and concerns for the condition of the environment have significantly increased the interest in renewable energy sources. Consequently, it led to a significant increase in the use of renewable energy sources in Poland and in other highly-developed countries. This increase has also forced measures of a legal nature, including obligations arising for instance from Directive 2009/28/EC [1] obliging Poland to reach in 2020 at least 15% share of energy from renewable sources in the consumption of gross final energy (20% at the EU level). Apart from the main objective, Poland is to achieve intermediate objectives: 9.54% until 2014, 10.71% until 2016 and 12.27% until 2018.

An important source of renewable energy in Poland, available for quick use, is biomass. One of biomass applications is the production of biomass-based liquid fuels. In the case of this biomass application, there are also legal regulations that enforce the increase in its application. Pursuant to the provisions of the "Act on Biocomponents and Liquid Biofuels" [2], entrepreneurs operating business activity within the scope of manufacture, import or purchase of fuels or liquid biofuels, who sell them in the territory of Poland, have been obliged (since 2008) to ensure in a given year at least a minimum share of biocomponents and other renewable fuels in the total quantity of fuels and liquid biofuels

[1] Department of Technologies and Installations for Waste Management, Silesian University of Technology, ul. S. Konarskiego 18, 40-100 Gliwice, Poland, phone +48 32 237 11 23, fax +48 32 237 11 26, email: michal.koziol@polsl.pl
[*] Contribution was presented during ECOpole'15 Conference, Jarnoltowek, 14-16.10.2015

sold. And the minimum share, as mentioned hereinabove, is calculated according to the calorific value of individual biocomponents. The minimum share of biocomponents in subsequent years is stipulated in the Regulation of the Council of Ministers on National Indicative Targets for the years 2008-2013 [3]. Accordingly, National Indicative Targets (*ie* minimum shares of biocomponents) amount to: from 2013 - 7.10%, in 2017 - 7.80% and in 2018 - 8.50% (in 2008 - the first year when the regulation came into force, it amounted to 3.45%). The implementation of the provisions of the aforementioned legal acts resulted in the increase in the production of bioethanol and esters. Figure 1 presents changes in the production volume of biocomponents and biofuels in Poland in the years 2008-2014.

It is worth mentioning that in Poland up to 5 percent of bioethanol is added to standard petrol and up to 7 percent of esters is added to diesel oil.

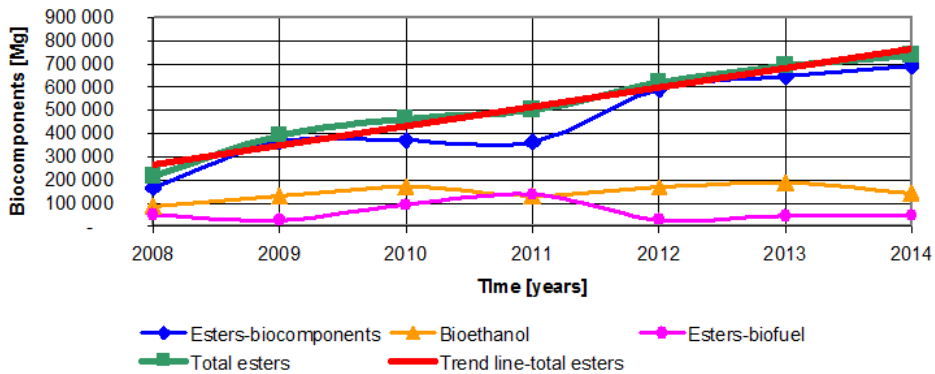

Fig. 1. Production volume of biocomponents and biofuels in Poland in the years 2008-2014 (own work based on data [4])

From the point of view of the research presented in the paper, the volume of esters production is important, as their production is accompanied by the creation of the glycerine phase. As a result of the process of vegetable oil esterification for fuel purposes, a relatively considerable quantity of glycerine phase is produced. The glycerine phase production amounts from several to twenty percent of the weight of esters produced.

According to the data presented in Figure 1, in the last five years in Poland there has been a rapid increase in the production of esters. Their production increased from the level of about 200 000 Mg to the value of nearly 700 000 Mg. Due to the further increase in obligatory National Indicative Targets, further increase in ester production is to be expected. With the increase in the quantity of produced esters, the quantity of produced glycerine phase will be also increasing.

It can be estimated that during the production of the mass of esters produced in 2014, about 80-130 thousand Mg of glycerine phase was created. The issue of effective management of the currently produced glycerine phase causes a number of problems. They result both from high changeability of glycerine phase properties depending on technology and raw materials used for ester production, and from the relatively high weight of this waste produced at the national level. There are several possibilities of managing the glycerine fraction. However, for majority of them, the glycerine fraction needs to be treated

to pure glycerine first, and this is an expensive process. Other applications include the use in agriculture or in thermal processes, *eg* in co-combustion processes.

In Poland, hard coal is still the basic fuel and its share in the structure of covering demand on primary energy will continue to be significant for a few decades.

One of the technologies for using coal is its combustion in stoker fired boilers, including with a mechanical grate. Boilers with mechanical grates are basic structures in Poland used for combusting coal in medium output facilities. They are present in boiler rooms, heat generating plants and municipal and industrial heat and power stations. A large tolerance of these boilers for parameters of combusted fuel causes that they are predisposed to carry out processes of fuel co-combustion. In addition, their prevalence causes that they can be used in the place where biomass or waste is produced. It is also relatively easy to perform modernisation in these boilers, *eg* of the fuel feeding system. The weak point of this type of structure is the relatively low energy efficiency and problems with adapting to the growing legal requirements in terms of environmental protection.

Testing methodology

As part of the testing presented, technical possibilities and selected environmental effects of the co-combustion process of hard coal with the glycerine phase in the stoker-fired boiler furnace were checked. Testing was conducted at a laboratory station allowing for conducting laboratory testing in a relatively large scale as the fuel mixture combusted at the station can have the maximum capacity of over 40 dm^3 and the weight of over 20 kg.

The basic element of the laboratory station is a boiler with a special design that allows for the simulation of combustion processes occurring in water boilers with a permanent grate and with a mechanical travelling grate. The boiler is composed of two basic parts:

- the lower one, with adjustable temperature,
- the upper one, equipped with a water jacket.

The lower part of the system, in connection with the possibility of being heated up to the assumed temperature, allows, inter alia, for the simulation of the operation of the ignition arch of the stoker-fired boiler. The heated chamber walls also simulate the impact of further parts of the boiler on the combusted fuel sample.

The upper part of the boiler allows for flue gas cooling in a manner similar to the one occurring in the upper part of combustion chambers in water boilers.

To ensure quick feeding of the fuel sample into the furnace chamber and to allow for the placing of fuel on the grate, it is possible to insert the grate into the lower chamber.

The combustion chamber is equipped in a number of nozzles, which enables performing temperature measurements and sampling in the different points of the chamber. The installation is equipped with a system of equipment, which makes it possible to control the size of the air stream supplied and to measure it.

Before starting tests, samples of the combusted fuel were prepared. The glycerine phase was mixed with coal in proportion by weight of 10 and 20%. Then the prepared mixture was poured on the travelling grate. After the lower part of the furnace was heated up to 900°C, the grate was inserted into the combustion chamber. The fuel was combusted in a 50 mm-thick layer. As a result of the combustion chamber cooling during the insertion

of the fuel sample, the process was carried out from the temperature of about 700-750°C. The temperature measurement was registered at the level of 200 mm above the combusted fuel layer.

Table 1 presents basic fuel parameters of substances used in testing.

Table 1

Selected fuel parameters of substances used in testing

Item	Unit	Hard coal*	Glycerine phase*
c	[%]	63.88	43.12
h		3.71	7.15
n		1.17	0.03
s		0.94	1.75
cl		0.11	-
o		6.34	48.02
p		18.47	0.12
w		6.51	0.29
Calorific value	[MJ/kg]	25.3	16.4

* Over 100% summary contents of components result from uncertainty in measurement and from the fact that oxygen was measured and not calculated

Further in the article, combustion results for coal and mixtures with 10 and 20% of glycerine phase content are presented. These results are compiled with the results obtained during hard coal combustion. Every fuel (coal and mixtures) combustion was repeated three times. These processes were defined respectively as: “Test I”, “Test II” and “Test III”.

During presented testing, the mixture was obtained by thorough mixing of the glycerine phase with coal. As a result of such mixing, the glycerine phase occurred only on coal grains, providing them with clear gloss. Therefore, the phenomenon of the flow of the glycerine phase down the fuel layer did not occur. Moreover, such creation of the mixture caused that, de facto, there was no increase in their capacity (in relation to the combustion of coal alone). The glycerine phase filled the irregularity of grains and spaces between them.

Measurements were started at the moment of the ignition (adopted to be the moment when over 0.5% of CO_2 in flue gas was reported); testing was conducted for the period of 90 minutes. During testing, air was supplied to the combustion chamber in the quantity ensuring the mean value (for the entire combustion process) of the excess air ratio λ equal to 1.5.

Test results

Ones of the most important flue gas parameters in terms of environmental protection are their concentrations and emissions of CO and NO. These combustion process compounds are largely affected by control factors, such as, *eg* quantity and time of air supply.

A more detailed analysis of changes in these concentrations during the combustion of tested fuels (coal and mixtures) is presented below.

Figure 2 presents changes in time of CO concentrations reported during the implementation of three repetitions of the combustion of the mixture with 20% of glycerine

phase content. In the figure, there is also a curve presenting changes in time of the mean concentration values from these three repetitions.

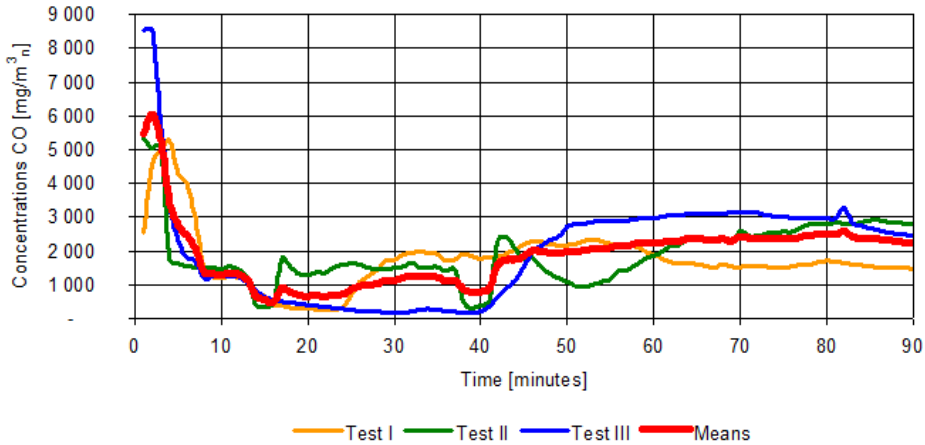

Fig. 2. CO concentrations during the combustion of the mixture with 20% of glycerine phase content

According to the data presented in Figure 2, for all tests we can observe that after the initial very significant increase in concentrations, they decrease very quickly (this stage lasts until c. 15th minute). At this stage, for all three repetitions of the mixture combustion process, maximum values were observed. Then, there is the stage of relatively low concentration values, and then their repeated increase. However, the duration of the last two stages of CO concentrations are very diversified for individual tests.

Despite relatively significant differences in the slopes of individual curves, the mean values of concentrations observed during individual repetitions are similar. These values are presented in Table 1.

Figure 3 presents mean CO concentrations obtained during the combustion of tested fuels.

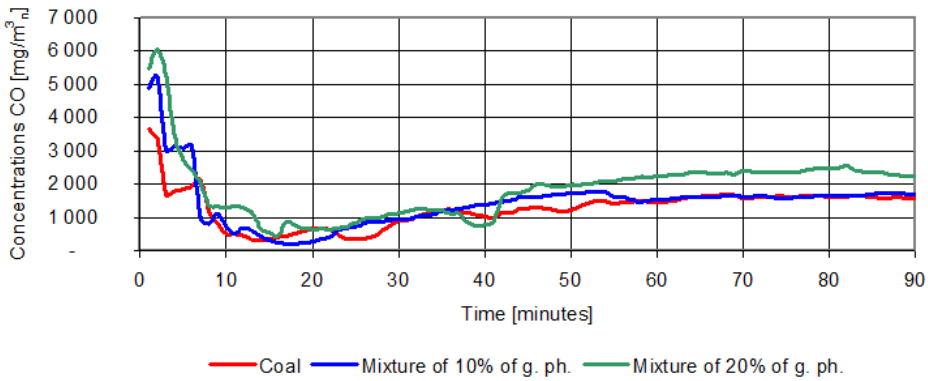

Fig. 3. Mean CO concentrations during the combustion of tested fuels (g. ph. - glycerine phase)

According to the data presented in Figure 3, in case of combustion of all tested fuels, a sudden increase and a very fast drop in CO concentrations in the period of the first 10 minutes is visible. In the second period, lasting for about 15 minutes, concentrations are of relatively low values. Then, there is an increase in concentrations, which continues till the end of testing.

The initial increase in CO concentrations results from the very intense process of volatile matter releasing. At the second stage, the fuel is combusted intensely, and CO is burned to CO_2. At the third stage, hydrogen radicals necessary for burning CO to CO_2 have already been used up. At the same time, there is a temperature drop, which also affects significantly CO burning.

Figure 3 also demonstrates that during the combustion of coal and mixture with 20% of glycerine phase content, starting from the 10th minute, we can observe relatively similar changes in concentration values. For the combustion of the mixture with 20% of glycerine phase content, increased (in relation to combustion processes of the other two fuels compared) CO concentrations at the first and at the last stage (from about 45th minute) of the combustion process were observed.

When comparing the mean values of concentrations reported during combustion of individual fuels (values presented in Table 2), it can be concluded that the least repeatable CO concentration results were characteristic for the coal combustion process, for which the relative error was over 30% (for the combustion of other fuels 11.0 and 7.3%). Along with the increase in the glycerine fraction content, CO concentrations are growing, and in the case of the combustion of the mixture with 10% of glycerine phase content, the increase is insignificant. For the combustion of the mixture with 20% of glycerine phase content the increase is over 30% (in relation to the concentrations observed during coal combustion).

Table 2

Mean values, standard deviations and relative errors, characteristic for the course of fuel combustion processes (coal and mixtures with 10 and 20% of glycerine phase content)

Gas	Mean values [mg/m^3_n]			Mean value for tests I to III [mg/m^3_n]	Standard deviation [mg/m^3_n]	Relative error [%]
	Test I	Test II	Test III			
	Coal					
CO	1462	951	1831	1415	442	31.2
NO	90	99	59	83	21	25.3
	Mixture with 10% of glycerine phase content					
CO	1423	1323	1636	1460	160	11.0
NO	92	50	57	66	22	33.3
	Mixture with 20% of glycerine phase content					
CO	1741	1904	2014	1887	137	7.3
NO	40	67	92	67	26	38.8

As in the case of CO, analyses conducted for NO lead to the conclusion that mean concentration values obtained are characterised by much less repeatability (relative error amounted from about 25 to nearly 40%). At the same time, adding the glycerine fraction resulted in the reduction in observed concentrations by about 20%. And concentrations observed during the combustion of mixtures with 10 and 20% of glycerine phase content were similar.

Conclusions

In Poland, in recent years, we have been observing a dynamic increase in ester production. The growing ester production is accompanied by an increasing production of the glycerine phase. Thus, the problem with the management of the glycerine fraction in a cheap and effective manner starts to occur. One of the methods meeting these criteria is the possibility of co-combusting the glycerine phase with coal. Testing conducted leads to the conclusion that combustion of mixture based on coal, characterised by a significant glycerine phase content (20% mass fraction), in the grate furnace, is possible. Glycerine does not cause the filling of spaces among the grains. And the co-combustion of the glycerine phase stabilises the process and increases its repeatability. Unfortunately, this co-combustion process is accompanied by an increase in concentrations, and thus, in CO emission.

References

[1] Directive 2009/28/EC, 23.04.2009. http://eur-lex.europa.eu/legal-content/EN/TXT/HTML/?uri=CELEX:32009L0028&from=EN.
[2] DzU 2006, Nr 169, poz. 1199. http://isap.sejm.gov.pl/DetailsServlet?id=WDU20061691199.
[3] DzU 2007, Nr 110, poz. 757. http://isap.sejm.gov.pl/DetailsServlet?id=WDU20071100757.
[4] URE: The market of biocomponents and liquid fuels. http://www.ure.gov.pl/pl/rynki-energii/paliwa-ciekle.

WYBRANE ASPEKTY EKOLOGICZNE WSPÓŁSPALANIA FAZY GLICERYNOWEJ Z WĘGLEM W PALENISKACH RUSZTOWYCH

Katedra Technologii i Urządzeń Zagospodarowania Odpadów, Politechnika Śląska, Gliwice

Abstrakt: Perspektywa wyczerpania się zapasów paliw kopalnych oraz obawy o stan środowiska naturalnego znacznie zwiększyły zainteresowanie odnawialnymi źródłami energii i w konsekwencji doprowadziły do dużego wzrostu ich wykorzystania zarówno w Polsce, jak i w pozostałych krajach Unii Europejskiej. Jednym z istotnych źródeł energii odnawialnej jest biomasa, która może być wykorzystana m.in. do produkcji biopaliw i biokomponentów płynnych, w tym estrów. Obowiązujące obecnie przepisy wymuszają rosnące zużycie tych substancji, a więc i rosnącą ich produkcję. Produkcji estrów towarzyszy produkcja fazy glicerynowej, której zagospodarowanie w sposób efektywny przysparza szereg problemów. Wynikają one zarówno z dużej zmienności właściwości fazy glicerynowej w zależności od technologii i surowców wykorzystywanych do produkcji estrów, jak i stosunkowo dużej masy tego odpadu powstającego w skali kraju. W pracy przedstawiono wyniki badań nad wybranymi aspektami środowiskowymi procesu współspalania fazy glicerynowej z węglem w paleniskach rusztowych. Specyfiką krajowej energetyki komunalnej jest występowanie stosunkowo dużej liczby kotłów z rusztami taśmowymi. W ramach prezentowanych badań zbadano proces spalania mieszanek o udziale masowym fazy glicerynowej wynoszącym od 5 do 20%. W pracy przedstawiono metodykę prowadzonych badań oraz wyniki dotyczące powstających emisji CO i NO.

Słowa kluczowe: faza glicerynowa, współspalanie, paleniska rusztowe, emisja

DOI: 10.2429/proc.2016.10(1)005 2016;10(1)

Małgorzata KUTYŁOWSKA[1]

SUPPORT VECTOR MACHINES AND NEURAL NETWORKS FOR FORECASTING OF FAILURE RATE OF WATER PIPES

METODA WEKTORÓW NOŚNYCH I SIECI NEURONOWE DO PRZEWIDYWANIA WSKAŹNIKA AWARYJNOŚCI PRZEWODÓW WODOCIĄGOWYCH

Abstract: The failure rate of water pipes was predicted using support vector machines (SVMs) and artificial neural networks (ANNs). Both algorithms are regression methods of so called machine learning. Operational data from the time span 2001-2012 were used for forecasting purposes. The length, diameter and year of construction of the distribution pipes and the house connections were treated as the independent variables. The computations were carried out using the Statistica 12.0 software.

Keywords: pipelines, prediction, radial basis functions

Introduction

Failure frequency is one among other indicators taken into account during the assessment of the reliability level of water supply systems [1, 2]. Nowadays, typical analysis of exploitation data related to the number and kinds of damages should be concerned together with the mathematical modelling. There are a lot of models which could be used for failure rate prediction [3-5]. They help us to assess the deterioration level of water conduits relatively quickly. The regression methods, for example support vector machines (SVMs) and artificial neural networks (ANNs) are nowadays very popular in solving many complex engineering problems [6-8]. It is the reason why such algorithms, based on radial basis functions (RBF), were used in this study to predict the values of failure rate of distribution pipes and house connections. The principal aim of this research was to find out, if an artificial neural network and support vector machine of the RBF type would predict (with an error acceptable for engineering purposes) the failure frequency indicator of water conduits

Materials and methods

The failure rate [λ, fail./(km·a)] of the house connections and the distribution pipes was predicted using the RBF-SVM and the RBF-ANN methods. The two approaches were based on radial basis functions. Exploitation data for the years 2001-2012 received from the water utility were used for forecasting purposes. In relation to SVM modelling, the whole data set was randomly divided into two equal (50%) subsets. The training and the testing sample had 147 data each for the house connections as well as respectively 124 and 125 data for the distribution pipes. The model was built using the training data and then it was tested on

[1] Faculty of Environmental Engineering, Wroclaw University of Science and Technology, Wybrzeże S. Wyspiańskiego 27, 50-370 Wrocław, Poland, phone +48 71 320 40 84, email: malgorzata.kutylowska@pwr.edu.pl
[*] Contribution was presented during ECOpole'16 Conference, Zakopane, 5-8.10.2016

different sample. In relation to ANNs, the methodology was a little bit different because of the peculiarities of such kind of modelling. The artificial neural network learning process consisted of several stages: a training stage (50% of the data), followed by a testing stage (25% of the data) and finally, the validation (25% of the data) of the created models. In the considered case, the whole data set (294 data for the house connections and 249 data for the distribution pipes) was used to learn the ANN. The training, testing and validation samples were chosen randomly from the whole data set. The prognosis was done on the basis of the unknown previously data set (created separately). The models were built separately for the distribution pipes and house connections. The calculations were done in the programme Statistica 12.0.

The relation between the dependent variables (the predicted value) and the independent variable need not to be known because the SVM method is a kind of nonparametric regression algorithm. V-fold cross validation was used to find the optimal model parameters [9]. Tenfold (V = 10) cross validation was used in the considered problem, whereby it was possible to select proper values for such parameters (learning constants) as capacity (C) and epsilon (ε), since they are not known *a priori*. In relation to artificial neural networks, model parameters (*eg* the number of hidden neurons and the type of activation functions) are determined during ANN learning using a suitable training algorithm. Many ANN models, for which the number of hidden neurons ranged from 1 to 30, were tested. The model characterized by the smallest mean-square error and the best fit between the real data and the predicted ones was selected. The results presented later in this paper are for this chosen optimal ANN model.

In both the methods the independent variables were: length (L_r, L_p), diameter (D_r, D_p) the year of construction (Y_r, Y_p) of the distribution pipes and the house connections.

Results and discussion

The parameters of the built ANN and SVM models for the different kinds of water pipelines are presented in Table 1. The validation error was considered for selecting an SVM model most accurately forecasting the failure rate. The validation error for the house connections and distribution pipes equalled to respectively 0.11 and 0.08. Nevertheless, the failure rate prediction on the basis of the testing sample was not satisfactory from the predicted/real data fit point of view. Moreover, the number of SVMs for the distribution pipes was high and as much as 82% of them were localized SVMs, *ie* with weights equal to ± the capacity value (Table 1), indicating a more complicated model structure. In the case of any kind of modelling, it is necessary to answer the question whether the aim is to obtain a perfect data fit at any cost, *ie* at the expense of model architecture complication, or rather to reveal the correlations between the dependent and independent variables.

In the case of the ANN models, Pearson's correlation coefficient (R), a determination coefficient (R^2) and a relative mean-square prediction error (amounting to about 20% for the distribution pipes and the house connections) would be compared. The value of this error is rather high in comparison to other results obtained using multilayer perceptron instead of radial basis functions. According to the literature [10] RBF ANNs were also less useful for hourly water demand prediction than the multilayer perceptron. Despite the fact that there were three times more hidden neurons in the house connections model than in the distribution pipes model (Table 1), the prediction results are worse and characterized by larger

discrepancies between the experimental and forecasted data (Figs. 1 and 2). Because of the nature of RBF ANNs, the activation functions and the training method were pre-imposed, which also can have a bearing on modelling quality in comparison with, *eg* artificial neural networks using the multilayer perceptron, where it is possible to use several different functions, such as the sigmoidal function, the exponential function and so on [11].

Table 1

Parameters of SVM and ANN models

Type of conduit/parameter	Distribution pipes	House connections
SVM model		
Gamma	0.333	0.333
Capacity (C)	3	1
Epsilon (ε)	0.2	0.5
Number of support vectors (localized)	56 (46)	14 (7)
Cross-validation error	0.081	0.110
ANN model		
Number of hidden neurons	8	27
Activation functions: hidden/output layer	Gaussian/linear	Gaussian/linear
Training algorithm	RBFT	RBFT
Correlation coefficient (learning/prognosis step)	0.956/0.859	0.997/0.897
Determination coefficient (learning/prognosis step)	0.914/0.737	0.994/0.805

The results of failure rate prediction for the learning sample are presented in Table 2 while the ones for the testing sample (the SVM model) and the prognosis stage (the ANN model) are shown in Figures 1 and 2. Such distinction, between the testing sample for the SVM model and the prognosis stage for the ANN model, is necessary to draw, since the testing sample data and the prognosis stage data were unknown to the model previously. Using such approach it is possible to establish the quality of the model and its applicability to failure rate prediction.

Table 2

Results of failure rate prediction - learning step

Year	House connections			Distribution pipes		
	Experimental	ANN-RBF	SVM-RBF	Experimental	ANN-RBF	SVM-RBF
2001	0.94	0.95	1.17	0.34	0.36	0.38
2002	0.84	0.84	1.16	0.34	0.36	0.38
2003	1.59	1.58	1.26	0.50	0.47	0.48
2004	1.07	1.07	1.32	0.37	0.39	0.41
2005	1.00	1.00	1.32	0.57	0.48	0.52
2006	1.15	1.15	1.33	0.42	0.42	0.42
2007	0.83	0.80	1.12	0.31	0.30	0.33
2008	0.65	0.63	0.79	0.22	0.21	0.22
2009	0.61	0.62	0.70	0.25	0.25	0.24
2010	0.50	0.50	0.63	0.27	0.26	0.24
2011	0.23	0.33	0.57	0.10	0.21	0.20
2012	0.38	0.38	0.51	0.24	0.25	0.24

An analysis of Table 2 clearly shows that prediction of failure rate λ of house connections using the RBF-ANN model is better than for the RBF-SVM model. For the

distribution pipes the differences in failure rate predictions between the two modelling methods are not so significant and one can say that these two methods are equally effective, as indicated by the fact that coefficients R = 0.96 and R^2 = 0.92 are identical for both methods. Considerable errors (over 100%) occur in the estimates of the failure rate for the distribution pipes only in 2011, which is undoubtedly due to the fact that this indicator is very much different from the values for the other analyzed years (could be treated as outlier). A similar situation is observed during forecasting the failure rate for the house connections in 2011.

Parallel correlations (as the ones described above) between real and forecasted data were found at the testing step (the SVM model) and the prognosis step (the ANN model), as shown in Figures 1 and 2. In relation to the house connections, good agreement between experimental and predicted values is generated by the ANN model, but for some years (*eg* 2003, 2006 and 2009) the discrepancies are much larger than the ones observed at the learning step. Despite many divergences, the trend in the changes of the forecasted values is similar to the trend in the variation of real values. In the years 2006-2008 a similar configuration is observed for the SVM model, but most of the λ values are much higher than the real ones.

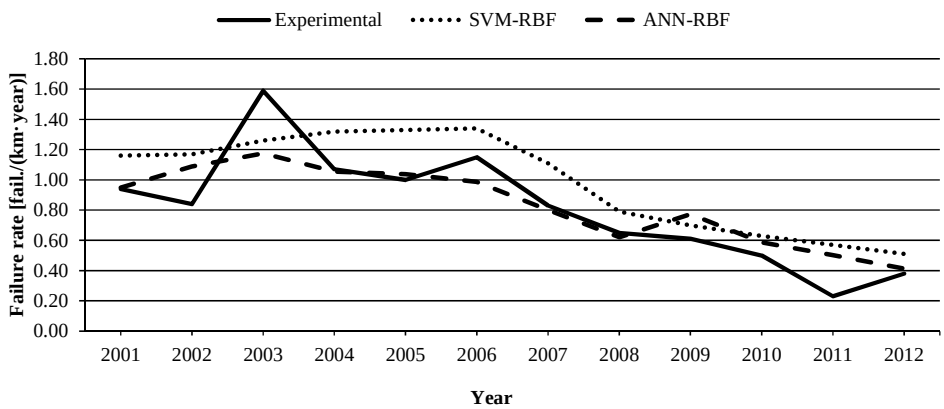

Fig. 1. Prediction results of house connections' failure rate - testing-SVM/prognosis-ANN

The estimation of the failure rate of the distribution pipes (Fig. 2) by the SVM method and the ANN method was characterized by acceptable agreement between the forecasted and real values in both cases. The Pearson correlation coefficient for the SVM model and the ANN model equalled to respectively 0.96 and 0.86, indicating that the SVM method is slightly better for predicting the failure rate of distribution pipes than the ANN method. The different situation is observed for house connections. It should also be noted that the results of predicting the failure rate of the distribution pipes and the house connections (Table 2, Figs. 1 and 2) by means of the SVM-RBF model are very similar for both the learning sample and the testing sample. Whereas the results of learning and prognosis by the ANN-RBF model show larger discrepancies for both types of pipelines. Even though at the learning stage the agreement between the experimental and forecasted values is satisfactory, the prognosis stage (using new data) gives a larger (but still acceptable from the engineering point of view) error. This is evidence of greater effectiveness of RBF-based

training by means of SVMs than ANNs. However, at the present step of the studies it cannot be explicitly pointed out which of the algorithm is better and should be widely adopted in the modelling of the failure rate of water pipelines. Further research in this area is needed, also on operational data from other water utilities, permitting more in-depth analyses and broader generalizations.

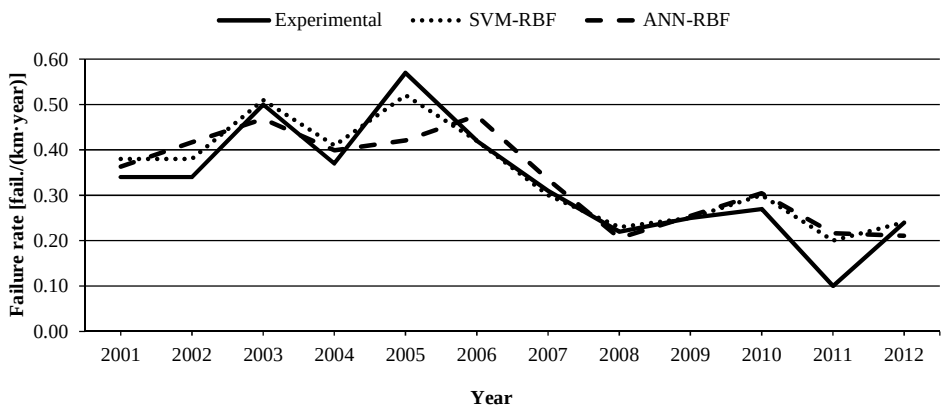

Fig. 2. Prediction results of distribution pipes' failure rate - testing-SVM/prognosis-ANN

Conclusions

Support vector machines and artificial neural networks were used for the prediction of the failure rate of the house connections and distribution pipes in one of the Polish city. Exploitation data for the time span 2001-2012 were chosen for prediction purposes. The problem is quite important for the correct and quick approximation of the reliability level. Both methods can be used to establish the failure rate of municipal systems. A relatively large database must be available in order to identify the relevant correlations between dependent and independent variables.

The optimal SVM model had gamma coefficient equalled to 0.33 for both the distribution pipes and the house connections. The capacity C and the number of SVMs were respectively 3 and 4 times greater in relation to the model describing the failure frequency of the distribution pipes. The error of the V-fold cross validation amounted to 0.110 and 0.081 for the model describing the failure rate of respectively the house connections and distribution pipes. The length, diameter and year of laying the water pipes in the ground were treated as independent variables. The optimal ANN-RBF model contained 27 and 8 hidden neurons for respectively house connections and distribution pipes. The coefficients R and R^2 are slightly higher at the step of learning than during prognosis of ANN model.

Acknowledgments

The work was realized within the allocation No. B50519 awarded for Faculty of Environmental Engineering Wroclaw University of Science and Technology by Ministry of

Science and Higher Education. The grant was allocated for scientific researches of young scientists in years 2015-2016.

References

[1] Tscheikner-Gratl F, Sitzenfrei R, Rauch W, Kleidorfer M. Struct Infrastruct Eng. 2016;12(3):366-380. DOI: 10.1080/15732479.2015.1017730.
[2] Kowalski D, Miszta-Kruk K. Eng Failure Analysis. 2013;35:736-742. DOI: 10.1016/j.engfailanal.2013.07.017.
[3] Scheidegger A, Leitao JP, Scholten L. Water Res. 2015;83:237-247. DOI: 10.1016/j.watres.2015.06.027.
[4] Nishiyama M, Filion Y. Can J Civ Eng. 2014;41(10):918-923. DOI: 10.1139/cjce-2014-0114.
[5] Tscheikner-Gratl F, Sitzenfrei R, Rauch W, Kleidorfer M. Struct Infrastruct Eng. 2016;12(3):366-380. DOI: 10.1080/15732479.2015.1017730.
[6] Kolasa-Więcek A. Ecol Chem Eng S. 2013;20(2):419-428. DOI: 10.2478/eces-2013-0030.
[7] Aydogdu M, Firat M. Water Resour Manage. 2015;29:1575-1590. DOI: 10.1007/s11269-014-0895-5.
[8] Rodolfi E, Servili F, Magini R, Napolitano F, Russo F, Alfonso L. Proced Eng. 2014;89:648-655. DOI: 10.1016/j.proeng.2014.11.490.
[9] Statistica 12.0, Electronic Manual. http://www.statsoft.pl/textbook/stathome_stat.html?http%3A%2F%2Fwww.statsoft.pl%2Ftextbook%2Fstmachlearn.html
[10] Siwoń Z, Cieżak W, Cieżak J. Modele neuronowe szeregów czasowych godzinowego poboru wody w osiedlach mieszkaniowych [Neural network models of hourly water demand time series in housing areas]. Ochr Środ. 2011;33(2):23-26. http://www.os.not.pl/docs/czasopismo/2011/2-2011/Siwon_2-2011.pdf.
[11] Kutyłowska M. Eng Failure Analysis. 2015;47:41-48. DOI: 10.1016/j.engfailanal.2014.10.007.

METODA WEKTORÓW NOŚNYCH I SIECI NEURONOWE DO PRZEWIDYWANIA WSKAŹNIKA AWARYJNOŚCI PRZEWODÓW WODOCIĄGOWYCH

Wydział Inżynierii Środowiska, Politechnika Wrocławska

Abstrakt: Wskaźnik awaryjności przewodów wodociągowych przewidywano za pomocą metody wektorów nośnych (SVM) i sztucznych sieci neuronowych (SSN). Oba algorytmy należą do metod regresyjnych, nazywanych metodami uczenia maszyn. Dane eksploatacyjne z lat 2001-2012 zostały wykorzystane w celach predykcji. Długość, średnica i rok budowy przewodów rozdzielczych i przyłączy były zmiennymi niezależnymi. Obliczenia przeprowadzono w programie Statistica 12.0.

Słowa kluczowe: rurociągi, przewidywanie, radialne funkcje bazowe

DOI: 10.2429/proc.2016.10(1)006 2016;10(1)

Kamila NOWAK[1]

NATURAL BACKGROUND GAMMA RADIATION IN THE URBAN SPACE OF WALBRZYCH

NATURALNE TŁO PROMIENIOWANIA GAMMA W PRZESTRZENI MIEJSKIEJ WAŁBRZYCHA

Abstract: Walbrzych is the second most populous city of dolnoslaskie voivodeship, with the population of over 117 000 inhabitants. It is one of the largest cities within the Sudety Mountains with the area of approximately 85 km^2. From the geological point of view it is situated at the junction of three units: the Gory Sowie Massif, the Swiebodzice Basin and the Intra-Sudetic Basin. Each of this unit consists of various rocks which are characterised by various natural radionuclides content, resulting in various gamma dose rates in air within Walbrzych area. The landscape of the city largely is formed by an anthropogenic activity, mainly coal mining. Within the city there are thirty two heaps of wastes after the coal mining. The gamma spectrometric research of natural background gamma radiation in the urban space of Walbrzych was carried out. *In situ* measurements were performed by means of portable gamma spectrometer RS 230 with a BGO detector and dimensions of 259 mm × 81 mm × 96 mm. The device displays potassium K [%], equivalent uranium eU [ppm] and equivalent thorium eTh [ppm] contents, as well as absorbed gamma dose rate in air at the height of 1 meter generated by these radionuclides [in nGy/h]. The investigations were divided into two stages. In the first one, the content of K, eU and eTh in various types of rocks was examined. Measurements were performed on 14 outcrops of various aged rocks within all the three units (from Proterozoic gneisses of the Gory Sowie Massif to Pleistocene sands and gravels covering the Swiebodzice Basin) and on a heap. In the second stage the spatial distribution of natural radionuclides and gamma dose rate within the city was examined. Forty measurements were performed in the nodes of regular grid with the mesh size of 1.5 km. Taking into account that gamma dose rate in air mostly is formed by radionuclides present in the top 30-centimetres ground surface, the type of material covering the ground in measurement points was noted. Performed investigations showed that among rocks occurring within Walbrzych city, late Carboniferous trachyandesites, outcropping in the old quarry in Podgorze II district (the Intra-Sudetic Basin), were the most radioactive. The mean content of K, eU and eTh was 3.8%, 4.0 and 18.3 ppm, respectively which generated absorbed gamma dose rate equal to 121.2 nGy/h. Late Carboniferous conglomerates and sandstones of the Glinik Formation (the Intra-Sudetic Basin) are characterised by the lowest radioactivity. The mean content of K, eU and eTh was 0.6%, 1.5 and 5.1 ppm, respectively which generated absorbed gamma dose rate equal to 29.6 nGy/h. The analysis of spatial distribution of absorbed gamma dose rate showed that Srodmiescie district and the vicinity of Ksiaz Castle are characterised by the highest natural background gamma radiation. Absorbed dose rates with values of over 100 nGy/h were noted in places where the ground was covered by granite cobblestone. The lowest natural background gamma radiation was observed in points situated on the outskirts of the city, in places with relatively natural soils.

Keywords: natural background gamma radiation, gamma radiation, potassium, uranium, thorium, Sudety Mts.

Introduction

Potassium ^{40}K and radionuclides of uranium ^{238}U and thorium ^{232}Th decay series are the main contributors to natural background gamma radiation. Contents of ^{40}K and radionuclides of ^{238}U and ^{232}Th decay series vary depending on the type of rock. Many papers describe radionuclides content in various rocks and analyse results in the context of human exposure on an open space depending on the lithology [1-5]. Whereas estimating

[1] Institute of Geological Sciences, University of Wroclaw, pl. M. Borna 9, 50-204 Wroclaw, Poland, email: kamila.nowak@ing.uni.wroc.pl
[*] Contribution was presented during ECOpole'15 Conference, Jarnoltowek, 14-16.10.2015

gamma dose rate on an open space is relatively simple because of an open field geometry, urban areas are much more complex and less studies are carried out in these environments. Urban areas are places with various geometries resulting from an urban structure. Furthermore, in urban areas the environment is modified by numerous and various building materials used for the construction of buildings, roads and pavements [6-9].

Urban areas are very important for estimating human exposure to gamma radiation. According to data from 2014 published by the Central Statistical Office [10] over 60% of total population in Poland lives in urban environments. The aim of this study was to estimate natural background gamma radiation in the urban space of Walbrzych, the second most populous city of dolnoslaskie voivodeship, with the population of over 117 000 inhabitants and one of the largest cities in Sudety Mountains with the area of approximately 85 km^2. Strzelecki et al [11] estimated gamma dose rate in Walbrzych on the basis of measurements performed in 900 measurment points. The lithological type of the bedrock was assigned to each measurement point. The results were analysed taking into account the geological structure of the area but the influence of building materials used in the urban space was not considered. Koperski [12] analysed background gamma radiation in cities of southern Poland, including Walbrzych, taking into account a type of material covering the ground. This paper presents the analysis of natural background gamma radiation in Walbrzych taking into account the type of rocks outcropping on this area but also considering the influence of building materials covering the roads and pavements. Furthermore, the spatial distributions of radionuclides and gamma dose rate were examined. Radioecological maps of Walbrzych were prepared and are presented in this paper.

Study area

The geology structure of Walbrzych area is very complex. The city is situated at the junction of three units: the Gory Sowie Massif, the Swiebodzice Basin and the Intra-Sudetic Basin. Each of this unit consists of various rocks which are characterised by various natural radionuclides content, resulting in various gamma dose rates in air. The Gory Sowie Massif is the oldest geological unit on the Walbrzych area. It is built of strongly metamorphosed Precambrian, Proterozoic and Archaic rocks which were the protoliths for gneisses. Some of the gneisses were exposed to high pressures and temperatures forming migmatites. The Swiebodzice Basin is a part of early Variscan sedimentary basin, filled in by coarse-grained sediments in late Devonian and early Carboniferous. Within the Swiebodzice Basin there are four formations, two Devonian: (1) Pogorzala Formation (consisted of mudstones, claystones and sandstones with insertions of conglomerates) and (2) Pelcznica Formation (consisted of mudstones and sandstones), and two Carboniferous: (3) Ksiaz Formation (consisted of conglomerates with approximately 80% of gneiss boulders) and (4) Chwaliszow Formation (consisted of conglomerates with approximately 32% of gneiss boulders). The Intra-Sudetic Basin consists of early and late Carboniferous sediments: conglomerates, sandstones, mudstones and claystones. Within the Intra-Sudetic Basin in the Walbrzych area there are two formations of early Carboniferous (Lubomin and Szczawno Formations) and five of late Carboniferous (Walbrzych, Bialy Kamien, Zaclerz, Glinik and Ludwikowice Formations). Within late Carboniferous sediments of Intra-Sudetic Basin there are igneous rocks, such as rhyolites, rhyodacites, volcanic tuffs, pyroclastic breccias,

trachyadesites and trachybasalts. Quaternary sediments (from Pleistocene and Holocene) are the youngest rocks of Walbrzych area. The landscape of the city is largely modified by an anthropogenic activity, mainly coal mining. Within the city there are thirty two heaps of wastes after the coal mining [13].

Fourteen outcrops of various aged rocks (from Proterozoic gneisses of the Gory Sowie Massif to Pleistocene sands and gravels covering the Swiebodzice Basin) characteristic for the Walbrzych area and one heap of mineral waste after coal mining were selected (Table 1). Not all of the outcrops were located within the Walbrzych area (Fig. 1).

Table 1

Location and stratigraphic position of the outcrops

ID	Longitude [ºE]	Latitude [ºN]	Unit	Rock type	System	Epoch	Formation
1	16.2788	50.7543	Intra-Sudetic Basin	Mineral wastes after coal mining	Holocene		
2	16.3114	50.8253	Swiebodzice Basin	Sands and gravels	Pleistocene		
3	16.3259	50.7931	Gory Sowie Massif	Boulder clays			
4	16.3057	50.7409	Intra-Sudetic Basin	Trachyandesites	Carboniferous	Late	
5	16.2732	50.7397	Intra-Sudetic Basin	Rhyodacites			
6	16.2188	50.7756	Intra-Sudetic Basin	Rhyolites			
7	16.2596	50.7383	Intra-Sudetic Basin	Conglomerates, sandstones			Glinik Formation
8	16.2847	50.7673	Intra-Sudetic Basin	Conglomerates, sandstones, claystones			Zaclerz Formation
9	16.2477	50.7889	Intra-Sudetic Basin	Conglomerates, sandstones			Bialy Kamien Formation
10	16.2849	50.7879	Intra-Sudetic Basin	Sandstones, conglomerates			Walbrzych Formation
11	16.2320	50.7997	Intra-Sudetic Basin	Sandstones, conglomerates		Early	Szczawno Formation
12	16.2296	50.8004	Intra-Sudetic Basin	Claystones			
13	16.2979	50.8384	Swiebodzice Basin	Conglomerates			Ksiaz Formation
14	16.2808	50.8189	Swiebodzice Basin	Conglomerates			Chwaliszow Formation
15	16.3404	50.7959	Gory Sowie Massif	Gneisses and migmatites	Proterozoic		

To examine the spatial distribution of natural radionuclides and gamma dose rate within the city, forty measurement points were selected within the city borders. Measurements were performed in the nodes of regular grid with the mesh size of 1.5 km (Fig. 2).

Measurements not always were performed strictly in a node of designed grid. Some points were planned on private properties or places hardly available so measurements were conducted as close designed points as possible. Taking into account that gamma dose rate in air mostly is formed by radionuclides present in the top 30-centimetres ground surface [14] and a bedrock in a city often is covered by a building material, the type of material covering the ground in measurement points was noted (Table 2).

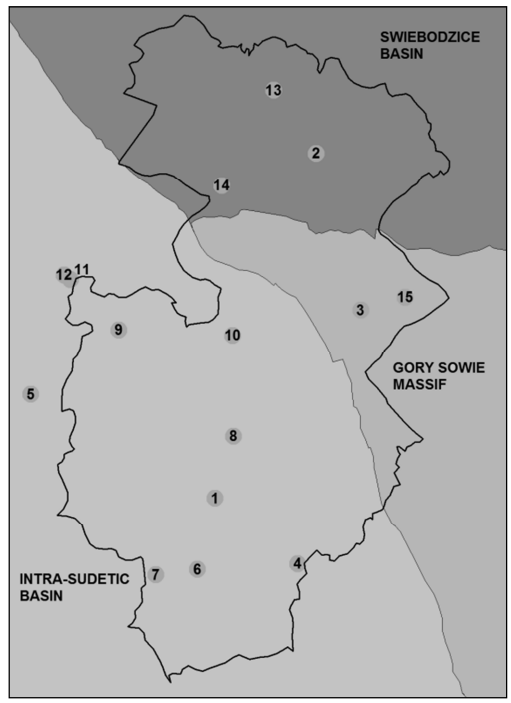

Fig. 1. Location of outcrops on the geological map (after Haydukiewicz et al [15] simplified)

Fig. 2. Location of measurement points

Table 2

Coordinates and ground coverage in measurement points

ID	Longitude [ºE]	Latitude [ºN]	Ground coverage	ID	Longitude [ºE]	Latitude [ºN]	Ground coverage
1	16.2579	50.8425	Soil	23	16.2783	50.7802	Asphalt
2	16.2795	50.8470	Soil	24	16.2580	50.7802	Soil
3	16.2976	50.8433	Granite	25	16.2578	50.7938	Asphalt
4	16.3197	50.8453	Soil	26	16.2376	50.7931	Crushed stone
5	16.3405	50.8308	Soil	27	16.2378	50.7805	Soil
6	16.3185	50.8303	Asphalt	28	16.2361	50.7679	Soil
7	16.2981	50.8297	Asphalt	29	16.2581	50.7666	Asphalt
8	16.2779	50.8306	Soil	30	16.2783	50.7678	Granite
9	16.2591	50.8309	Soil	31	16.2981	50.7674	Crushed stone
10	16.2782	50.8182	Asphalt	32	16.3211	50.7688	Soil
11	16.2987	50.8184	Asphalt	33	16.3388	50.7675	Soil
12	16.3163	50.8157	Soil	34	16.3160	50.7569	Soil
14	16.3389	50.8060	Soil	35	16.2975	50.7547	Asphalt
15	16.3180	50.8055	Soil	36	16.2789	50.7543	Soil
16	16.2972	50.8057	Concrete	37	16.2609	50.7557	Soil
17	16.2782	50.8057	Asphalt	38	16.2376	50.7539	Soil
18	16.3002	50.7924	Soil	39	16.2588	50.7420	Soil
19	16.3184	50.7926	Soil	40	16.2782	50.7425	Soil
20	16.3386	50.7929	Soil	41	16.2976	50.7435	Soil
21	16.3181	50.7804	Soil	43	16.2732	50.7294	Asphalt
22	16.3018	50.7796	Soil				

Methods

Portable gamma spectrometers are convenient devices to estimate natural background gamma radiation in urban environments with complex geometry of the source. Measurements of terrestrial background gamma radiation were conducted by means of gamma spectrometer RS 230 with a BGO detector and dimensions of 259 mm × 81 mm × 96 mm. The device displays potassium K [%], equivalent uranium eU [ppm] and equivalent thorium eTh [ppm] contents, as well as absorbed gamma dose rate in air at the height of 1 meter generated by these radionuclides [nGy/h]. Potassium K content is calculated on the basis of gamma photons emitted by ^{40}K (1461 keV). Uranium ^{238}U and thorium ^{232}Th contents are calculated on the basis of gamma photons emitted by ^{214}Bi (1765 keV) and ^{208}Tl (2615 keV), respectively. The secular equilibrium between all of the radioisotopes within the decay series is assumed. Uranium and thorium contents obtained in this way are denoted as equivalent uranium (eU) and equivalent thorium (eTh) content, respectively. Measurements on outcrops were performed placing the device directly on a rock. The result is representative for a sample of a radius of 0.5 m, a thickness of 25 cm and a mass exceeding 100 kg [14]. On each outcrop three measurements were performed. Measurements in regular grid were performed at the standard height of 1 meter above the ground. At this height 90% of photons reaching the gamma spectrometer originates from the area of a radius of 10 m [16]. In each point one measurement was performed. Additionally, equivalent gamma dose rate [μSv/h] generated by both, terrestrial and cosmic, radiations was measured in each point by means of radiometer ECO-D.

Results and discussion

Results of K, eU, eTh content in examined waste after coal mining and rocks, characteristic for the Walbrzych area, as well as absorbed dose rate in air generated by these radionuclides are presented in Table 2. Results varied in wide ranges depending on a type of rock. Mean K content varied from 0.6% for conglomerates and sandstones of Glinik Formation to 4.4% for Carboniferous rhyodacites. Mean eU content ranged from 1.5 ppm for conglomerates and sandstones of Glinik Formation to 6.5 ppm for sandstones and conglomerates of Walbrzych Formation. Mean eTh content varied from 5.1 ppm for conglomerates and sandstones of Glinik Formation to 29.1 ppm for Carboniferous rhyolites. Mean absorbed dose rate in air ranged from 29.6 nGy/h for conglomerates and sandstones of Glinik Formation to 121.2 nGy/h for Carboniferous trachyandesites. Contribution of K, eU and eTh in forming absorbed dose rate varied in ranges 13.7-51.5%, 17.7-33.7% and 25.6-66.0%, respectively. According to Strzelecki et al [11] absorbed dose rate at the Walbrzych area ranges between 24.1 and 138.5 nGy/h. They observed the highest absorbed dose rates on heaps of wastes after coal mining and in Kozice district, in a place with the uranium mineralization within gneisses.

Table 3

Results depending on the bedrock lithology

ID*	Terrestrial absorbed dose rate [nGy/h]	K			eU			eTh		
		[%]	[nGy/h]	Contribution [%]	[ppm]	[nGy/h]	Contribution [%]	[ppm]	[nGy/h]	Contribution [%]
1	109.5	3.1	42.2	38.5	4.9	26.2	23.9	15.3	41.1	37.5
2	53.5	1.7	22.9	42.8	2.1	11.2	20.8	7.3	19.5	36.4
3	66.5	1.9	25.1	37.8	3.0	16.1	24.2	9.4	25.3	38.0
4	121.2	3.8	50.7	41.8	4.0	21.4	17.7	18.3	49.1	40.5
5	114.2	4.4	58.8	51.5	4.4	23.2	20.3	12.0	32.2	28.2
6	118.3	1.2	16.2	13.7	4.5	24.1	20.4	29.1	78.1	66.0
7	29.6	0.6	8.1	27.3	1.5	8.0	26.9	5.1	13.6	45.8
8	83.6	3.0	40.8	48.8	3.7	19.6	23.5	8.6	23.1	27.7
9	87.9	3.2	42.6	48.5	3.0	15.8	17.9	11.0	29.5	33.6
10	102.8	2.7	36.3	35.3	6.5	34.7	33.7	11.9	31.8	30.9
11	52.0	1.6	22.0	42.3	2.3	12.2	23.5	6.6	17.8	34.2
12	111.4	3.7	49.3	44.3	4.6	24.3	21.8	14.1	37.8	33.9
13	78.5	2.7	36.3	46.3	3.3	17.3	22.1	9.3	24.8	31.6
14	90.5	3.1	41.3	45.6	4.4	23.4	25.8	9.7	25.9	28.6
15	94.4	3.3	44.4	47.1	4.9	25.8	27.4	9.0	24.1	25.6

*Description of the lithology in Table 1

Table 4 presents results of measurements performed in measurement points of regular grid. Among 40 measurements, 26 were performed above relatively natural soils, 9 above a ground covered by an asphalt, 2 above a crushed stone, 2 above granite cobblestones and 1 above a ground covered by a concrete (Table 4). Such a large contribution of places with soils is a result of a large contribution of farmlands and forests (almost 70%) and low contribution of urban areas (about 13%) within Walbrzych area [17]. The lowest absorbed dose rate was observed in the places with relatively natural soils. Nevertheless, absorbed

dose rate above soils ranged in wide limits, from 22 to 81 nGy/h with a mean of 47 nGy/h. The highest absorbed dose rate was observed in the places with granite cobblestones (mean absorbed dose rate equal to 106 nGy/h). Results obtained by Koperski [12] are similar to the results obtained in this study. The highest absorbed dose rate was noted in places covered by granite cobblestones, lower in places covered by an asphalt and a concrete and the lowest in places with soils.

Mean terrestrial absorbed dose rate in Walbrzych obtained on the basis of 40 measurement points of regular grid was equal to 52 nGy/h. This value is lower than mean absorbed dose rate estimated by Strzelecki et al [11] which was 72.35 nGy/h.

Table 4

Results depending on the ground coverage

	Soil	**Concrete**	**Granite**	**Crushed stone**	**Asphalt**	**Total**
Number of measurements	26	1	2	2	9	40
Mean terrestrial absorbed dose rate [nGy/h]	47	42	106	62	53	52
Standard deviation [nGy/h]	11	-	5	1	9	16
Min [nGy/h]	22	-	100	61	50	22
Max [nGy/h]	81	-	111	63	56	111
Mean contribution of K [%]	38	35	38	37	38	38
Mean contribution of eU [%]	27	33	25	30	26	27
Mean contribution of eTh [%]	35	32	37	33	36	35

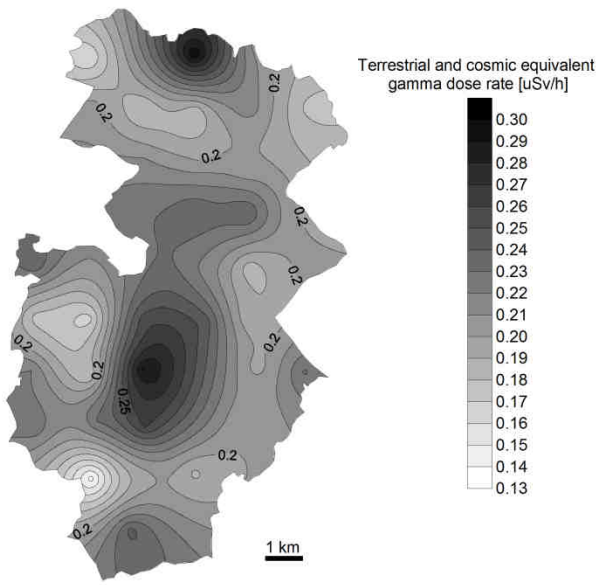

Fig. 3. Spatial distribution map of terrestrial and cosmic equivalent gamma dose rate [μSv/h] measured by means of ECO D radiometer

Figures 3 and 4 present radioecological maps of Walbrzych area. The analysis of spatial distribution of gamma dose rate showed that Srodmiescie district and the vicinity of Ksiaz Castle are characterised by the highest natural background gamma radiation. Also contents of K, eU and eTh are the highest in these places. It is a result of the presence of granite cobblestones used for a construction of roads and pavements. The lowest natural background gamma radiation was observed in points situated on the outskirts of the city, in places with relatively natural soils.

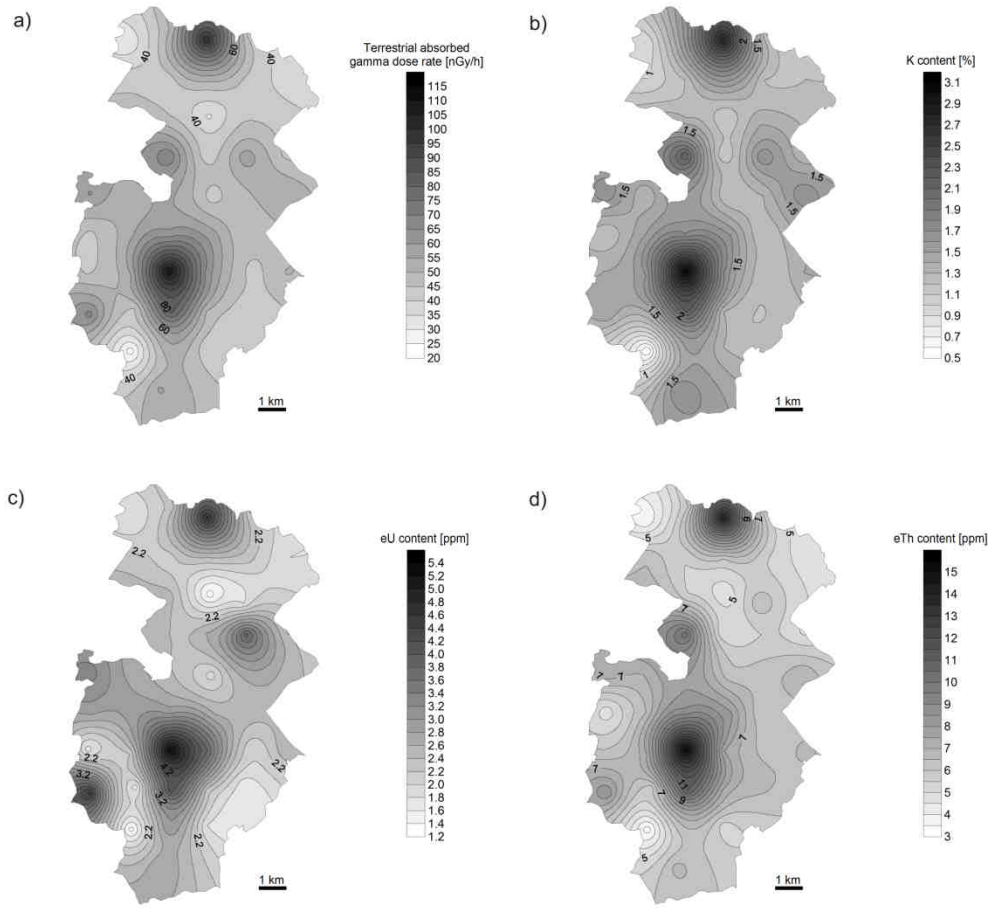

Fig. 4. Spatial distribution maps of: a) terrestrial absorbed gamma dose rate [nGy/h], b) potassium content [%], c) equivalent uranium content [ppm], d) equivalent thorium content [ppm] measured by RS 230 gamma spectrometer

Conclusions

Natural background gamma radiation in Walbrzych ranges in wide limits as a result of a complex geological structure of this area. Nevertheless, the type of the ground coverage plays a significant role in forming gamma dose rate on urban areas. High dose rates are observed on urban areas with a ground covered by granite cobblestones and on heaps of wastes which means that people largely form background gamma radiation in which they live.

Acknowledgements

The project is co-financed by the European Union under the European Social Fund.

References

[1] Orgün Y, Altinsoy N, Sahin SY, Güngör Y, Gültekin AH, Karahan G, et al. Natural and anthropogenic radionuclides in rocks and beach sands from Ezine region (Canakkale), Western Anatolia, Turkey. Appl Radiat Isotopes. 2007;65:739-747. DOI: 10.1016/j.apradiso.2006.06.011.

[2] El Galy MM, El Mezayn AM, Said AF, El Mowafy AA, Mohamed MS. Distribution and environmental impacts of some radionuclides in sedimentary rocks at Wadi Naseib area, southwest Sinai, Egypt. J Environ Radioact. 2008;99(7):1075-82. DOI: 10.1016/j.jenvrad.2007.12.012.

[3] Joshuaa EO, Ademolaa JA, Akpanowoa MA, Oyebanjoa OA, Olorodeb DO. Natural radionuclides and hazards of rock samples collected from Southeastern Nigeria. Radiat Meas. 2009;44:401-404. DOI: 10.1016/j.radmeas.2009.04.002.

[4] Rafiquea M, Khana AR, Jabbarb A, Rahmanc SU, Kazmia SJA, Nasird T, et al. Evaluation of radiation dose due to naturally occurring radionuclides in rock samples of different origins collected from Azad Kashmir. Russ Geol Geophys. 2014;55:1103-1112. DOI: 10.1016/j.rgg.2014.08.005.

[5] Rani A, Mittal S, Mehra R, Ramola RC. Assessment of natural radionuclides in the soil samples from Marwar region of Rajasthan, India. Appl Radiat Isot. 2015;101:122-6. DOI: 10.1016/j.apradiso.2015.04.003.

[6] Clouvas A, Xanthos S, Antonopoulos-Domis M. Extended survey of indoor and outdoor terrestrial gamma radiation in Greek urban areas by in situ gamma spectrometry with a portable Ge detector. Radiat Prot Dosim. 2001;94(3):233-246. DOI: 10.1093/oxfordjournals.rpd.a006495.

[7] Cresswell AJ, Sanderson DCW, Harrold M, Kirley B, Mitchell C, Weirb A. Demonstration of lightweight gamma spectrometry systems in urban environments. J Environ Radioactiv. 2013;124:22-28. DOI: 10.1016/j.jenvrad.2013.03.006.

[8] Licínio MV, Freitas AC, Evangelista H, Costa-Gonçalves A, Miranda M, Alencar AS. A high spatial resolution outdoor dose rate map of the Rio de Janeiro city, Brasil, risk assessment and urbanization effects. J Environ Radioactiv. 2013;126:32-39. DOI: 10.1016/j.jenvrad.2013.07.012.

[9] Nowak KJ, Solecki AT. Factors affecting background gamma radiation in the urban space. J Elem. 2015;20(3):653-665. DOI: 10.5601/jelem.2014.19.4.755.

[10] Stańczak J, Znajewska A, Cierniak M, Daniłowska A, Urbanowicz M, Kostrzewa Z, et al. Size and structure of population and vital statistics in Poland by territorial division in 2014. Warszawa: Central Statistical Institute; 2015. http://stat.gov.pl/download/gfx/portalinformacyjny/en/defaultaktualnosci/3286/3/8/1/p_population_size_structure_31-12-2013.pdf (in Polish and English).

[11] Strzelecki R, Wołkowicz S, Nałęcz T. Radioactive elements and radioecological hazard in towns of the Sudetic region (SW Poland). Prz. Geol. 2000;48:1139-1150. https://geojournals.pgi.gov.pl/pg/article/view/15435/13029.

[12] Koperski J. Exposure of urban populations to natural gamma background in Poland. Radiat Prot Dosim. 1984;8(3):163-17l. http://rpd.oxfordjournals.org/content/8/3/163.

[13] Solecki AT, Śliwiński WR, Tchorz-Trzeciakiewicz DE. The Świebodzice and Intra-Sudetic basins - geosites of syn- and postorogenic Variscan molasse. In: Solecki AT, editor. Geoeducational Potential of the Sudety Mts. Wrocław: Drukarnia Argi Wrocła; 2008. http://geopark.org.pl/Rozne/geoeducationalpotential.pdf.

[14] IAEA. Guidelines for radioelement mapping using gamma ray spectrometry data. IAEA-TECDOC-136. 2003. http://www-pub.iaea.org/mtcd/publications/pdf/te_1363_web.pdf.

[15] Haydukiewicz A, Olszewski S, Porębski S, Teisseyre A. Szczegółowa mapa geologiczna Sudetów w skali 1:25000 [Detailed geological map of Sudety Mts. in the scale of 1:25000]. Wałbrzych: Arkusz Wałbrzych (Walbrzych sheet). Państwowy Instytut Geologiczny; 1982. http://sudety.pgi.gov.pl/Arkusze/as77.htm.
[16] Papastefanou C. Measurement of naturally occurring radionuclides with several detectors: advantages and disadvantages. In: Aycik GA, editor. NATO Science for Peace and Security. Series B: Physics and Biophysics 2009:221-246. http://www.australasiancancer.org/journal__/download-article.php?id=333.
[17] http://www.um.walbrzych.pl/sites/default/files/statystyka_i_gospodarka_gminy.pdf.

NATURALNE TŁO PROMIENIOWANIA GAMMA W PRZESTRZENI MIEJSKIEJ WAŁBRZYCHA

Instytut Nauk Geologicznych, Uniwersytet Wrocławski

Abstrakt: Wałbrzych jest drugim najludniejszym miastem województwa dolnośląskiego, liczącym ponad 117 tys. mieszkańców. Jest jednym z największych miast Sudetów, o powierzchni ok. 85 km^2. Pod względem geologicznym leży na styku trzech jednostek geologiczno-strukturalnych: bloku sowiogórskiego, depresji Świebodzic oraz niecki śródsudeckiej. Każdą z tych jednostek budują różnorodne skały, charakteryzujące się zróżnicowaną zawartością naturalnych pierwiastków promieniotwórczych, co sprawia, że moc dawki promieniowania gamma w powietrzu pochodząca od naturalnych radionuklidów rozproszonych w skałach podłoża i glebie waha się w szerokich granicach na terenie Wałbrzycha. Krajobraz miasta w dużej mierze ukształtowany jest przez działalność człowieka. Pozostałością po eksploatacji węgla kamiennego są 32 hałdy. Przeprowadzono gamma spektrometryczne badania naturalnego tła promieniotwórczego w przestrzeni miejskiej Wałbrzycha. Pomiary *in situ* były wykonywane przy pomocy przenośnego spektrometru gamma RS 230 o wymiarach 259 mm × 81 mm × 96 mm, wyposażonego w detektor BGO. Urządzenie podaje zawartość potasu K [%] oraz równoważne zawartości uranu eU [ppm] i toru eTh [ppm], a także moc dawki pochłoniętej w powietrzu na wysokości 1 metra generowanej przez te radionuklidy [nGy/h]. Badania składały się z dwóch etapów. W pierwszym zbadano zawartość K, eU i eTh w różnych typach skał podłoża, wykonując pomiary na 14 wychodniach różnowiekowych skał w obrębie trzech jednostek geologiczno-strukturalnych (od proterozoicznych gnejsów bloku sowiogórskiego po plejstoceńskie piaski i żwiry pokrywające depresję Świebodzic) oraz na hałdzie odpadów powęglowych. W drugim etapie zbadano przestrzenny rozkład zawartości naturalnych radionuklidów oraz mocy dawki promieniowania gamma na terenie miasta, wykonując 40 pomiarów w węzłach regularnej siatki o wielkości oczek 1,5 km. Uwzględniając fakt, że moc dawki promieniowania gamma w powietrzu kształtują głównie radionuklidy znajdujące się w 30-centymetrowej wierzchniej warstwie podłoża, zanotowano rodzaj pokrycia gruntu w badanych punktach. Przeprowadzone badania wykazały, że wśród skał występujących na terenie Wałbrzycha najbardziej radioaktywne są późnokarbońskie trachyandezyty odsłaniające się w starym kamieniołomie w dzielnicy Podgórze II (niecka śródsudecka). Zawartość K, eU i eTh wynosi średnio 3,8%, 4,0 i 18,3 ppm, odpowiednio, generując moc dawki pochłoniętej w powietrzu równą 121,2 nGy/h. Najniższą radioaktywnością charakteryzują się późnokarbońskie zlepieńce i piaskowce formacji z Glinika (niecka śródsudecka). Zawartość K, eU i eTh wynosi średnio 0,6%, 1,5 i 5,1 ppm, odpowiednio, generując moc dawki pochłoniętej w powietrzu równą 29,6 nGy/h. Analiza przestrzennego rozkładu mocy dawki pochłoniętej wykazała, że najwyższym tłem promieniowania gamma charakteryzuje się dzielnica Śródmieście oraz rejon zamku Książ. Moc dawki pochłoniętej o wartości ponad 100 nGy/h odnotowano w miejscach, w których grunt pokryty został kostką granitową. Najniższe tło promieniowania gamma zaobserwowano natomiast w punktach znajdujących się na obrzeżach miasta, w miejscach występowania względnie naturalnej gleby.

Słowa kluczowe: naturalne tło promieniotwórcze, promieniowanie gamma, potas, uran, tor, Sudety

DOI: 10.2429/proc.2016.10(1)007 2016;10(1)

Robert OLENIACZ[1], Mateusz RZESZUTEK[1] and Marek BOGACKI[1]

ASSESSMENT OF CHEMICAL TRANSFORMATION MODULES FOR SECONDARY INORGANIC AEROSOL FORMATION IN CALPUFF MODEL

OCENA MODUŁÓW PRZEMIAN CHEMICZNYCH TWORZENIA SIĘ WTÓRNYCH AEROZOLI NIEORGANICZNYCH W MODELU CALPUFF

Abstract: Air quality impact assessment is usually carried out with the application of simplified stationary dispersion models, which omit the chemical transformation process of air pollutants. Omission of this effect in the calculation process increases the uncertainty of the obtained results, and hinders the decision making process, related to air quality management. The paper presents a comparison of atmospheric dispersion modeling related to pollutants emitted from high industrial emitters, performed with and without consideration of various chemical transformation modules pertaining to the formation of inorganic aerosols, available in the CALMET/CALPUFF modeling system. A mechanism of inorganic aerosol formation in a liquid phase, considered in the ISORROPIA/RIVAD+AQUA module was observed to exert strong influence on calculation results referring to concentration levels of some air contaminants. The following was found out: more than a double decrease of the annual average concentration of SO_2, and even more significant increase (from 7 to 10 times) of the annual average concentration of PM10 (as a sum of primary and secondary particles) in comparison to other considered chemical transformation modules (MESOPUFF, RIVAD/ARM3, ISORROPIA/RIVAD), and a variant with a chemical transformation module switched off (without taking into account the secondary inorganic aerosol formation).

Keywords: air pollution, chemical transformations, secondary inorganic aerosols, atmospheric dispersion modeling, CALPUFF, ISORROPIA, RIVAD, MESOPUFF

Introduction

A significant role in the system of air quality management is played by methods of mathematic modeling of air pollutant dispersion. There are plenty of atmospheric dispersion models applied around the world, with various characteristics, and each country usually possesses its own model for regulatory purposes. Here, some stationary models, characterized by simplicity of spatial data preparation, which encompass, among others: AERMOD, ISC3, CTDMPLUS, OCD, ADMS, OML or AUSTAL [1, 2], as well as non-stationary models, capable of simulating meteorological conditions, variable in space and time, out of which the most popular are: WRF/Chem, CAMX, CMAQ, UAM-V and MCCM [3, 4]. The first group is usually applied in the system of air quality impact assessment, and it treats the chemical transformations, which apply mainly to NO_x chemistry, with simplicity, and omits reactions taking place on the boundary of the gas - liquid - solid states. The second group is characterized by a high level of requirements related to preparation of input data and high level of calculation costs. There are usually applied in the performance of complex air pollutant dispersion simulation in a mesoscale [2].

[1] AGH University of Science and Technology, Department of Environmental Management and Protection, al. A. Mickiewicza 30, 30-059 Krakow, Poland, email: oleniacz@agh.edu.pl
[*] Contribution was presented during ECOpole'15 Conference, Jarnoltowek, 14-16.10.2015

Particular attention is deserved by the CALMET/CALPUFF modeling system [5, 6], which may be successfully applied in the two cases mentioned above, and it is additionally provided with a relatively comprehensive module of chemical transformations, when compared to stationary models. As suggested by works [7, 8], the application of this module in a current version 6.42, should reflect the processes of chemical transformations taking place in the atmosphere in a more favorable manner. The CALMET/CALPUFF modeling system itself is recommended by the US EPA, for calculations carried out in the area not exceeding 50 km. In a specific situation, when a research field is characterized by a complicated landscape and meteorological conditions changing in time, this model may be applied in areas smaller than 50 km [9].

This paper includes an initial analysis of the importance for air quality impact assessment of chemical transformation modules of the secondary inorganic aerosol formation, available in the CALPUFF model. The simulations were carried out for a real object (a heat and power plant in Krakow, Poland), in 6 variants, to compare the effects of various modules of chemical transformation applications, and to determine the uncertainty level pertaining to the omission of this effect in evaluation of air quality influence. Previous works were mainly focused on validation and adjustment of the input settings of the model [10-13], and they did not pay any attention to consequences pertaining to evaluation of the influence exerted by the analyzed object on the air quality.

Purposeful and correct application of advanced atmospheric dispersion modeling systems, which consider chemical transformation modules, may bear special significance for areas, where standards for air quality are not followed, as it happens *eg* in the Krakow urban area [14]. In such a case, it greatly improves reliability of evaluation of influence on air quality, carried out for a given object, especially when it may pose the cause for excessive air pollution.

Methods

In calculations of atmospheric dispersion of pollutants performed within the scope of this work, the real data related to air emissions from two high point emitters that belong to the heat and power plant EDF Poland S.A. Branch No. 1 in Krakow, located near the city center of Krakow (South Poland), were applied. Regarding the character of the combusted fuels (mainly hard coal) and the installed power (460 MWe and 1118 MWt), this combined heat and power station constitutes one of the largest dust and gaseous emission sources, located in the vicinity of Krakow. Thus it has an important role in shaping the air quality in Krakow, especially in situations of abnormal boiler operating conditions (boiler startups) [15]. For the needs of this work, the data coming from the continuous emission monitoring system (pertaining to emissions of particulate matters, SO_2 and NO_x, and parameters of flue gases) from 2012 were applied, with a one-hour step. The results of manual measurements posed a basis for the assumption of air emissions for installations (boilers) startup phases. The basic data of the considered emitters are presented in Table 1.

The calculations were carried out in the CALMET/CALPUFF modeling system [5, 6], with and without consideration of various chemical transformation modules for the formation of secondary inorganic aerosols, including the ISORROPIA/RIVAD+AQUA module, available in the latest version of the CALPUFF program (ver. 6.42) [7, 8]. The

basic calculation domain was the 38 km × 26 km area, with grid resolution of 200 m. The topography and land cover data were obtained respectively from SRTM3 and CLC2006 databases. The spatial data were processed initially in the ArcGIS software, and in so called preprocessors of geophysical data, according to the procedure described in papers [16, 17]. Results of meteorological parameters observations were obtained from numerous sources for 2012. In total, 18 surface stations located within Krakow and its boundaries, together with 3 upper stations (Poprad, Legionowo, Wroclaw) were employed.

Table 1

Dimensions of the analyzed emitters, average parameters of flue gases and total air emissions in 2012

Emitter number	Stack dimensions		Average parameters of flue gases		Total annual emissions to air [Mg y^{-1}]		
	high [m]	diameter [m]	stack gas velocity [m s^{-1}]	temperature [K]	dust (PM)	SO_2	NO_x
E1	225	6.5	7.57	415	700	6505	4178
E2	260	7.0	7.77	406			

Afterwards, the three-dimensional fields of wind and temperature, together with a two-dimensional field of micro-climate parameters (PG stability class, mixing height, Monin-Obukhov length, friction velocity, convective velocity scale) were generated through the CALMET diagnostic model. CALMET model output data were then used as input for the CALPUFF model.

Table 2

A comparison of calculation variants, and their corresponding settings, input data, name of models and source materials

Variant	Settings		Background concentrations			NO_x emission	Model	Reference
	MCHEM	MAQ CHEM	NH_3	O_3	H_2O_2			
V1	0	0	-	-	-	NO_x	-	-
V2	1	0	month	1-hour	-	NO_x	MESOPUFF	[21-23]
V3	3	0	month	1-hour	-	NO/NO_2	RIVAD/ARM3	[24]
V4	6	0	month	1-hour	-	NO/NO_2	ISORROPIA/ RIVAD	[7, 8, 25-27]
V5	6	1	month	1-hour	season	NO/NO_2	ISORROPIA/ RIVAD+AQUA	
V6	6	1	month	month	season	NO/NO_2		

Calculations of atmospheric dispersion of air pollutants were carried out in 6 variants, including the variant without application of the chemical transformations module. The remaining variants differed among each other with application of MCHEM (chemical transformation module selection) and MAQCHEM (not including or including liquid state for the conversion of SO_2), and the introduced input data (Table 2). Variants 3-5 required determination of separate emission of NO and NO_2. Emission of these substances was estimated on the basis of results of NO_x emission measurements, assuming percentage shares of NO and NO_2 on the level of 95 and 5% respectively [18]. Particulate matter grain size fractions were determined on the basis of literature data [19]. Monthly average background concentrations of NH_3, indispensable during the process of calculations, were

determined on the basis of data coming from continuous monitoring carried out in stations of urban background in various European cities, and the H_2O_2 concentrations were assumed on the basis of a measurement campaign performed in Wroclaw [20]. Concentrations of ozone were introduced with 1-hour (variants V2-V5) or 1-month (variant V6) temporal resolution, on the basis of data coming from the urban background station situated in Krakow, at Bujaka street.

There were calculations of maximum 1-hour, 24-hour and annual average concentrations in the air at the land surface, carried out for NO, NO_2 (and/or NO_x), SO_2, primary particulate matter (PPM), secondary inorganic aerosol (NO_3, and SO_4), and the sum of secondary particulate matter (SPM), as well as total primary and secondary particulate matter (PPM+SPM) with consideration of fractions below 10 µm (PM10). The calculations results obtained for particular variants underwent a comparative analysis.

Results and discussion

Results of calculations of the highest values for maximum 1-hour and 24-hour concentrations and maximum and average annual concentrations of the analyzed substances, for a given area, obtained in the assumed computational field for particular variants, are presented in Tables 3 and 4.

Table 3

The highest values of maximum 1-hour and 24-hour concentrations in the air, obtained within the assumed computational area for particular variants

Air pollutant	The highest 1-hour average concentration in the variant [µg m^{-3}]						The highest 24-hour average concentration in the variant [µg m^{-3}]					
	V1	V2	V3	V4	V5	V6	V1	V2	V3	V4	V5	V6
NO	-	-	53.6	62.4	62.4	66.5	-	-	3.27	3.28	3.28	3.91
NO_2	-	-	165.8	162.7	162.6	138.6	-	-	20.51	20.50	20.50	20.30
NO_x (NO_2)	241.3	230.1	240.3	240.1	240.1	240.4	21.62	21.57	21.60	21.60	21.60	21.61
SO_2	582.1	576.8	581.1	581.2	491.3	492.4	34.09	33.72	34.01	34.03	33.22	33.22
PPM (PM10)	449.1	449.1	449.1	449.1	449.1	449.1	29.09	29.09	29.09	29.09	29.09	29.09
SPM (NO_3)	-	7.0	4.6	5.3	5.3	4.9	-	0.47	0.25	0.28	0.28	0.33
SPM (SO_4)	-	13.3	3.2	2.5	264.6	263.4	-	0.78	0.21	0.16	23.66	24.00
SPM (total)	-	20.3	5.6	5.7	264.6	263.4	-	1.18	0.36	0.33	23.66	24.01
PPM+SPM	449.1	449.3	449.1	449.1	466.4	466.0	29.09	29.11	29.10	29.10	31.87	31.78

It should be noticed that the highest values of maximum 1-hour and 24-hour concentrations, listed in Table 3, could exist in various spots of the computational area, and at a various time. Nevertheless, in case of all primary pollutants, maximum values of those concentrations for variants V1-V4 were obtained on the similar level, and in case of PPM and NO_x - the same or similar concentration values were also obtained for V5 and V6 variants.

As suggested by the presented data, application of various chemical transformation modules usually does not influence significantly the obtained results of calculations of the maximum 1-hour and 24-hour concentrations of NO and NO_2 in the air. However, it is possible to obtain an understated value for the highest of maximum 1-hour concentrations of NO_2 during application of the latest version of the CALPUFF model with the

ISORROPIA/RIVAD+AQUA module in ozone background, in a form of monthly average concentrations (variant V6), instead of 1-hour average concentrations (variant V5).

Table 4

The highest and mean values of annual average concentrations in the air, obtained within the assumed computational area for particular variants

Air pollutant	The highest annual average concentration in the variant [µg m^{-3}]						The mean of annual average concentrations in the variant [µg m^{-3}]					
	V1	V2	V3	V4	V5	V6	V1	V2	V3	V4	V5	V6
NO	-	-	0.369	0.371	0.371	0.429	-	-	0.024	0.025	0.025	0.027
NO_2	-	-	1.443	1.438	1.439	1.367	-	-	0.198	0.196	0.196	0.192
NO_x (NO_2)	1.999	1.980	1.993	1.992	1.993	1.993	0.240	0.222	0.235	0.234	0.234	0.233
SO_2	3.108	3.104	3.106	3.104	2.610	2.625	0.363	0.360	0.361	0.361	0.172	0.174
PPM (PM10)	0.307	0.307	0.307	0.307	0.307	0.307	0.028	0.028	0.028	0.028	0.028	0.028
SPM (NO_3)	-	0.019	0.010	0.005	0.005	0.006	-	0.006	0.003	0.001	0.001	0.002
SPM (SO_4)	-	0.013	0.008	0.006	1.955	1.952		0.005	0.003	0.002	0.250	0.249
SPM (total)	-	0.031	0.017	0.011	1.956	1.954	-	0.011	0.006	0.003	0.251	0.251
PPM+SPM	0.307	0.320	0.313	0.310	2.130	2.127	0.028	0.039	0.034	0.032	0.279	0.280

Application of chemical transformation modules for the analyzed objects did not exert any greater influence on the maximum 1-hour or 24-hour PM10 (PPM+SPM) concentrations measured in the air. It was caused by a fact that the maximum values were recorded in a situation of abnormal operating conditions of the installation (the boiler startup, with an electrostatic precipitator turned off), which was accompanied by significant dust emission, resulting in extremely high maximum values of PM10 concentration in air (PPM). In such a situation, omission of chemical transformation modules in the evaluation of this object impact on the air quality is not burdened with a high level of error, regarding an insignificant share of the secondary inorganic aerosols in the total level of PPM+SPM concentration in the air in that period. If the periods of boilers startups are not considered in calculations, it is possible to obtain great discrepancies between the calculations results of the maximum 1-hour and 24-hour concentrations of PM10 in the air, obtained with and without consideration of chemical transformation modules.

Great disproportions between the analyzed variants were obtained in case of calculation results for annual average concentration for PM10 and maximum 1-hour and annual average concentrations of SO_2. Omission of the chemical transformation module causes that results of evaluation of influence on air quality, carried out for sources, which emit these substances in significant amounts, will always be burdened with considerable uncertainty, and they may bear great differences when compared to the modeling results obtained with consideration of the inorganic aerosol creation module. In this case, special role is played by a module of chemical transformations in a liquid state, implemented in version 6.42 of the CALPUFF model, which intensifies the conversion process of SO_2 to sulfate forms. Omission of this effect in the process of atmospheric dispersion modeling may contribute to overprediction of SO_2 concentration calculations (to various degrees, depending on the average period), and significant underprediction of annual average PM10 concentrations in the air. For the object in consideration, the maximum 1-hour and annual average concentrations of SO_2 were overpredicted on the level of ca. 15-16%, regarding the reference variants (V5 and V6). More than double overprediction of annual SO_2

concentrations, and underprediction of maximum and average (in the computational area) annual average PM10 concentrations, by *ca* 7-10 times, was also obtained for the variant V1, V2, V3, and V4, in comparison with the variant V5 or V6. In particular variants, there were maximum annual concentrations of those substances in the air recorded also in other places, what is illustrated on the example of annual PM10 concentrations obtained for V1 and V5 variants in Figures 1 and 2.

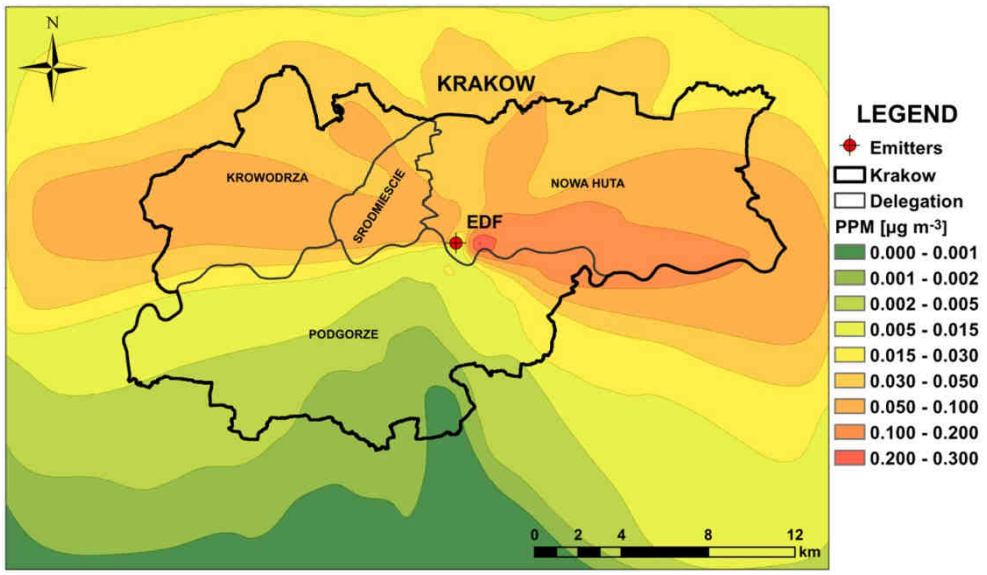

Fig. 1. Spatial distribution of annual average PM10 (PPM) concentrations in the air, obtained for the variant V1

SPM share in the total annual concentration of PM10 (PPM+SPM) is elevated along with an increase of distance from the emission source, what is especially observable in areas located along dominating wind directions, which are exposed to the influence of the analyzed object to the highest extent. Within the whole computational area, average SPM share in relation to the sum of annual average PPM+SPM concentrations for variants V2, V3, V4, V5 and V6 was as follows: 38.45; 25.70; 17.77; 90.08 and 90.10% respectively. Even greater shares of SPM in relation to PPM+SPM were present in case of the maximum values of annual concentrations, which were as follows for the variants mentioned above: 72.26; 53.28; 48.15; 95.96 and 95.95%. It proves large influence of SO_2 and NO_x emission of the analyzed object on the caused total level of annual concentrations of PM10 (PPM+SPM) in the air. In case of V5 and V6 variants, a surge of this influence was caused first of all by secondary inorganic aerosols, formed as a result of chemical transformations of SO_2 in the air, in a liquid state. What is more, in variants V4-V6, in comparison to variants V2 and V3, annual concentrations of secondary nitrate aerosols were significantly reduced. It results from the reduction or elimination of the phenomenon of overpredicting their concentrations, characteristic for MESOPUFF and RIVAD/ARM3 modules, presented among others in the paper [28].

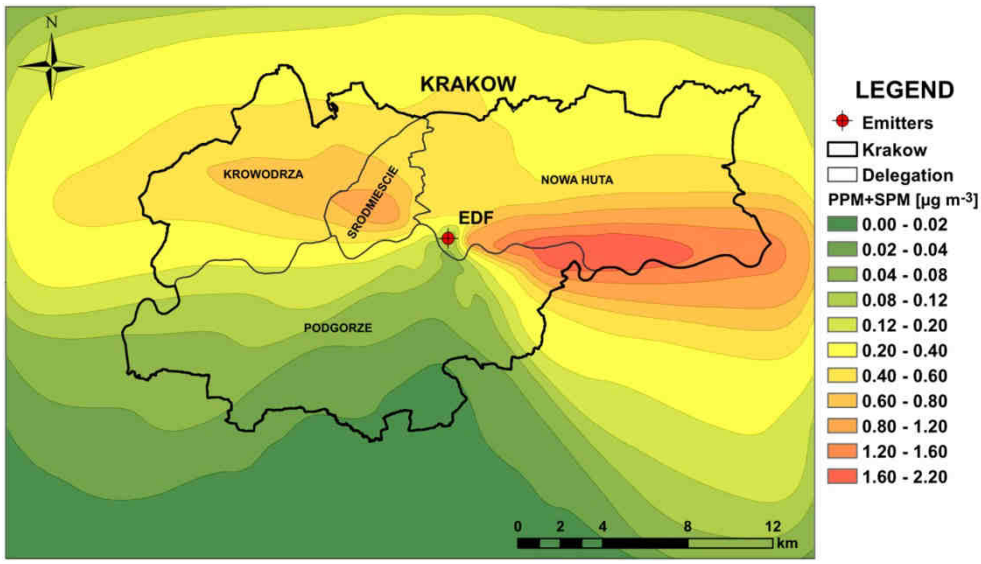

Fig. 2 Spatial distribution of annual average PM10 (PPM+SPM) concentrations in the air, obtained for the variant V5

Conclusions

Application of advanced atmospheric dispersion models for air quality impact assessment, allows to consider chemical transformation modules available in the model for air pollutants emitted from the analyzed emission source, including reactions that lead to formation of secondary inorganic aerosols. In the CALMET/CALPUFF modeling system, several features of chemical transformation modules may be applied for this purpose, including the following modules: MESOPUFF, RIVAD/ARM3, ISORROPIA/RIVAD and ISORROPIA/RIVAD+AQUA.

Calculations of pollutant dispersion in the air, carried out for a large combustion plant, with consideration of the CALMET/CALPUFF modeling system, allow to conclude that the chemical transformations modules exert no significant influence on calculations results for concentrations of NO, NO_2, and NO_x in the air. However, they may influence the calculation results for SO_2 and PM10 concentrations significantly, especially in case of applying the version 6.42 of the CALPUFF model with the ISORROPIA/RIVAD+AQUA module, taking conversion of SO_2 in a liquid phase into consideration [7, 8]. In calculations applying the model version mentioned above, maximum1-hour and annual average SO_2 concentrations were higher by *ca* 15-16%, and the annual average PM10 (primary and secondary particle matter) concentrations were at least 7 times higher, when compared to the remaining analyzed variants, including the one that does not consider the chemical transformations.

Therefore, omission of chemical transformations of the secondary inorganic aerosols in the process of atmospheric dispersion of air pollutants may lead to a wrong conclusion in the scope of evaluation of the emission sources impact on air quality, if SO_2 emission from

those sources is significant. If the CALPUFF model is applied for this evaluation, it is recommended to apply the ISORROPIA/RIVAD+AQUA module, allowing better reflection of the sulfate aerosol formation, hence to obtain more probable air concentrations of SO_2 and secondary particle matter. In this module, it is advisable to consideration of the ozone background with 1-hour temporal resolution, if such data are available. The use of monthly average concentration values may cause certain underprediction of maximum values of 1-hour and annual concentrations of NO_2 in the air. Moreover, application of the ISORROPIA/RIVAD or ISORROPIA/RIVAD+AQUA modules allows elimination the phenomenon of overprediction of secondary inorganic nitrate aerosols concentrations, characteristic for MESOPUFF and RIVAD/ARM3 modules.

Acknowledgments

The paper has been prepared within the scope of the AGH UST statutory research no. 11.11.150.008.

References

[1] Cimorelli AJ, Perry SG, Venkatram A, Weil JC, Paine RJ, Wilson RB, et al. A dispersion model for industrial source applications. Part I: General model formulation and boundary layer characterization. J Appl Meteorol. 2005;44(5):682-693. DOI: 10.1175/JAM2227.1.

[2] Holmes NS, Morawska L. A review of dispersion modelling and its application to the dispersion of particles: An overview of different dispersion models available. Atmos Environ. 2006;40:5902-5928. DOI: 10.1016/j.atmosenv.2006.06.003.

[3] Karamchandani P, Vijayaraghavan K, Yarwood G. Sub-grid scale plume modeling. Atmosphere (Basel). 2011;2(3):389-406. DOI: 10.3390/atmos2030389.

[4] Suppan P, Skouloudis A. Inter-comparison of two air quality modelling systems for a case study in Berlin. Int J Environ Pollut. 2003;20:75-84. DOI: 10.1504/IJEP.2003.004250.

[5] Scire JS, Robe FR, Fernau ME, Yamartino RJ. A user's guide for the CALMET meteorological model (Version 5). Concord, MA: Earth Tech, Inc; 2000. http://www.src.com/calpuff/download/CALMET_UsersGuide.pdf.

[6] Scire JS, Strimaitis DG, Yamartino RJ. A user' s guide for the CALPUFF dispersion model (Version 5). Concord, MA: Earth Tech, Inc; 2000. http://www.src.com/calpuff/download/CALPUFF_UsersGuide.pdf.

[7] Karamchandani P, Chen S-Y, Balmori R. Evaluation of original and improved versions of CALPUFF using the 1995 SWWYTAF data base. AER Report CP281-09-01 prepared for API, Washington, DC. San Francisco, CA: Atmospheric and Environmental Research, Inc.; 2009. http://mycommittees.api.org/rasa/amp/CALPUFF%20Projects%20and%20Studies/CALPUFF%20Evaluation%20with%20SWWYTAF,%202009,%20Kharamchandani%20et%20al.pdf.

[8] Karamchandani P, Chen S, Seigneur C. CALPUFF Chemistry Upgrade. AER Final Report CP277-07-01 prepared for API, Washington, DC. San Ramon, CA; Atmospheric & Environmental Research, Inc.; 2008. https://www3.epa.gov/ttn/scram/11thmodconf/200802-CALPUFF_Chemistry_Upgrade.pdf.

[9] U.S. EPA. Guideline on Air Quality Models: Revision to the Guideline on Air Quality Models: Adoption of a Preferred General Purpose (Flat and Complex Terrain) Dispersion Model and Other Revisions. Federal Register, 40 CFR Part 51, Appendix W. https://www3.epa.gov/scram001/guidance/guide/appw_05.pdf.

[10] Cui H, Yao R, Xu X, Xin C, Yang J. A tracer experiment study to evaluate the CALPUFF real time application in a near-field complex terrain setting. Atmos Environ. 2011;45(39):7525-7532. DOI: DOI:10.1016/j.atmosenv.2011.08.041.

[11] Dresser AL, Huizer RD. CALPUFF and AERMOD model validation study in the near field: Martins Creek revisited. J Air Waste Manage. Assoc. 2011;61(6):647-659. DOI: 10.3155/1047-3289.61.6.647.

[12] Brode RW. CALPUFF near-field validation. In: 10th US EPA Conference on Air Quality Modeling. Research Triangle Park, North Carolina, March 2012.

[13] Rood AS. Performance evaluation of AERMOD, CALPUFF, and legacy air dispersion models using the Winter Validation Tracer Study dataset. Atmos Environ. 2014;89:707-720. DOI: 10.1016/j.atmosenv.2014.02.054.
[14] Oleniacz R, Bogacki M, Rzeszutek M, Kot A. Meteorologiczne determinanty jakości powietrza w Krakowie. In: Konieczyński J, editor. Ochrona powietrza w teorii i praktyce, T. 2. Zabrze: IPIŚ PAN; 2014. DOI: 10.13140/RG.2.1.4200.3044.
[15] Apostoł M, Bąkowski A, Chronowska-Przywara K, Kot M, Monieta J, Oleniacz R, et al. Wybrane zagadnienia inżynierii mechanicznej, materiałowej i środowiskowej. Kraków: Wyd. Katedra Automatyzacji Procesów, Akademia Górniczo-Hutnicza; 2015. DOI: 10.13140/RG.2.1.2907.1440.
[16] Oleniacz R, Rzeszutek M. Determination of optimal spatial databases for the area of Poland to the calculation of air pollutant dispersion using the CALMET/CALPUFF model. Geomatics Environ Eng. 2014;8(2):57-69. DOI: 10.7494/geom.2014.8.2.57.
[17] Oleniacz R, Rzeszutek M. Assessment of the impact of spatial data on the results of air pollution dispersion modeling. Geoinformatica Polon. 2014;13:57-68. DOI: 10.2478/gein-2014-0006.
[18] U.S. EPA. AP42 Fifth Ed. Vol. 1, 1.1, 1998. http://www.epa.gov/ttn/chief/ap42/ch01/final/c01s01.pdf.
[19] U.S. EPA. AP42 Fifth Ed. Vol. 1, 1.1, 1993. http://www.epa.gov/ttn/chief/ap42/ch01/bgdocs/b01s01.pdf.
[20] Sówka I. Określenie czynników fizycznych i chemicznych determinujących zawartość substancji utleniających w atmosferze miejskiej. [PhD Thesis]: Wrocław: Politechnika Wrocławska; 2001.
[21] Stelson AW, Seinfeld JH. Relative humidity and temperature dependence of the ammonium nitrate dissociation constant. Atmos Environ. 1982;16:983-992. DOI: 10.1016/0004-6981(82)90184-6.
[22] Atkinson R, Lloyd AC, Winges L. An updated chemical mechanism for hydrocarbon/NO_x/SO_x photo oxidation suitable for inclusion in atmospheric simulation models. Atmos Environ. 1982,16:1341-1355. DOI: 10.1016/0004-6981(82)90055-5.
[23] Stelson AW, Bassett ME, Seinfeld JH. Thermodynamic equilibrium properties of aqueous solutions of nitrate, sulfate and ammonium. In: Teasley J, editor. Acid Precipitation, Chemistry of Particles, Fog and Rain. Woburn, MA: Ann Arbor Science; 1983.
[24] Morris RE, Kessler RC, Douglas SG, Styles KR, Moore GE. Rocky Mountain Acid Deposition Model Assessment: Acid Rain Mountain Mesoscale Model (ARM3). San Rafael, CA.: Systems Applications, Inc., U.S. EPA, Research Triangle Park, NC, Atmospheric Sciences Research Laboratory; 1988. https://ntrl.ntis.gov/NTRL/dashboard/searchResults/titleDetail/PB89124408.xhtml.
[25] Walcek CJ, Taylor GR. A theoretical method for computing vertical distributions of acidity and sulfate production within cumulus clouds. J Atmos Sci. 1986;43:339-355. DOI: 10.1175/1520-0469(1986)043<0339:ATMFCV>2.0.CO;2.
[26] Nenes A, Pandis SN, Pilinis C. ISORROPIA: A new thermodynamic equilibrium model for multiphase multicomponent inorganic aerosols. Aquatic Geochem. 1998;4(1):123-152. DOI: 10.1023/A:1009604003981.
[27] Fountoukis C, Nenes A. ISORROPIA II: a computationally efficient thermodynamic equilibrium model for K^+–Ca^{2+}–Mg^{2+}–$NH4^+$–Na^+–SO_4^{2-}–NO_3^-–Cl^-–H_2O aerosols. Atmos Chem Phys. 2007;7(17):4639-4659. DOI: 10.5194/acp-7-4639-2007.
[28] Scire JS, Strimaitis DG, Wu Z-X. New developments and evaluations of the CALPUFF model exponent. In: 10th EPA Conference on Air Quality Modeling. Research Triangle Park, North Carolina; 2012. https://www3.epa.gov/scram001/10thmodconf/presentations/3-5-CALPUFF_Improvements_Final.pdf.

OCENA MODUŁÓW PRZEMIAN CHEMICZNYCH TWORZENIA SIĘ WTÓRNYCH AEROZOLI NIEORGANICZNYCH W MODELU CALPUFF

AGH Akademia Górniczo-Hutnicza w Krakowie, Katedra Kształtowania i Ochrony Środowiska

Abstrakt: Ocena wpływu źródeł emisji na jakość powietrza wykonywana jest zwykle przy użyciu uproszczonych stacjonarnych modeli dyspersji, pomijających procesy przemian chemicznych zanieczyszczeń powietrza. Pominięcie tych efektów w procesie obliczeniowym powoduje zwiększenie niepewności uzyskanych wyników oraz utrudnia proces podejmowania prawidłowych decyzji związanych z zarządzaniem jakością powietrza. Praca przedstawia porównanie wyników modelowania dyspersji atmosferycznej zanieczyszczeń emitowanych z wysokich emitorów przemysłowych prowadzonych bez uwzględniania i z uwzględnianiem różnych modułów przemian chemicznych tworzenia się nieorganicznych aerozoli, dostępnych w systemie modelowania

CALMET/CALPUFF. Wykazano istotny wpływ mechanizmu tworzenia się wtórnego aerozolu nieorganicznego w fazie wodnej, uwzględnianego w module ISORROPIA/RIVAD+AQUA, na wyniki obliczeń poziomów stężeń niektórych zanieczyszczeń w powietrzu. Stwierdzono m.in. ponad 2-krotny spadek średniego poziomu stężeń średniorocznych SO_2 i jeszcze większy (od 7 do 10 razy) wzrost średnich wartości stężeń średniorocznych pyłu PM10 (suma cząstek pierwotnych i wtórnych) w porównaniu z innymi rozpatrywanymi modułami przemian chemicznych (MESOPUFF, RIVAD/ARM3, ISORROPIA/RIVAD) oraz wariantem z wyłączonym modułem przemian chemicznych (bez uwzględniania tworzenia się wtórnego aerozolu nieorganicznego).

Słowa kluczowe: zanieczyszczenie powietrza, przemiany chemiczne, wtórne aerozole nieorganiczne, modelowanie dyspersji atmosferycznej, CALPUFF, ISORROPIA, RIVAD, MESOPUFF

DOI: 10.2429/proc.2016.10(1)008 2016;10(1)

Barbara PIECZYKOLAN[1] and Izabela PŁONKA[1]

SORPTION PROCESS OF ACID YELLOW 36 ON SLUDGE-BASED ACTIVATED CARBON

SORPCJA BARWNIKA ACID YELLOW 36 ZA POMOCĄ WĘGLA AKTYWNEGO WYTWORZONEGO Z OSADU CZYNNEGO

Abstract: The study of sorption of dye Acid Yellow 36 on SAC (sludge-based activated carbon) was conducted. For this purpose, anaerobically digested and dewatered sewage sludge was dried at 105ºC to constant weight. Next this sludge was milled to a particle with a diameter of 0.5-1.0 mm and subjected to chemical activation by hydrogen peroxide. After oxidation process the sludge was subjected to thermal transformation in a muffle furnace at 600ºC. In this way obtained a powder activated carbon based on activated sludge (so-called SAC). Based on the results of the study the most favorable parameters of sorption process was achieved as follows: pH value equaled to 2.5 and reaction time equaled to 30 minutes. The linearized forms of Freundlich and Langmuir isotherms showed that the highest value of correlation factor was obtained in the case of Langmuir model. However, in this case, the negative value of constant isotherm was achieved. Therefore, it can be assumed that more accurately in this case is the Freundlich model or other model which was not examined during that studies.

Keywords: sewage sludge, activated carbon, dyes, sorption isotherm, sorption kinetic, Freundlich isotherm, Langmuir isotherm

Introduction

The synthetic dyes are widely used in different kind of industry such as textile, leather, paint, etc. therefore during production a colored wastewater are generated. That wastewater has to be purified and uncolored. Some dyes used in industry are toxic to the water environment. The can also be carcinogenic. The process of photosynthesis may be disturbed as a result of the discharge the untreated colored wastewater into the receiver.

The Acid Yellow 36 is one of that kind of dye which has negative impact on water environment. It has the very toxic and carcinogenic properties. Moreover the dye involves negatively on fishes. The mortality, the loss of weight, changes in body colours and restlessness of fishes during the toxicity tests were observed. Moreover, it has an adverse effect on the nervous system of fishes causing involuntary movements of their body. The Acid Yellow 36 is widely used in paper, soap, tannery, cosmetics, wax, polishes and many others industries [1, 2].

There are many different methods used for treatment of colored wastewater. These methods include: membrane techniques [3, 4], sorption [5] and advanced oxidation processes [6, 7]. The sorption has high efficiency, low-cost, availability, and is easy to design. The most often applied sorbent is the activated carbon. It has a very high efficiency however this sorbent is also very expensive. Therefore, the adsorbents produced from wastes are more and more often examined. That kind of sorbents are much cheaper. The wastes such as waste paper [8], kernel plum [9], rice hull [10], olive cake [11], corncob

[1] Faculty of Energy and Environmental Engineering, Silesian University of Technology, ul. S. Konarskiego 18, 44-100 Gliwice, Poland, phone +48 32 237 16 98, fax +48 32 237 10 47, email: barbara.pieczykolan@polsl.pl, rie4@polsl.pl

* Contribution was presented during ECOpole'15 Conference, Jarnoltowek, 14-16.10.2015

[12], apricot stone [13], date stone [14] and coconut husk [15] may be used as sorbents. During the last few years the studies of application of sewage sludge as a sorbent are carrying out. The digested sewage sludge (both anaerobically and aerobically) can be used to produce so called "sludge-based activated carbon". The kind of application of the sewage sludge is also the new way of utilization of that waste. Nowadays the sewage sludge is mainly used as a fertilizer for soil amendment. However, the amount of the sites at which the sewage sludge can be applied is limited. Thus, the use of sewage sludge for production of activated carbon can be an alternative method of final management of that waste.

The isotherm of sorption is used in order to examine that process. Equilibrium relationships between sorbent and sorbate are described by sorption isotherms. The ratio between the quantity sorbed and that remaining in the solution at a fixed temperature at equilibrium describes the sorption isotherm [16, 17].

There are several isotherm models available for analyzing experimental data and for describing the equilibrium of adsorption. The most commonly models used for examination of dye adsorption process are the Freundlich isotherm and Langmuir isotherm [18-21]. The Freundlich isotherm is the earliest known relationship describing the sorption equation. This fairly satisfactory empirical isotherm can be used for non-ideal sorption that involves heterogeneous sorption. The theoretical Langmuir isotherm is often used to describe sorption of a solute from a liquid solution. The development of the Langmuir isotherm assumes monolayer adsorption on a homogenous surface.

The results of the studies of sorption process of dye Acid Yellow 36 are presented in that publication. During the tests the most favorable pH value and reaction time were established. Moreover as a result of the studies the isotherm of sorption was examined according two models: Freundlich and Langmuir.

Experimental

Material of sorbent

During the sorption process an anaerobically digested and dewatered sewage sludge (mixture of excess and raw sludge) was used. It was transformed into sludge-based activated carbon by chemical activation and next combustion in muffle furnace. The sludge was dried into constant mass in 105ºC and milled in laboratory grinder to a particle with a diameter of 0.5-1.0 mm. A hydrogen peroxide was used for chemical activation. Next the sludge was combusted in two stages in muffle furnace. First step was carried out in temperature of 300ºC and next a temperature was risen up to 600ºC. The combustion in both temperatures was carried out by 45 minutes.

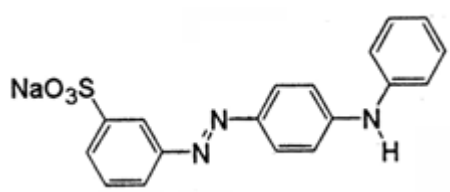

Fig. 1. The chemical structure of Acid Yellow 36 [22]

During the studies an anionic dye Acid Yellow 36 was used (Fig. 1). The working solution of the dye had a concentration equaled to 5 g/dm^3.

Sorption process

The tests of sorption of the dye Acid Yellow 36 was carried out in a static system. The sample of activated carbon (based on the sewage sludge) in a weight of 0.1 g was placed in a closed Erlenmeyer flasks with a capacity of 50 cm^3. During the study a working solution of Acid Yellow 36 witch concentration was equaled to 5 g/dm^3 was used. A suitable amount of working solution of the dye was added into distilled water to obtain required concentration of the Acid Yellow 36. The flasks were placed on a laboratory shaker to ensure constant stirring the contents. The concentration of the dye after sorption process was determined by photometric measurement on the basis of the calibration curve.

Impact of pH value

During the first stage of study the most favorable pH value of the process was chosen. The tests were conducted by using six different value of pH of the dye solutions: 2.5; 4.0; 5.5; 8.5. During that tests the solution of the dye was the same for each sample and was equaled to 70 mg/dm^3. The sorption process was conducted by one hour and after that time the concentration of Acid Yellow 36 was measured in each sample.

Contact time

In order to choose the most favorable sorption time the tests were carried out in different contact times. During that phase of study the concentration of the dye and the pH value of each samples were the same and were equaled to 70 mg/dm^3 and 2.5 respectively. The value of pH was chosen during the first stage of the study.

Sorption isotherm

In the last phase of the tests the isotherm of sorption of the dye on SAC (sludge-based activated carbon) was conducted. In order to obtain that goal, sorption process was carried out for different concentration of Acid Yellow 36. However the sorption time and value of pH were the same for each sample (chose during earlier steps of study).

Based on the results of sorption isotherm, two models of sorption process were analyzed. The Freundlich isotherm is expressed by the following empirical equation (1):

$$q_e = K_F \cdot C_e^n \tag{1}$$

where K_F is the Freundlich adsorption constant [dm^3/g] and n is a measure of the adsorption intensity. This equation is usually linearized in order to determine K_F and n constants. As a result of taking the logarithm of both sides of equation a linear form is obtained (Eq. (2)):

$$\log q_e = \log K_F + n \cdot \log C_e \tag{2}$$

The Langmuir isotherm is expressed by the following equation (3):

$$q_e = \frac{q_m \cdot C_e \cdot K_a}{1 + K_a \cdot C_e} \tag{3}$$

where C_e is the equilibrium concentration [mg/dm^3], q_e the amount adsorbed [mg/g], q_m is q_e for complete monolayer adsorption capacity [mg/g], and K_a is the equilibrium adsorption constant [dm^3/mg]. The linear forms of that equation are expressed as equations (4), (5) and (6):

$$\frac{C_e}{q_e} = \frac{1}{q_m} \cdot C_e + \frac{1}{K_a \cdot q_m} \tag{4}$$

$$\frac{1}{q_e} = \left(\frac{1}{K_a \cdot q_m}\right) \cdot \frac{1}{C_e} + \frac{1}{q_m} \tag{5}$$

$$q_e = q_m - \left(\frac{1}{K_a}\right) \cdot \frac{q_e}{C_e} \tag{6}$$

Results and discussion

Impact of pH value

The tests has shown, that the value of pH of solution during sorption process is very important. It can be observed that as the value of pH increased the effectiveness of sorption process decreased. The smallest concentration of the dye was obtained when the pH value was equaled to 2.5 (Fig. 2). An increase of pH value to 4.0 caused an increase of content of Acid Yellow 36 up to 69.8 mg/dm^3. In the case of other pH value the concentration of Acid Yellow 36 did not significantly change and were in the range of 69.6-69.9 mg/dm^3. This phenomenon could prove that the SAC (used during that research) has negative electric charge of its surface. The Acid Yellow is also an anionic dye. Therefore the use of such a low pH value (what is connected with large amount of hydrogen ions) caused the change of electric charge of SAC surface. The sorption of the dye was thus possible by obtaining a positive surface charge of the SAC.

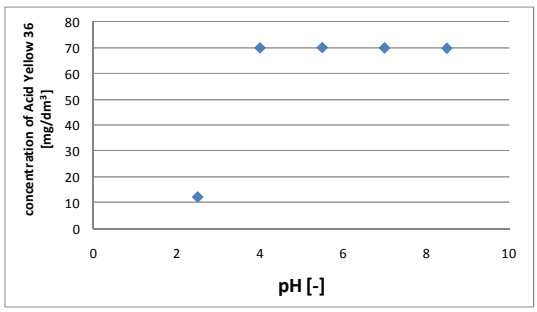

Fig. 2. The impact of pH value on efficiency of dye adsorption

Impact of contact time

Based on the results obtained during the first stage of the study, the impact of contact time of the dye solution with SAC on sorption efficiency was examined.

It could be observed (Fig. 3) that after 30 minutes of contact the SAC with the dye solution the effectiveness of dye sorption obtained the very high level and was equaled to 83.4%. Further increasing the contact time did not significantly improve the efficiency.

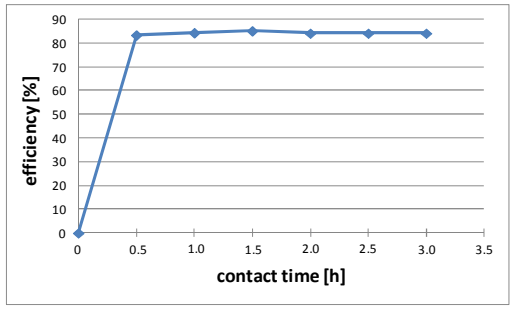

Fig. 3. The impact of contact time on color removal efficiency

Sorption isotherm

During the third stage of the study the isotherm of sorption was examined. Following process parameters were used at that tests: 2 g_{SAC}/dm^3, pH 2.5 and contact time equaled to 30 minutes. The concentration of the dye was in the range of 10-160 mg/dm^3.

Table 1

Parameters of sorption isotherms

Freundlich		**Langmuir**	
K_F [dm^3/g]	1.1071	K_a [dm^3/g]	–0.019
n [-]	1.4622	q_m [mg/g]	–133.3
R^2[-]	0.9314	R^2 [-]	0.9677

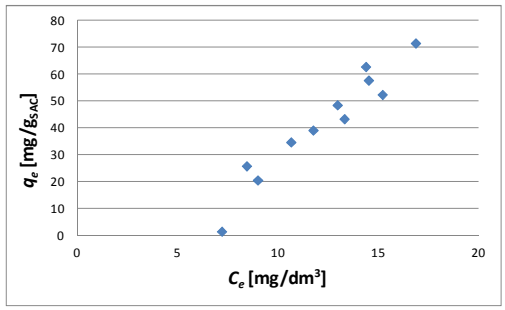

Fig. 4. Sorption isotherm

As a result of that tests the graph of isotherm was plotted (Fig. 4). Moreover, the models of Freundlich and Langmuir were examined. The graph of linearized forms of that models were plotted (Figs. 5a-d). In the case of all prepared graph, the correlation factors were calculated. In the case of Langmuir model the q_m (complete monolayer adsorption capacity [mg/g]), and K_a (the equilibrium adsorption [dm^3/g]) were established for that linearized form which graph obtained the highest correlation factor R^2. The correlation factors and other parameters for Freundlich and Langmuir isotherm are presented in Table 1.

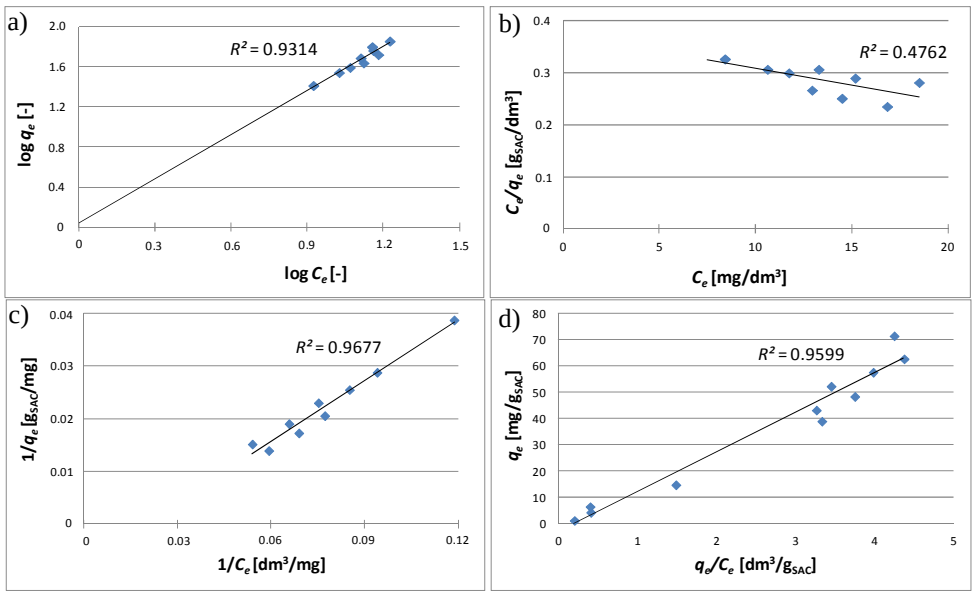

Fig. 5. The linearized forms of isotherm models: a) Freundlich, b) Langmuir according eq. (4), c) Langmuir according eq. (5), d) Langmuir according eq. (6)

Conclusions

1. The study showed that the sewage sludge may be a material from which an activated carbon can be produced. It was also proved that this kind of activated carbon may be used for removal the dye Acid Yellow 36 from its aqueous solution.
2. The most favorable pH value was equaled to 2.5. It can be concluded that the electric charge of SAC is negative. Therefore it was necessary to change the surface charge of the SAC by decreasing pH value.
3. Based on the results of the study it is observed that the adsorption of the dye on the SAC occurred in the first 30 minutes of the process.
4. The study showed that the highest value of correlation factor of linearized forms was obtained in the case of Langmuir model. However in that case the value of q_m was negative. Therefore, it can be assumed that more accurately in this case is the Freundlich model or other model which was not examined during that studies.

References

[1] Malik PK. Dyes Pigments. 2003;56:239-249. DOI: 10.1016/S0143-7208(02)00159-6.
[2] Clarke CE, Kielar F, Johnson KL. J Hazard Mater. 2013;246-247;310-318. DOI: 10.1016/j.jhazmat.2012.12.018.
[3] Buonomenna MG, Gordano A, Golemme G, Drioli E. React Funct Polym. 2009;69:259-263. DOI: 10.1016/j.reactfunctpolym.2009.01.004.
[4] Saffaj N, Persin M, Alami-Younssi S, Albizane A, Bouhria M, Loukili H, et al. Sep Purif Technol. 2005;47:36-42. DOI: 10.1016/j.seppur.2005.05.012.
[5] Ko DCK, Porter JF, Mckay G. Adsorption. 2002;8:171-188. DOI: 10.1023/A:1021283731952.

[6] Hsing HJ, Chiang PC, Chang EE, Chen M. J Hazard Mater. 2007;141:8-16. DOI: 10.1016/j.jhazmat.2006.05.122.
[7] Szpyrkowicz L, Juzzolino C, Kaul SN. Water Res. 2001;35:2129-2136. DOI: 10.1016/S0043-1354(00)00487-5.
[8] Okada K, Yamamoto N, Kameshima Y, Yasumori A. J Colloid Interface Sci. 2003;262:179-193. DOI: 10.1016/S0021-9797(03)00107-3.
[9] Juang RS, Wu FC, Tseng RL. J Colloid Interface Sci. 2000;227:437-444. DOI: 10.1006/jcis.2000.6912.
[10] Guo YP, Rockstraw DA. Micropor Mesopor Mater. 2007;100:12-19. DOI: 10.1016/j.micromeso.2006.10.006.
[11] Aljundi IH, Jarrah NJ. Anal Appl Pyrolysis. 2008;81:33-36. DOI: 10.1016/j.jaap.2007.07.006.
[12] Tseng RL, Tseng SK, Wu FC. Colloids Surf A. 2006;279:69-78. DOI: 10.1016/j.colsurfa.2005.12.042.
[13] Karagozoglu B, Tasdemir M, Demirbas E, Kobya M. J Hazard Mater. 2007;147:297-306. DOI: 10.1016/j.jhazmat.2007.01.003.
[14] Bouchelta C, Medjram MS, Bertrand O, Bellat JP. J Anal Appl Pyrolysis. 2008;82:70-77. DOI: 10.1016/j.jaap.2007.12.009.
[15] Tan IAW, Ahmad AL, Hameed BH. J Hazard Mater. 2008;154:337-346. DOI: 10.1016/j.jhazmat.2007.10.031.
[16] Turabik M. J Hazard Mater. 2008;158:52-64. DOI: 10.1016/j.jhazmat.2008.01.033.
[17] Crini G, Badot PM. Prog Polym Sci. 2008;33:399-447. DOI: 10.1016/j.progpolymsci.2007.11.001.
[18] Hameed BH, El- Khaiary MI. J Hazard Mater. 2008;154:639-648. DOI: 10.1016/j.jhazmat.2007.10.081.
[19] Ho YS, Chiu WT, Wang CC. Biores Techn. 2005;96:1285-1291. DOI: 10.1016/j.biortech.2004.10.021.
[20] Carrillo F, Lis MJ, Valldeperas J. Dyes and Pigments. 2002;53:129-136. DOI: 10.1016/S0143-7208(02)00007-4.
[21] Tehrani-Bagha AR, Nikkar H, Mahmoodi NM, Markazi M, Menger FM. Desal. 2011;266:274-280. DOI: 10.1016/j.desal.2010.08.036.
[22] http://www.worlddyevariety.com/acid-dyes/acid-yellow-36.html.

SORPCJA BARWNIKA ACID YELLOW 36 ZA POMOCĄ WĘGLA AKTYWNEGO WYTWORZONEGO Z OSADU CZYNNEGO

Instytut Inżynierii Wody i Ścieków, Wydział Inżynierii Środowiska i Energetyki, Politechnika Śląska, Gliwice

Abstrakt: Przeprowadzono badania sorpcji barwnika Acid Yellow 36 z użyciem węgla aktywnego bazującego na osadzie ściekowym. W tym celu ustabilizowany beztlenowo i odwodniony osad czynny wysuszono w 105ºC do stałej masy. Następnie osad ten zmielono do ziaren o średnicy 0,5-1,0 mm i poddano chemicznej aktywacji za pomocą nadtlenku wodoru. Po tym procesie osad spalono w piecu muflowym w 600ºC, uzyskując w ten sposób pylisty węgiel aktywny bazujący na osadzie czynnym (tzw. SAC - czyli „sludge-based activated carbon"). Dla tak spreparowanego węgla aktywnego przeprowadzono badania procesu sorpcji statycznej względem barwnika Acid Yellow 36. Na podstawie przeprowadzonych eksperymentów stwierdzono, że najkorzystniejsza wartość pH wynosi 2,5, a czas kontaktu jest równy 30 minut. Natomiast bazując na graficznych formach zlinearyzowanych modelów sorpcji według Langmuira i Freundlicha, stwierdzono, że największą wartość współczynnika korelacji odnotowano w przypadku zlinearyzowanej formy równania Langmuira. Jednakże w tym przypadku uzyskano ujemne wartości stałych izotermy, dlatego można przypuszczać, że jednak bardziej prawidłowy jest model Freundlicha lub inny rodzaj izotermy, który nie był analizowany w toku tych badań.

Słowa kluczowe: osad czynny, węgiel aktywny, barwniki, izoterma sorpcji, kinetyka sorpcji, izoterma Fruendlicha, izoterma Langmuira

DOI: 10.2429/proc.2016.10(1)009 2016;10(1)

Agata ROSIŃSKA[1]

INFLUENCE OF SELECTED COAGULANTS OF INDICATOR AND DIOXIN-LIKE PCB REMOVAL FROM DRINKING WATER

WPŁYW WYBRANYCH KOAGULANTÓW NA USUWANIE WSKAŹNIKOWYCH I DIOKSYNOPODOBNYCH PCB Z WODY PRZEZNACZONEJ DO SPOŻYCIA

Abstract: The aim of the research was to compare selected coagulants efficiency in indicator and chosen dioxin-like PCB removal from surface water. As coagulants, there were used aluminium sulfate and 5 hydrolyzed polyaluminium chlorides, with trade names: PAX-XL1, PAX-XL10, PAX-XL19, PAX-XL60, PAX-XL69. For the research, surface water was used, collected from dam reservoir. The water composition was modified with standard mixtures PCB MIX24 and MIX13, in order to obtain concentration of each congener equal to 300 ng/dm^3. The PCB MIX24 mixture was composed of indicator congeners solution: 28, 52, 101, 118, 138, 153, and 180, whereas the MIX13 mixture - solution of three dioxin-like PCB 77, PCB 126, and PCB 169. It was demonstrated that the application of aluminium sulfate allowed for reaching better effects for purifying water of PCB, than with the usage of pre-hydrolyzed salts, polyaluminium chlorides. Out of the studied coagulants, the best effects for indicator PCB removal were obtained with the application of aluminium sulfate, total PCB concentration was decreased by 65%. The highest efficiency for indicator congeners removal (90%) was obtained for PCB 138 and 153. After the application of hydrolyzed polyaluminium chlorides PAX-XL1, PAX-XL10 decrease in higher chlorinated PCB concentration was obtained, in the range of 23 to 74%. Selectivity of chosen PCB congener removal, depending on applied coagulant, was demonstrated; with the usage of aluminium sulfate, removal of heptachlorobiphenyl PCB 180 at the level of 34% was obtained, whereas with the application of PAX-XL1 and PAX-XL10 higher reduction efficiency for this congener was obtained, *ie* 83 and 74% respectively. For dioxin-like PCB, after application of aluminium sulfate, total concentration reduction by 74% was obtained, efficiency of this congeners removal amounted to from 54 (PCB 77) up to 72% (PCB 126), similar results were obtained after the usage of PAX-XL1. The lowest PCB removal from water rate was stated for coagulants PAX-XL60 and PAX-XL69.

Keywords: polychlorinated biphenyls, coagulation, aluminium sulphate, hydrolyzed polyaluminium chlorides, removal efficiency, drinking water

Introduction

In recent years, significant increase in interest in micropollutants present in water can be observed. For this purpose, further normative quality indicators for drinking water and water for economical purposes are being introduced in proper pieces of legislation. Moreover, worldwide tendency can be observed to reduce their permissible concentration to a level, at which no pathological changes in water consumers are discovered. Micropollutants occurring in water are divided into several categories, one of the classification is division into organic micropollutants (*eg* polycyclic aromatic hydrocarbons, polychlorinated biphenyls, surface active substances, pesticides) and inorganic micropollutants, primarily heavy metals [1-3].

[1] Department of Chemistry, Water and Wastewater Technology, Faculty of Infrastructure and Environment, Czestochowa University of Technology, ul. J. H. Dąbrowskiego 69, 42-200 Częstochowa, Poland, phone +48 34 325 04 96, email: rosinska@is.pcz.czest.pl
[*] Contribution was presented during ECOpole'15 Conference, Jarnoltowek, 14-16.10.2015

209 polychlorinated biphenyl (PCB) congeners are known, a number of which are characterized by high bioaccumulation, toxicity or potential carcinogenicity, and simultaneously high persistence in the environment. So called dioxin-like PCB, which include coplanar congeners with codes: 77, 81, 126, 169, are considered to be the most toxic [4]. Three of them (PCB 77, PCB 126 and PCB 169) are spatial analogues of the most toxic dioxin, *ie* 2,3,7,8-tetrachlorodibenzo-p-dioxin (TCDD). According to the U.S. Environmental Protection Agency, 7 indicator congeners should be determined in the environment, with codes: 28, 52, 101, 118, 138, 153, and 180. Water ecosystems pollution occurs indirectly (from the atmosphere) or directly (discharge of waste water containing PCB, run-off from fields, leakages from transformers and condensers, landfills). Because of hydrophobic properties, PCB have a strong tendency to transition from liquid phase to phases with higher hydrophobicity, *eg* through bioaccumulation or sorption, by binding to sediment particles or to suspended solids present in water [5].

Negative influence of micropollutants on water consumers health causes the need to remove these substances from drinking water. The choice of micropollutant removal processes is determined by their type, properties, and form of occurrence. Current literature reports emphasize the need for basic research regarding the removal mechanism of trace organic pollutants, using different coagulants. In recent years the use of new generation coagulants, with high efficiency, can be observed [1]. These coagulants reflect the properties of trace organic pollutants which are being removed (*eg* hydrophobicity, charge, polarizability, the presence of particular functional groups). It was also demonstrated that combined processes have a high efficiency in removal of organic micropollutants from water [6, 7]. In the literature there are few examples of research regarding PCB removal from contaminated surface water. Due to the similarities in chemical properties of PCB and PCDD, for removing polychlorinated biphenyls from water, research developments in PCDD/Fs removal [7] can be used.

PCB pollution monitoring is particularly important for reservoirs, which are sources of drinking water for supplying the population. Research conducted in 2009-2011 for chosen water reservoir in Poland, which is the source of water for water treatment plant, showed that the water and the bottom sediments are contaminated with PCB [8]. The scope of PCB concentration in the reservoir water ranged from 1.0 to 8.1 ng/dm^3, whereas the concentration of these compounds in the bottom sediments ranged from 0.12 to 2.78 µg/kg. The most commonly used coagulant in water treatment plants in Poland is aluminium sulphate $Al_2(SO_4)_3$. Also, there are studies conducted regarding the application of pre-hydrolyzed coagulants, *ia* polyaluminium chlorides with general formula $Al_n(OH)_mCl_{3n-m}$. The mechanism of coagulation with aluminium salts, non-hydrolyzed and pre-hydrolyzed, is the same, however the presence of aluminium polymeric forms in polyaluminium chloride solutions cause them to be more stable in water, resulting in more efficient removal of pollutants [1, 9].

The aim of this research was to compare the efficiency of chosen coagulants in removal of indicator and dioxin-like PCB from surface water.

Materials and methods

Research material

Kozlowa Gora water reservoir is created by damming the river Brynica. It is located on the south-eastern edge of Swierklaniec municipality. It occupies an area of approx. 5.5 km^2, its capacity equals to approx. 13 millions m^3, and its average depth is 4.5 m. Currently it constitutes water source for water treatment plant in Wymyslow, which belongs to Gornoslaskie Przedsiebiorstwo Wodociagow. The reservoir also fulfils flood prevention objectives, and it is used, to a limited extend, for touristic and recreational purposes.

Water from the reservoir, sampled in November 2011, was used for the research. Positions were situated in southern, outlet (by the dam) part of the reservoir. At each measuring point, 20 dm^3 of water was collected. The water composition was modified in order to obtain concentration of each PCB congener equal to 400 and 300 ng/dm^3 respectively, by introducing to water appropriate amounts of standard solutions - PCB MIX 13 and MIX 24.

As the coagulants there were used $Al_2(SO_4)\cdot 18H_2O$ produced by Przedsiebiorstwo Handlowe Polskie Odczynniki Chemiczne in Gliwice, and five hydrolyzed polyaluminium chlorides with trade names Kemira: PAX-XL1, PAX-XL10, PAX-XL19, PAX-XL60, PAX-XL69 produced by KEMIPOL in Police. Commercial solutions of polyaluminium chlorides were characterized by alkalinity equal to respectively 70 ±5%; 70 ±10%; 85 ±5%; 40 ±10%; 60 ±10%; 85 ±5%, and contained respectively 10.0 ±0.6%; 9.4 ±0.4%; 9.4 ±0.4%; 14.4 ±0.6%, and 11.3 ±0.9% of Al_2O_3 [10]. For the research, 1% solution of aluminium sulphate, and solutions of polyaluminium chlorides were prepared, by diluting commercial products so that they contained 1.0 g Al/dm^3.

Coagulation process

The coagulation process was conducted in glass vessels, to each 2 dm^3 of studied water was measured. The coagulants were introduced in the amount of 4 mg Al/dm^3, and fast stirring was performed for 2 minutes (applying 250 rpm) with the use of mechanical stirrer. Next slow stirring (20 rpm) was conducted for 15 minutes. After this time the samples were subjected to 1-hour sedimentation. Then 0.7 dm^3 of water was decanted. Before and after the coagulation process, water analysis was performed, including determination of: pH, turbidity, colour, total organic carbon (TOC), and PCB analysis [8, 11].

Analysis methodology

For the PCB analysis, hexane was added to 0.5 dm^3 of sampled water, and it was stirred with magnetic stirrer. Next, after separation of hexane fraction in a separator, the solution was mixed with fresh batch of hexane. Hexane extracts were combined. The extract was dried by seeping it through a layer of anhydrous Na_2SO_4. Hexane was evaporated near to dryness from the dried extract under vacuum, and it was poured into a tube. The flask was further washed with hexane, and combined with the solution, and then transferred into the tube. For mineralization of organic compounds, obtained solution was shaken with concentrated H_2SO_4. After separation of the mixture, 5% solution of KOH in ethanol was added to hexane layer. The tube was closed tightly and heated in a water bath.

After cooling, ethanol-water solution was added (1:1, v/v). Next, the hexane layer was separated, which was concentrated in a vacuum evaporator to a volume of 1 cm^3. The obtained extracts were analyzed qualitatively and quantitatively by means of capillary gas chromatography with mass spectrometry (CGC/MS) according to literature data [12]. For the chromatographic analysis there were used standards by dr Ehrenstorfer company, *ie* PCB MIX24 mixture, which was a solution of indicator congeners: 28, 52, 101, 118, 138, 153 and 180, and PCB MIX13 solution, which contained three coplanar PCB congeners with codes: 77, 126 and 169. For their chromatographic separation, a DB-5 column was used. For detection, quadrupole mass spectrometer MS 800 by Fisons was used, which was operating in a selective ion monitoring mode. PCB quantification was achieved by single ion monitoring (SIM) [13].

Results and discussion

The analysed surface water had slightly alkaline pH (7.9), colour equal to 30 mg Pt/dm^3, and turbidity of 17 NTU [8].

Total concentration of indicator and dioxin-like PCB in sampled water was low and amounted to 32.3 and 4.7 ng/dm^3 respectively. Research results of PCB removal from water, for the coagulant dose of 4 mg Al/dm^3 with additional amount of standard solutions of indicator and dioxin-like PCB are presented in Table 1.

Table 1

PCB concentration in modified surface water after coagulation process

Congeners	Concentration [ng/dm^3]					
	$Al_2(SO_4)_3$	PAX-XL1	PAX-XL10	PAX-XL19	PAX-XL60	PAX-XL69
Indicator						
PCB 28	165.7	178.9	186.3	285.9	290,4	287.9
PCB 52	159.2	174.4	180.4	261.9	272.5	274.8
PCB 101	62.0	146.4	157.5	185.5	210.8	215. 6
PCB 118	44.1	125.6	138.9	164.0	195.3	202.7
PCB 138	31.4	89.0	95.3	134.9	180.5	192.6
PCB 153	31.3	240	235.9	230.0	252.0	263.0
PCB 180	198.0	52.1	78.7	118.8	164..6	170.3
Dioxin-like						
PCB 77	138.0	140.6	179.7	236.3	262.1	260.0
PCB 126	84.5	74.9	119.4	179.5	211.7	214.3
PCB 169	90.0	110.7	173.2	180.3	184.9	187.5

Out of studied coagulants better effects of indicator PCB removal were obtained after the usage of aluminium sulphate, total PCB concentration decreased by 65%. The highest efficiency of indicator congener removal was obtained for PCB 138 and 153, which amounted to 90% (Fig. 1). The concentrations of other PCB were reduced in the range of 85 (PCB 118) to 34% (PCB 180).

Among hydrolyzed polyaluminium chlorides, the best results of indicator PCB removal were obtained after application of PAX-XL1 and PAX-XL10. For these coagulants, decrease in total PCB concentration by 53 and 50% respectively was obtained.

Greater reduction of higher chlorinated congener, *ie* PCB 180, 138 and 118, concentration was achieved, in the range of 54 to 83%.

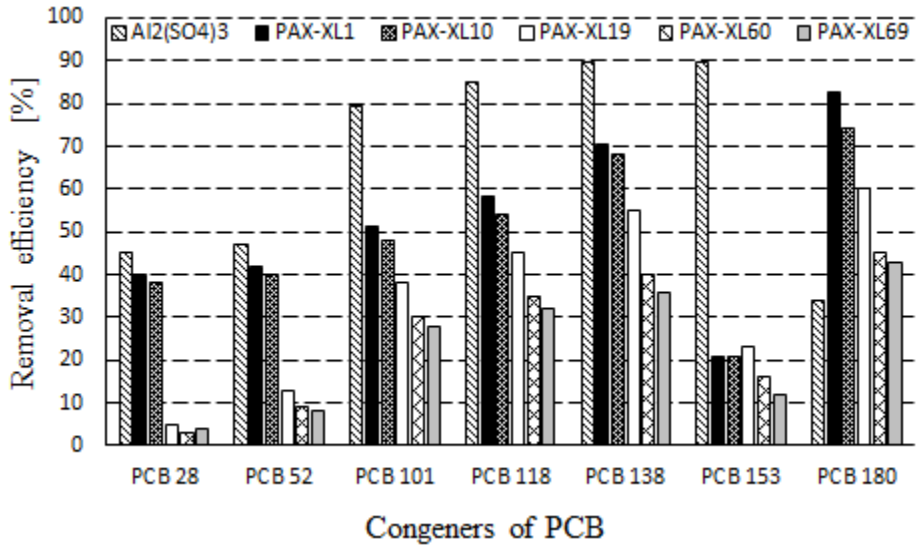

Fig. 1. Removal efficiency of indicator PCBs from water

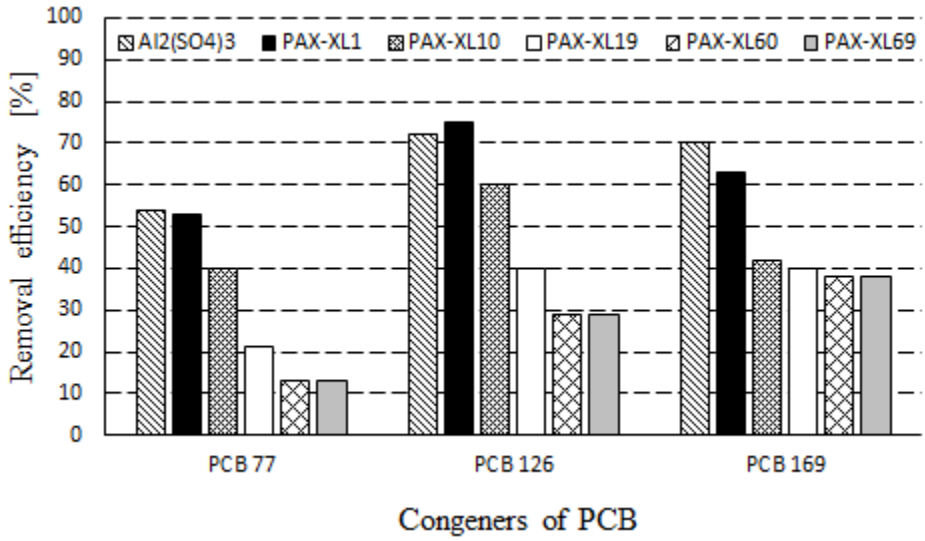

Fig. 2. Removal efficiency of dioxin-like PCBs from water

Selectivity in removal of chosen PCB congeners, depending on applied coagulant, was demonstrated; the usage of aluminium sulphate resulted in achieving heptachlorobiphenyl

PCB 180 removal rate at the level of 34%, while using PAX-XL1 and PAX-XL10 resulted in obtaining higher reduction efficiency for this congener, *ie* 83 and 74% respectively.

For dioxin-like PCB after the application of aluminium sulphate total concentration reduction by 74% was obtained, congener removal efficiency amounted to from 54 (PCB 77) to 72% (PCB 126) (Fig. 2). Similar effects were achieved after the usage of PAX-XL1, total PCB concentration decreased by 73%, reduction of PCB 77, 126 and 169 concentration amounted to 53, 75 and 63% respectively.

The smallest degree of removal from water, both for indicator and dioxin-like PCB, was stated for coagulants PAX-XL60 and PAX-XL69. After the application of these coagulants, decrease in PCB concentration in the range of 3 to 45% (indicator PCB), and 13 to 38% (dioxin-like PCB), was obtained.

According to the literature data, the coagulation process with aluminium sulphate, apart from desirable effects, may cause negative changes in physico-chemical composition of purified water, *eg* an increase in aluminium ion concentration or intensification of water corrosivity [1]. Increased aluminium ion concentration in drinking water may also pose a potential threat to human health. Therefore, despite demonstrated in the research, higher efficiency of aluminium sulphate in PCB removal from water, it is suggested to use polyaluminium chlorides PAX-XL1 and PAX-XL10, which have alkalinity equal to 70 ±5%, 85 ±5% respectively, and which contain approx. 10 and 3% of Al_2O_3. The application of polyaluminium chlorides as coagulants for organic pollutant removal, is recommended by many authors [1, 2]. Higher efficiency is explained by the fact that polyaluminium chloride solutions contain more polycationic and polymerized products of controlled prehydrolysis than aluminium sulphate. In the pH range of natural waters and with their alkalinity, hydrolysis of aluminium cations present in aluminium sulphate occurs almost immediately after their contact with treated water, therefore the precipitation of aluminium hydroxide occurs faster than the desired reaction of colloids and organic pollutant anions neutralization [2].

The obtained results suggest that in case of removal from water indicator and dioxin-like PCB using polyaluminium chlorides, their alkalinity is important, which should amount to approx. 70%. Alkalinity of PAX-XL60 and PAX-XL69 was lower and amounted to approx. 40 and 60%, which can explain lower efficiency of these coagulants in PCB removal. PAX-XL1 coagulant efficiency in congener removal is confirmed by results obtain for dioxin-like PCB. Also the literature data confirm the effectiveness of polyaluminium chloride in dioxin and dioxin-like compound removal. Li et al [7] demonstrated 99% efficiency in PCDD/Fs removal after application of ferric chloride and polyaluminium chloride, slightly lower (97-98%) was obtained for aluminium sulphate. Applied coagulants were selective in removal of chosen PCDD/Fs. The literature data and own research indicate that significant improvement of polyaluminium chloride efficiency in PCB removal from water is achieved by application of coagulation process enhancement with powder-activated carbon. Liyan et al. [14] demonstrated the effectiveness of powder-activated carbon (PAC), granular-activated carbon (GAC) in hydrophobic organic chemicals (HOCs) removal, in the range of 73.4 to 89.2%, which is the next stage of own research.

Conclusions

Conducted research allowed for formulating the following conclusions:

- good effects of indicator and dioxin-like PCB removal from surface water were obtained after the application of aluminium sulphate, and hydrolyzed polyaluminium chlorides PAX-XL1 and PAX-XL10,
- after the coagulation process using aluminium sulphate and coagulants PAX-XL1 and PAX-XL10, total concentration of indicator PCB decreased in water by 65, 53, and 50% respectively,
- for dioxin-like PCB, after using aluminium sulphate and hydrolyzed polyaluminium chloride PAX-XL1, total concentration reduction by 74 and 73% was achieved,
- selectivity in chosen PCB congener removal was demonstrated, depending on applied coagulant; with the usage of aluminium sulphate removal of heptachlorobiphenyl PCB 180 at the level of 34% was obtained, whereas with the application of PAX-XL1 and PAX-XL10 higher efficiency of this congener reduction was obtained, *ie* 83 and 74% respectively.

Acknowledgements

This work was carried out within the research project No. BS-PB-402/301/2011.

References

[1] Alexander JT, Faisal I, Hai FI, Al-aboud TM. Chemical coagulation-based processes for trace organic contaminant removal. Current state and future potential. J Environ Manage. 2012;111:195-207. DOI: 10.1016/j.jenvman.2012.07.023.

[2] Zhao YX, Phuntsho S, Gao BY, Yang, Kim J-H, Shon HK. Comparison of a novel polytitanium chloride coagulant with polyaluminium chloride: Coagulation performance and floc characteristics. J Environ Manage. 2015;147:194-202. DOI: 10.1016/j.jenvman.2014.09.023.

[3] Deborde M, von Gunten U. Reactions of chlorine with inorganic and organic compounds during water treatment-Kinetics and mechanisms: A critical review. Water Res. 2008;42:13-51. DOI: 10.1016/j.watres.2007.07.025.

[4] Van den Berg M, Birnbaum LS, Denison M, De Vito M, Farland W, Feeley M, et al. The 2005 World Health Organization reevaluation of human and Mammalian toxic equivalency factors for dioxins and dioxin-like compounds. Toxicol Sci. 2006;93:223-241. DOI: 10.1093/toxsci/kfl055.

[5] Howell NL, Suarez MP, Riafi HS. Koenig L. Concentration of polychlorinated biphenyls (PCBs) in water, sediment and aquatic biota in the Huston Ship Chanel, Texas. Chemosphere. 2008;70:593-606. DOI: 10.1016/j.chemosphere.2007.07.031.

[6] Ternes, TA, Meisenheimer M, McDowell D, Sacher F, Brauch HJ, Haist-Gulde B, et al. Removal of pharmaceuticals during drinking water treatment. Environ Sci Technol. 2002;36:3855-3863. DOI: 10.1021/es015757k.

[7] Li X, Peng P, Zhanga S, Man R, Sheng G, Fu J. Removal of polychlorinated dibenzo-*p*-dioxins and polychlorinated dibenzofurans by three coagulants in simulated coagulation processes for drinking water treatment. J Hazard Mater. 2009;162:180-185. DOI: 10.1016/j.jhazmat.2008.05.030.

[8] Rosińska A, Dąbrowska L. Concentrations of PCBs and heavy metals in water of the dam reservoir and use of pre-hydrolyzed coagulants to micropollutants removal from surface water. Desalin Water Treat. 2013;51:1657-1663. DOI: 10.1080/19443994.2012.695045.

[9] Dąbrowska L. Removal of organic matter from surface water using coagulants with various basicity. J Ecol Eng. 2016;17:66-72. DOI: 10.12911/22998993/63307.

[10] Charakterystyka wodnych roztworów chlorków poliglinu. (Characteristics aqueous solution of polyaluminum chloride) (30.12.2012). http://www. kemipol.com.pl/produkt.

[11] Dąbrowska L, Rosińska A. Usuwanie PCB i jonów metali ciężkich z wody powierzchniowej w procesie koagulacji. (Removal of PCBs and heavy metal ions from surface water by coagulation). Roczn Ochr Środ. 2013;15:1228-1242. http://ros.edu.pl/index.php?option=com_content&view=article&id=247:084-usuwanie-pcb-i-jonow-metali-ciezkich-z-wody-powierzchniowej-w-procesie-koagulacji&catid=22&lang=pl&Itemid=119.
[12] Lazzari L, Sperni L, Salizzato M, Pavoni B. Gas chromatographic determination of organic micropollutants in samples of sewage sludge and compost: Behaviour of PCB and PAH during composting. Chemosphere. 1999;38:1925-1935. DOI: 10.1016/S0045-6535(98)00406-8.
[13] Sapota G. Polychlorinated biphenyls (PCBs) and organochlorine pesticides (OCPs) in seawater of the Southern Baltic Sea. Desalination. 2004;162:153-157. DOI: 10.1016/S0011-9164(04)00038-4.
[14] Liyan S, Youcai Z, Weimin S, Ziyang L. Hydrophobic organic chemicals (HOCs) removal from biologically treated landfill leachate by powder-activated carbon (PAC), granularactivated carbon (GAC) and biomimetic fat cell (BFC). J Hazard Mater. 2009;163:1084-1089. DOI: 10.1016/j.jhazmat.2008.07.075.

WPŁYW WYBRANYCH KOAGULANTÓW NA USUWANIE WSKAŹNIKOWYCH I DIOKSYNOPODOBNYCH PCB Z WODY PRZEZNACZONEJ DO SPOŻYCIA

Katedra Chemii, Technologii Wody i Ścieków, Wydział Infrastruktury i Środowiska, Politechnika Częstochowska

Abstrakt: Celem badań była porównanie efektywności wybranych koagulantów w usuwaniu z wody powierzchniowej wskaźnikowych i wybranych dioksynopodobnych PCB. Jako koagulanty wykorzystano siarczan glinu oraz 5 zhydrolizowanych chlorków poliglinu o nazwach handlowych: PAX-XL1, PAX-XL10, PAX-XL19, PAX-XL60, PAX-XL69. Do badań wykorzystano wodę powierzchniową. Skład wody zmodyfikowano mieszaniną wzorcową PCB MIX24 oraz MIX13 w celu uzyskania stężenia każdego kongeneru 300 ng/dm^3. Mieszaninę PCB MIX24 stanowił roztwór wskaźnikowych kongenerów: 28, 52, 101, 118, 138, 153 i 180, a mieszaninę MIX13 roztwór trzech dioksynopodobnych PCB 77, PCB 126 oraz PCB 169. Wykazano, że zastosowanie siarczan glinu pozwoliło na uzyskanie lepszych efektów oczyszczania wody z PCB niż przy wykorzystaniu wstępnie zhydrolizowanych soli, chlorków poliglinu. Z przebadanych koagulantów najlepsze efekty usuwania wskaźnikowych PCB otrzymano po zastosowaniu siarczanu glinu, sumaryczne stężenie PCB zmniejszyło się o 65%. Najwyższą efektywność usuwania wskaźnikowych kongenerów (90%) uzyskano dla PCB 138 i 153. Po zastosowaniu zhydrolizowanych chlorków poliglinu PAX-XL1, PAX-XL10 uzyskano obniżenie stężenia wyżej chlorowanych PCB w zakresie od 23 do 74%. Wykazano selektywność usuwania wybranych kongenerów PCB w zależności od zastosowanego koagulantu; przy wykorzystaniu siarczanu glinu uzyskano usunięcie heptachlorobifenylu PCB 180 na poziomie 34%, natomiast przy wykorzystaniu PAX-XL1 i PAX-XL1o uzyskano większą efektywność redukcji tego kongeneru, tj. odpowiednio 83 i 74%. Dla dioksynopodobnych PCB po zastosowaniu siarczanu glinu uzyskano redukcję sumarycznego stężenia o 74%, efektywność usuwania tych kongenerów wynosiła od 54 (PCB 77) do 72% (PCB 126), podobne rezultaty otrzymano po zastosowaniu PAX-XL1. Najmniejszy stopień usuwania PCB z wody stwierdzono dla koagulantów PAX-XL60 i PAX-XL69.

Słowa kluczowe: polichlorowane bifenyle, koagulacja, siarczan glinu, zhydrolizowane chlorki poliglinu, efektywność usuwania, woda pitna

DOI: 10.2429/proc.2016.10(1)010 2016;10(1)

Zbigniew SUCHORAB[1], Danuta BARNAT-HUNEK[2] and Małgorzata FRANUS[2]

ANALYSIS OF HEAT-MOISTURE PROPERTIES OF HYDROPHOBISED GRAVELITE-CONCRETE WITH SEWAGE SLUDGE

ANALIZA CECH CIEPLNO-WILGOTNOŚCIOWYCH HYDROFOBIZOWANYCH KERAMZYTOBETONÓW Z OSADEM ŚCIEKOWYM

Abstract: The article presents the laboratory examinations of the basic physical parameters of gravelite-concrete modified by municipal sewage sludge and gravelite-concrete, obtained of light aggregates, commonly applied in Polish building market. To decrease water absorptivity of the concrete blocks, the admixture of water emulsion of reactive polisiloxanes was applied. For the presented blocks, capillary rise process was monitored together with moisture influence on heat conductivity coefficient λ determined using TDR probes and plate apparatus. Analysis of heat-moisture properties of concrete confirmed usefulness of gravelite with sewage sludge addition for further production.

Keywords: capillary rise, heat conductivity coefficient, gravelite-concrete, hydrophobisation

Introduction

Production of energy-saving and ecological building materials becomes a common technology to improve energetic effectiveness of the buildings according to European Union Directive 2006/32/WE3. One of the popular materials applied for the energy-saving civil engineering is gravelite-concrete, especially due to its thermal and moisture parameters.

Increased environmental and economic benefits can be achieved only if for gravelite-concrete production waste materials will be used [1-3]. To product gravelite-concrete, more often light aggregates, modified with municipal sewage sludge.

Sewage sludge may threat human health and thus should be suitably proceeded. Acts and regulations imposed by European Union limit sewage sludge deposition on landfills and its reuse in agriculture. One of the common utilization methods is application for production of ceramic materials [4, 5] and energy-saving gravelite-concrete blocks [6, 7]. Unfortunately sewage sludge is characterized by high moisture absorptivity, being the result of the structure of light aggregates. It is a serious problem in composition of the gravelite-concrete mixtures and ready-products because it intensifies transport of water due to capillary forces. It essentially influences heat flow process by the increase of the heat conductivity of the materials.

Differences between volumetric densities of the light aggregates and cement mortar cause the aggregates to flow out when cement mortar has no suitable viscosity. To minimize unfavorable phenomenon of water subtraction required for hydration process by the gravelite, several procedures should be conducted. One of them is initial wetting to

[1] Faculty of Environmental Engineering, Lublin University of Technology, ul. Nadbystrzycka 40B, 20-618 Lublin, Poland, email: Z.Suchorab@pollub.pl
[2] Civil Engineering and Architecture Faculty, Lublin University of Technology, ul. Nadbystrzycka 40, 20-618 Lublin, Poland, email: d.barnat-hunek@pollub.pl; m.franus@pollub.pl
[*] Contribution was presented during ECOpole'15 Conference, Jarnoltowek, 14-16.10.2015

protect the aggregates from autogenic contraction. Other solution is to cover the aggregates with cement grout, that provides lower water absorptivity of the aggregates, increases the density of particles and thus essentially influences concrete strength. A new technology is aggregates impregnation, that closes air gaps preventing them from water penetration with constant adherence of the particles to the cement matrix [8, 9].

The results of the present research can be possibly applied to establish guidelines for practical applications of lightweight concrete supplemented with sewage sludge foamed by hydrophobic agent, which has slightly different parameters compared to traditional lightweight concrete.

Materials and methods

Two types of gravelite-concrete samples were prepared, that differed in aggregates type. First type of aggregates were hand-made of clay from Light Aggregates Company "Keramzyt" in Mszczonow, Poland and from 10% additives of sewage sludge from municipal wastewater treatment plant "Hajdow" in Lublin, Poland. Sewage sludge from the Sewage Treatment Plant "Hajdow" in Lublin was described by following parameters: moisture content of sludge was 80.43%, alkalinity - 750 mg $CaCO_3/dm^3$, pH 7.68, VFAs - 92 mg/dm^3, COD - 136.423 mg O_2/dm^3, dry mass - 19.57%, loss on ignition - 60.65%, the residue on ignition - 39.35%, density - 0.795 g/cm^3. Sewage sludge samples were taken from the temporary storage site, and then dried to a constant weight at 110°C. Dried sludge was ground and then added to clay (90% by weight) in the amount of 10% by weight. The process of making the substance homogeneous was based on mixing components with the corresponding portion of water until a plastic consistency was achieved. Then the formed balls of 16 mm coarse fraction were dried to a state of air-dry and kept in a laboratory oven at 110°C for 2 h. Dried samples were placed in a chamber furnace and fired at 1150°C for 30 minutes.

Second type of aggregates came from Ligth Aggregates Company "Keramzyt" in Mszczonow, Poland. Basic characteristics of the applied aggregates are presented in Table 1.

Table 1

Basic characteristics of gravelite applied for research

Type of aggregates	Density [g/cm^3]	Apparent density [g/cm^3]	Absorptivity [%]	Porosity [%]
Gravelite from Mszczonow	2.48	1.050	20	30.0
Gravelite with sewage sludge	2.59	0.812	16.2	40.0

Samples with the following dimensions: 150×150×150 mm were formed directly after concrete compounds had been mixed. They were condensed in two layers by vibrations until cement grout appeared at the surface of the mortar. The samples were disassembled after 24 hours of maturation and placed in water basin according to the PN-EN 206:2014-4 [10] standard until full average strength was reached (examined samples age - 28 days).

Within the experiment the following measurements were conducted:

- Real density was determined using PN-EN 1936:2010 [11] standard A - method with pycnometer, in laboratory conditions, at the temperature of 20°C.

- Apparent density determination were conducted after 28 days of concrete maturation. Apparent volume was determined using the following standards: PN-EN 1389:2005 [12], PN-EN 12390-7:2011P [13].
- Absorptivity.
- Porosity.
- Capillary rise, determined using the TDR (Time Domain Reflectometry) technique, previously described in the following papers [14, 15].
- Microstructure of gravelite-concrete using SEM (Scanning Electron Microscope).
- Heat Conductivity Coefficient using FOX 314 by Laser Comp, plate apparatus.

It is worth mentioning in here, that the applied TDR (Fig. 1) technology required modification of the traditional reflectometric sensors which in standard version are small and not stiff enough to be inserted into the hard structure of gravelite-concrete. For that aim there were intentionally developed TDR sensors that could be used in this particular experiment. Heads of the manufactured sensors were made of polyamide cylinders with the diameter of 46 mm and the measuring elements were made of steel rods 50 mm long and 5 mm wide in diameter. Spacing between the rods was equal 24 mm. Probes were inserted into the examined sample in the following levels: 5 cm above water table and 10 cm above water table. Duration of the whole experiment was set to 350 hours until no significant water increase was observed. Capillary suction experiment was conducted on both samples (i) gravelite-concrete with aggregates from Mszczonow and (ii) gravelite concrete with aggregates from sewage sludge.

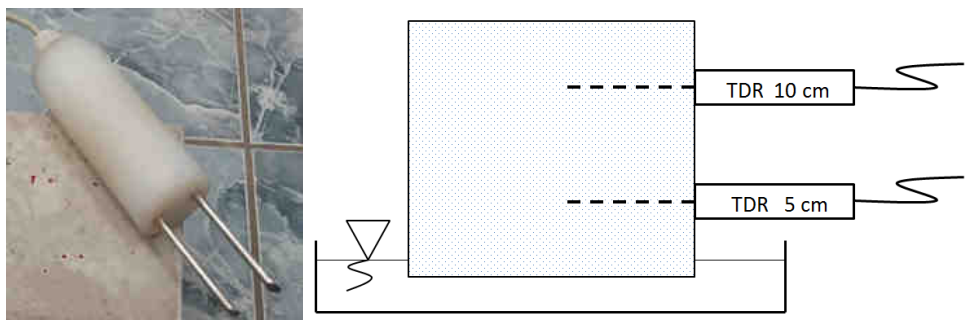

Fig. 1. Capillary uptake process determination - probe used for experiment and schematic view of measuring setup

To measure heat conductivity coefficient using FOX apparatus, 3 plates of each gravelite-concrete type were prepared. The dimension of each plate was 300 × 300 × 50 mm. Examinations were conducted for both dry samples and 3% moist (achieved by concrete saturation in a space with relative humidity about 70%). Period assumed for concretes saturation was established as 4 weeks. To determine heat conductivity coefficient of the material it was set the temperature gradient of 20°C between heating and cooling plate. For that aim the following temperatures were applied: 20°C for heating plate and 0°C for the cooling plate. Average temperature was equal 10°C.

Results and discussion

Obtained results are presented in Table 2.

Table 2

Physical properties of the examined gravelite-concretes

Type of concrete	Density [g/cm^3]	Apparent density [g/cm^3]	Absorptivity [%]	Porosity [%]	Heat conductivity λ [W/mK]	
					Dry	3% moist
With aggregates from Mszczonow	2376	1442	7	39.3	0.67	0.72
With aggregates from sewage sludge	2450	1344	4	45.1	0.52	0.58

According to the above described measurements and calculations, the real mass of the concrete unit (volumetric density) equals ρ_p = 1344-1442 kg/m^3. Determined with pycnometer real density equals ρ = 2376 and 2450 kg/m^3. Percentage volume of pores in concrete with sewage sludge reaches 45.1 and is 12.86% greater from light concrete with aggregates from Mszczonow.

Heat conductivity coefficient λ of gravelite-concrete with aggregates from Mszczonow in dry state is about 7% smaller comparing to moist material (3% of moisture) and 10% smaller comparing to concrete with sewage sludge. Difference between examined light concretes with moisture equal 3% is about 19.44% and indicates better thermal parameters of gravelite-concrete with sewage sludge.

Results of capillary rise phenomenon determined using TDR method are presented on Figure 2. Conducted research confirmed the decreased capillary parameters of the examined concretes.

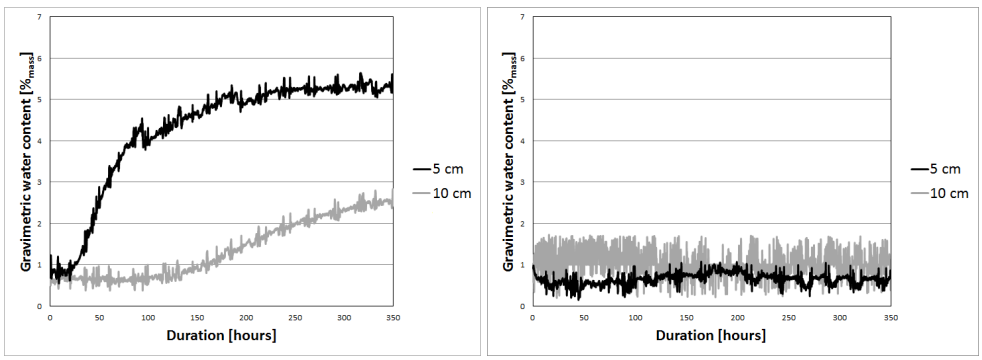

Fig. 2. Capillary rise phenomenon determined within the described research. Left - gravelite-concrete with aggregates from Mszczonow, right - gravelite concrete with aggregates from sewage sludge

In case of the sample with aggregates from Mszczonow the progress of the process was slow. The first moisture increase readouts were observed by the probe placed at level of 5 cm above water table. It was noticed after about 24 hours since the beginning of the experiment. Within next 150 hours the progress of the phenomenon was significant to reach the level of 5%. Maximum water content read by the bottom probe was reached after the

period of about 250 hours and it was still below 6%. It should be mentioned that this value was close to maximum material absorptivity (7%). In case of the second probe, mounted at the level of 10 cm above water table, moisture increase was significantly slower. The first water appearance was read after about 150 hours since the experiment was started. Maximum moisture read by the reflectometer was about 2.5%.

In case of the second sample - with aggregates from sewage sludge almost no significant water increase was observed. Readouts of two probes were unstable and varying between 0 and 2%. This ought to be considered as standard uncertainty of the TDR method, which according to many literature sources is about 2% [16, 17].

Scanning Electron Microscope (SEM) research was conducted on samples of gravelite-concrete obtained from aggregates modified with municipal sewage sludge and aggregates from Mszczonow. SEM photographs of microstructure of cement mortars are supplemented with EDS diagrams. Hardened cement mortar from Portland cement consists of 70% of hydrated calcium silicates, so called C-S-H phases. About 30% are calcium hydroxide and products of aluminate hydration and calcium aluminate-ferrate. Microscopic research confirmed good adhesion in contact points between gravelite aggregates and cement mortar. No empty gaps, cracks or scratches were noticed in the above mentioned contact points (Fig. 3).

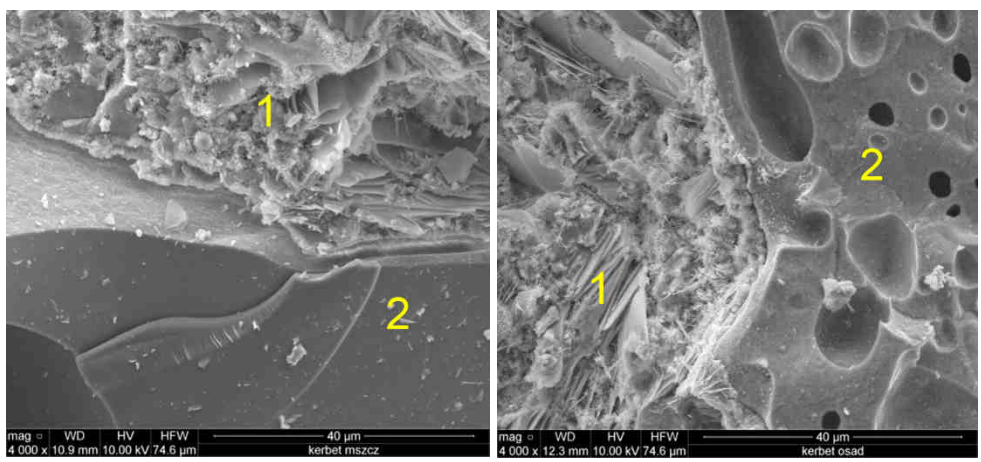

Fig. 3. SEM investigation in contact point: left - between gravelite aggregates from Mszczonow and cement mortar supplemented with spectrum of chemical composition; right - between gravelite with sewage sludge and cement mortar supplemented with spectrum of chemical composition (1 - mortar, 2 - gravelite)

Conclusions

By the use of gravelite-concrete modified with sewage sludge it is possible to produce lightweight concrete with the apparent densities of 1400-1960 kg/m^3.

Supplementation with sewage sludge caused the decrease of material apparent density for about 7% and the increase of total porosity for 12.86% comparing to the concrete from gravelite available on building market. This was also confirmed by verifications using SEM technique. Microscopic observations of contact points between gravelite aggregates and

cement mortar confirmed good adhesion. No empty gaps, cracks or scratches were noticed in above mentioned contact points.

Absorptivity of both gravelite-concretes is between 3 and 7%, especially because of the application of hydrophobic preparation as concrete additive. It should be emphasized that gravelite with sewage sludge, due to greater absorptivity and porosity absorbed more impregnate which decreased the total absorptivity of light concrete for about 57%. Time Domain Reflectometry measurement of capillary rise phenomenon proved total inhibition of capillary rise process.

Sewage sludge additives in gravelite-concretes enable to decrease heat conductivity coefficient for about 7-10%.

Presented examinations proved that sewage sludge can be applied as an additive for light concretes production. Anyhow, to completely verify this conclusion it should be supplemented with strength examinations of concretes with sewage sludge additives.

References

[1] Lin DF, Weng CH. Use of sewage sludge ash as brick material. J Env Eng. 2001;10:922-927. DOI: 10.1061/(ASCE)0733-9372(2001)127:10(922).

[2] Xu G, Song X, Liu W, Han J. Experimental study on preparation of high strength lightweight aggregate concrete by combined admixture of fly ash and mineral powder. Mechanic Automation and Control Engineering (MACE) 2010, China, Int Conf. DOI: 10.1109/MACE.2010.5535639.

[3] Kayali OA, Haque MN. A new generation of structural lightweight concrete. Int Conf. Advances in Concrete Technology. Proceedings Third CANMET/ACI. https://trid.trb.org/view/1997/C/475702

[4] Tay J H, Show KY. Resources recovery of sludge as a building and construction material - a future trend in sludge management. Water Sci Technol. 1997;11:259-266. DOI: 10.1016/S0273-1223(97)00692-6.

[5] Jordán MM, Almendro-Candel MB, Romero M, Rincón JM. Application of sewage sludge in the manufacturing of ceramic tile bodies. Appl Clay Sci. 2005;30:219-224. DOI: 10.1016/j.clay.2005.05.001.

[6] Gonzalez-Corrochano B, Alonso-Azcarate J. Rodas M. Production of lightweight aggregates from mining and industrial waste. J Env Manage. 2009; 90:2801-2812. DOI: 10.1016/j.jenvman.2009.03.009.

[7] Cheeseman CR, Virdi GS. Properties and microstructure of lightweight aggregate produced from sintered sewage sludge ash. Res Cons Rec. 2005;45:18-30. DOI: 10.1016/j.resconrec.2004.12.006.

[8] Muller HS, Haist M., Mechtcherine V. Selbstverdichtender Hochleistungs-Leichtbeton. Beton- und Stahlbetonbau. 2002;97(6). DOI: 10.1002/best.200201480.

[9] Kaszyńska M. Lekkie betony samozagęszczalne do konstrukcji mostowych. Mosty. 2009, marzec-kwiecień. http://www.nbi.com.pl/assets/NBI-pdf/2009/2_23_2009/pdf/19_lekkie_betony.pdf.

[10] PN-EN 206:2014-4 Beton - Wymagania, właściwości, produkcja i zgodność. http://sklep.pkn.pl/pn-en-206-2014-04p.html.

[11] PN-EN 1936:2010 Metody badań kamienia naturalnego - Oznaczanie gęstości i gęstości objętościowej oraz całkowitej i otwartej porowatości. http://sklep.pkn.pl/pn-en-1936-2010p.html.

[12] PN-EN 1389:2005 Techniczna ceramika zaawansowana. Kompozyty ceramiczne monolityczne. Właściwości fizyczne. Oznaczanie gęstości i porowatości otwartej. http://sklep.pkn.pl/pn-en-1389-2005p.html.

[13] PN-EN 12390-7:2011P Badania betonu - Część 7: Gęstość betonu. http://sklep.pkn.pl/pn-en-12390-7-2011p.html.

[14] Suchorab Z, Widomski MK, Łagód G, Barnat-Hunek D, Smarzewski P. Methodology of moisture measurement in porous materials using time domain reflectometry. Chem Didact Ecol Metrol. 2014;19(1-2):97-107. DOI: 10.1515/cdem-2014-0009.

[15] Pavlik Z, Jirickova M, Cerny R, Sobczuk H, Suchorab Z. Determination of moisture diffusivity using the Time Domain Reflectometry (TDR) method. J Build Phys. 2006;30(1):59-70. DOI: 10.1177/1744259106064356.

[16] Noborio K. Measurement of soil water content and electrical conductivity by time domain reflectometry: a review. Comp El Agr. 2001; 31: 213-237. DOI:10.1016/S0168-1699(00)00184-8.

[17] Amato M, Ritchie JT. Small spatial scale soil water content measurement with time-domain reflectometry. Soil Sci Soc Am J. 1995;59:325-329. DOI: 10.2136/sssaj1995.03615995005900020008x.

ANALIZA CECH CIEPLNO-WILGOTNOŚCIOWYCH HYDROFOBIZOWANYCH KERAMZYTOBETONÓW Z OSADEM ŚCIEKOWYM

[1] Wydział Inżynierii Środowiska, Politechnika Lubelska
[2] Wydział Budownictwa i Architektury, Politechnika Lubelska

Abstrakt: Produkcja ekologicznych i energooszczędnych materiałów budowlanych staje się powszechną technologią poprawy efektywności energetycznej budynków zgodnie z przepisami dyrektywy UE 2006/32/WE3. Jednym z materiałów stosowanym w budownictwie energooszczędnym ze względu na swoje właściwości cieplno-wilgotnościowe jest keramzytobeton. Do otrzymywania keramzytobetonu coraz częściej stosuje się kruszywa lekkie modyfikowane komunalnym osadem ściekowym. Osady ściekowe stwarzają zagrożenie dla zdrowia ludzi i środowiska naturalnego, dlatego też muszą być poddawane odpowiedniej przeróbce. Jedną z metod ich utylizacji jest zagospodarowanie do produkcji energooszczędnych bloczków keramzytobetonowych. Często jednak charakteryzują się one wysoką nasiąkliwością, co powoduje transport wody podciąganej kapilarnie. Wpływa to w istotny sposób na proces przepływu ciepła, tym samym zwiększając kilkukrotnie przewodnictwo cieplne materiałów. Artykuł przedstawia badania podstawowych cech fizycznych keramzytobetonu modyfikowanego komunalnym osadem ściekowym oraz keramzytobetonu uzyskanego z kruszywa lekkiego powszechnie stosowanego na rynku. W celu obniżenia nasiąkliwości betonów jako domieszkę zastosowano wodną emulsję reaktywnych polisiloksanów. Dodatkowo wykonano pomiary podciągania kapilarnego oraz jego wpływu na współczynnik przewodzenia ciepła λ w próbkach modelowych przy wykorzystaniu sond TDR i aparatu płytowego. Analiza cech cieplno-wilgotnościowych betonów potwierdziła przydatność keramzytu z dodatkiem osadu ściekowego do ich produkcji.

Słowa kluczowe: podciąganie kapilarne, współczynnik przewodzenia ciepła, keramzytobeton, hydrofobizacja

DOI: 10.2429/proc.2016.10(1)011 2016;10(1)

Wojciech UCHMAN[1], Sebastian WERLE[2] and Anna SKOREK-OSIKOWSKA[1]

ENERGY CROPS AS LOCAL ENERGY CARRIER

ROŚLINY ENERGETYCZNE JAKO LOKALNY NOŚNIK ENERGII

Abstract: The experimental investigation of energy crops (*Miscanthus* x *giganteus, Sida hermaphrodita, Spartina pectinata, Panicum virgatum*) gasification was carried out. The influence of excess air ratio (λ) on lower heating value (*LHV*) was investigated. Downdraft fixed bed gasifier was used. For all types of biomass, the highest *LHV* value was achieved for λ = 0.18. Compositions of gases obtained during the experimental study were used for thermodynamic and economic analysis of CHP system with gas piston engine. The system quality indices and input data for economic analysis were calculated. For the economic analysis the net present values method was adopted. Given the assumptions, despite biomass type, the *NPV* indice did not reach positive values. Break even price of electricity and break even cost of fuel were calculated. The economic viability of such systems is strongly influenced by economic and legal environment. The paper includes sensitivity analysis of change of the selected parameter such as annual availability of the system, price of fuel and price of green certificates.

Keywords: biomass, gasification, cogeneration, energy crops, gas piston engine

Introduction

Energy crops are in the area of interest because of multiple ways of advantageous utilization. They can be used for biofuels (solid, liquid and gaseous) and biocomponents production. Examples of commonly used plants are *Salix* L., *Miscanthus* x *giganteus*, *Spartina pectinata*, *Panicum virgatum*, *Sida hermaphrodita*, *Rosa multiflora* [1].

In Poland, agro-biomass is not widely used, which becomes a reason for underdeveloped cultivation techniques, lack of methods of preventing crop diseases and other detrimental external factors. That has a great impact on the volume of production and the quality of fuel. Other factors that affect an agro-fuel production are soil fertility, quality of agricultural treatment and field preparation (*eg* number of weeds). However, the current state of the Polish agro-energy sector gives number of opportunities for relatively easy and quick progression.

Energy crops utilization can be useful in more than one field. Phytoremediation is one of the techniques used for remediation of contaminated areas. Soil contamination can be found close to landfills, heavy-metal/oil industry areas. There are energy crops which can be grown on contaminated areas and have a potential to accumulate contaminants. The reasonable method of contaminated biomass utilization is gasification [2].

Gasification is a thermo-chemical conversion of solid feedstock into a gaseous fuel. Because of the low amount of the oxidizer used in the process and the reducing atmosphere, gasification prevents sulphur and nitrogen oxides emission, also it is possible to accumulate part of the contaminants in the solid residues. Gasification is a way to utilize contaminated biomass while useful syngas is produced. Syngases are mostly low-calorific gases (depends

[1] Institute of Power Engineering and Turbomachinery, Silesian University of Technology, ul. S. Konarskiego 18, 44-100 Gliwice, Poland
[2] Institute of Thermal Technology, Silesian University of Technology, ul. S. Konarskiego 22, 44-100 Gliwice, Poland, phone +48 32 237 29 83, email: sebastian.werle@polsl.pl
* Contribution was presented during ECOpole'15 Conference, Jarnoltowek, 14-16.10.2015

on the feedstock and gasification agent) that can be used in power boilers, industrial furnaces, gas turbines or piston engines [3]. Biomass gasification gases, as a fuel that might be received from local energy sources shows a great potential as fuel for combined heat and power (CHP) plants [4]. Combined heat and electricity generation in distributed energy systems with internal combustion piston engines is a good option for local communities due to a relatively low investment cost and the high efficiency of electricity production. What is more, the market of commercial solutions for low-calorific value gases (*eg* biogas, syngas) is constantly growing [5].

In this study the experimental investigation of four types of energy crops gasification was carried out. Compositions of gases obtained during the experimental study were used for thermodynamic and economic analysis of CHP system with gas piston engine.

Feedstock and apparatus

Four types of energy crops were gasified: *Miscanthus* x *giganteus*, *Sida hermaphrodita*, *Spartina pectinata* and *Panicum virgatum*. Picture of the feedstock samples is presented in Figure 1. Main properties of the studied plants are presented in Table 1.

Table 1

Properties of the analyzed energy crops (dry basis)

	Unit	***Miscanthus* x *giganteus***	***Sida hermaphrodita***	***Panicum virgatum***	***Spartina pectinata***
C	[%]	46.6	44.8	45	45.8
H	[%]	7.16	7.4	6.9	7.28
N	[%]	0.16	0.37	0.55	0.26
S	[%]	1.35	1.4	1.43	1.45
O	[%]	44.73	46.03	46.12	45.21
Cl	[ppm]	417.4	98.3	343.4	174.4
Pb	[ppm]	35	56.84	88.96	92.66
Cd	[ppm]	1.55	5.2	1.34	1.25
Zn	[ppm]	83.28	146.5	122.4	147.7
Ash	[%]	1.36	2.6	3.23	3.24
Volatiles	[%]	75.4	78.8	78.1	77.5
Moisture	[%]	7.6	9	8.5	8
LHV_{bio}	[MJ/kg]	19.45	19	18.35	19.29

Fig. 1. Samples of gasified energy crops

The experimental study was conducted using laboratory-scale fixed-bed gasification facility. The scheme of the installation is shown in Figure 2.

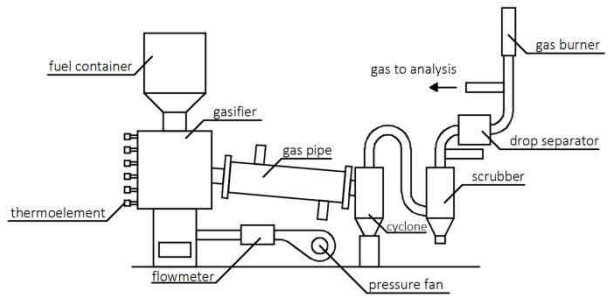

Fig. 2. Scheme of the gasification installation

The main part of the system is a fixed-bed gasifier with the maximum weight of the feedstock of 5 kg. The gasified material was fed into the reactor form the fuel container above. Gasification agent (air) was fed from the bottom by pressure fan. Air flowmeter allows to set the desirable air excess ratio in the gasifier. Produced gas passes basic gas cleaning equipment and the sample to analysis is taken. The internal temperature profile in the reactor is measured by six thermoelements located along the vertical axis of the reactor.

There are four main zones in the reactor: drying zone (water is evaporated), pyrolysis zone (thermal decomposition to volatiles and solid char), reduction zone (where main combustible gas components are produced) and combustion zone (where part of the biomass is combusted to generate heat for endothermic reactions).

Gasification process was carried out for six air excess ratios: 0.12, 0.14, 0.16, 0.18, 0.23, 0.27.

Results of experimental investigation

Figure 3 shows the dependence of lower heating values (*LHV*) on air excess ratio in reactor during the gasification. Gas with the highest *LHV*, 3.68 MJ/m^3_n, was produced using *Miscanthus* x *giganteus*. It can be seen that for particular type of biomass there is a certain range of the lower heating value of the syngas that can be obtained in the gasification process. Also, there is an optimal air excess ratio for studied energy crops gasification (the highest *LHV*). It is caused by the best thermal conditions for endothermic reactions that result in CO, CH_4 and H_2.

The lower heating value depends on the amount of combustible gases in the syngas. The main combustible gas in the syngases is carbon oxide. Figure 4 shows molar fraction of the main components of the gases for the optimum air excess ratio $\lambda = 0.18$, but the relation between the amount of particular compounds was similar for the air ratios used in the experiment. Also, minor differences in the gas compositions are related to minor differences in biomass composition. Analyzing this figure it can be confirmed that the gas with the highest *LHV* consists of the highest amount of CO and CH_4.

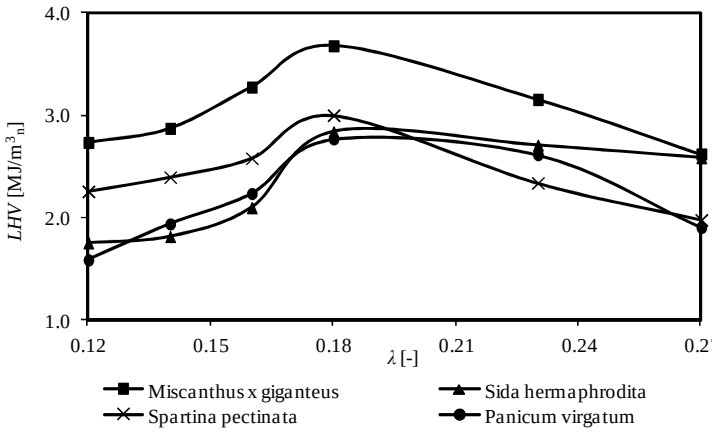

Fig. 3. Dependence on the lower heating value as a function of air excess ratio

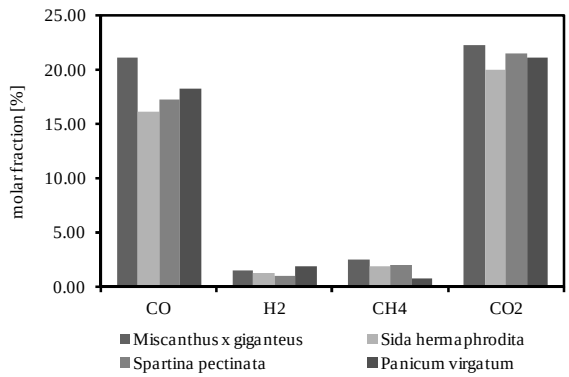

Fig. 4. Molar fraction of main components of produced gas (λ = 0.18) for all types of energy crops

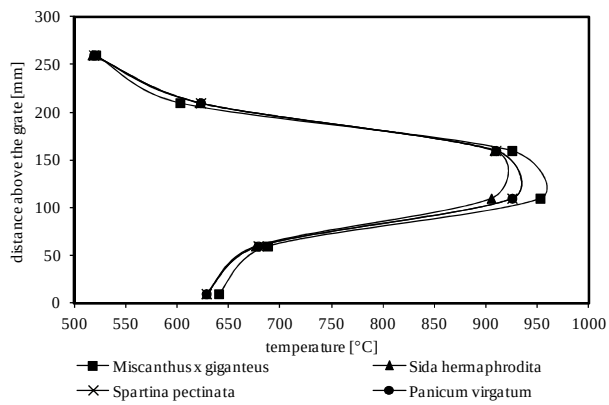

Fig. 5. Temperature profiles for λ = 0.18

Temperature in the gasifier is an important parameter, which allows to define where the particular zones of gasifier are. Figure 5 shows the temperature profile in the reactor (λ = 0.18). Despite the biomass type, the highest temperature is about 110 mm above the grate where the oxidation zone is located. This zone generates heat for the drying, devolatilization and endothermic gasification reactions.

Energetic analysis of the CHP system with gas piston engine

Calculations of CHP unit were based on the gas compositions delivered by the experimental investigation. Gas compositions with the highest *LHV* for each type of biomass were used.

Most manufacturers of gas piston engines for CHP systems does not provide detailed information about engines parameters fuelled with alternative fuels *eg* low-calorific value gases. Common way is to use the indicators describing the relative change in the engine parameters. For the purpose of the analysis, the indicators were adopted following [5] and defined by equations (1) and (2). The indicators are ratios of the parameter with alternative fuel to the parameter with nominal fuel. The indicator of the relative change in the electricity generation efficiency was defined as:

$$c_\eta = \frac{\eta_{el}}{\eta_{el}^*} \tag{1}$$

The indicator of the relative change in exhaust gas temperature was defined as:

$$c_{T_{sp}} = \frac{T_{sp}}{T_{sp}^*} \tag{2}$$

The superscript "*" refers to the values of characteristics of the engine operating at nominal conditions.

For the calculations the following values of the indicators was assumed: c_η = 0.909, $c_{T_{sp}}$ = 0.979 [5].

The database of the engines available on the Polish market (with electric power under 2.2 MW) was created. The transition functions that allow to estimate the electricity generation efficiency and the exhaust gas temperature as a function of nominal electric power were made. The functions are described by the equations:

$$T_{sp}^* = 618.07 \cdot N_{el}^{*\,-0.043} \tag{3}$$

$$\eta_{el}^* = 0.2967 \cdot N_{el}^{*\,0.0468} \tag{4}$$

For all types of syngases, thermal efficiency of the engine was calculated. The thermal efficiency describes the potential of generating useful heat. Heat produced within gas piston engine can be classified into two groups: high- and low-temperature heat. Low-temperature heat is obtained from the engine body and intercooler of the turbocharger. High-temperature heat is generated in the heat exchanger powered with exhaust gases. It was assumed that the efficiency of low-temperature heat generation is the same as with the nominal fuel.

To determine the high-temperature generation efficiency, it is necessary to calculate the amount of heat obtained from the heat-exchanger which is expressed by the following formula:

$$\dot{Q}_h = \dot{m}_{sp} \cdot \eta_{he} \cdot (h_{32} - h_{33}) \tag{5}$$

The efficiency of the heat exchanger (η_{he}) in equation (5) was assumed at 98%. Calculations of the enthalpy for semi-deal gas at points 32 and 33 require the knowledge of the exhaust gas composition and its temperature. Exhaust gas temperature was calculated using equations (2) and (3). Exhaust gas composition comes from stoichiometric calculations wherein the following assumptions were made: combustion is complete, air excess ratio is λ = 1.5 and the fuel is syngas with the highest *LHV* for each type of biomass. Temperature of the exhaust gas leaving the heat exchanger was assumed at 120°C.

For the annual biomass consumption the gasification efficiency was needed. Cold gasification efficiency was defined as follows:

$$\eta_{CGE} = \frac{\dot{E}_{ch_{LCVG}}}{\dot{E}_{ch_b}} = \frac{\dot{m}_{LCVG} \cdot LHV_{LCVG}}{\dot{m}_{bio} \cdot LHV_{bio}} \tag{6}$$

Assuming the cold gasification efficiency at 60%, the mass stream of used biomass was calculated.

The overall performance of the CHP system integrated with biomass gasification is characterized by several indices:

- Energy Utilization Factor *EUF*:

$$EUF = \frac{N_{el}+Q}{E_{ch_b}} \tag{7}$$

- Cogeneration index σ:

$$\sigma = \frac{N_{el}}{Q} \tag{8}$$

- Primary Energy Saving index *PES*:

$$PES = \left(1 - \frac{1}{\frac{\eta_{qe}}{\eta_{refe}} + \frac{\eta_{qc}}{\eta_{refc}}}\right) \cdot 100\% \tag{9}$$

- Energy Replacement Index *ERI* [6]:

$$ERI = \frac{EUF - \eta_{el}}{\eta_{Ek}} + \frac{\eta_{el}}{\eta_{el,ref}} \tag{10}$$

According to the methodology described earlier, thermodynamic analysis for CHP unit with electric power N_{el} = 500 kW and electricity generation efficiency η_{el} = 38% was made. Results of the analysis are presented in Table 2.

Table 2

The results of energetic analysis for CHP system integrated with biomass gasification

Quantity	**Unit**	***Miscanthus* x *giganteus***	***Sida hermaphrodita***	***Spartina pectinata***	***Panicum virgatum***
Q	[kW]	658	711	697	711
η_q	[%]	0.5	0.54	0.53	0.54
LHV_g	[MJ/m^3_n]	3.679	2.838	3.000	2.769
LHV_{bio}	[MJ/kg]	19.45	19	19.29	18.35
EUF	[%]	53	55	55	55
PES	[%]	42	43	43	43
ERI	[GJ/GJ$_{bio}$]	0.84	0.91	0.89	0.91
σ	[-]	0.76	0.70	0.72	0.70

The results of calculations match the data available in the literature [4, 7]. Systems fuelled with gases obtained from *Sida hermaphrodita* and *Panicum virgatum* present the highest value of thermal efficiency (54%) what effects in the highest value of the *ERI* = 0.91 GJ/GJ$_{bio}$. The *EUF* and *PES* index are similar for most energy crops, the only exception is system fuelled with *Miscanthus* x *giganteus* syngas, with the indices lower by 2 and 1 percentage point respectively. The same system presents the highest value of cogeneration index $\sigma = 0.76$.

Methodology of economic efficiency analysis

One of the commonly used indicators of economic efficiency is a Net Present Value (*NPV*) described by the following formula [8]:

$$NPV = \sum_{t=0}^{t=n} \frac{CF_t}{(1+r)^t} \tag{11}$$

The *NPV* depends on the net cash flow (CF_t), the discount rate (r) and the number of working years (n). The net cash flow can be determined as:

$$CF_t = \left[-J + S - \left(K_{op} + P_d + K_{obr}\right) + A + L\right]_t \tag{12}$$

where J is the investment cost, S is the value of sold production (electricity and heat), K_{op} is the operating cost, P_d is the income tax, K_{obr} is the change of working capital (not considered in this work), A is the amortization, L is the salvage value of the company [10].

Using the *NPV* as an indicator of economic efficiency allows to calculate a Break Even Point [8], which, for the purpose of this analysis can be defined as the minimum price of the electricity (k_{el}^{BE}) or the maximum price of the biomass (k_{bio}^{BE}), from the condition:

$$NPV = 0 \tag{13}$$

Investment cost formulas were adopted from [7]. Total investment cost of the installation consists of the gasification system (gasifier with the gas cleaning unit) cost and the CHP system cost. Unit investment cost of the gasification system, expressed in €/kW, can be estimated using following equation:

$$i_{GU} = -59.72 \ln(\dot{E}_{ch_b}) + 895.95 \tag{14}$$

and the unit CHP system cost, expressed in €/kW$_{el}$, can be described by the equation:

$$i_E = -144.80 \ln(N_{el}^*) + 1802.87 \tag{15}$$

The unit cost of biomass was assumed to be 246 PLN/Mg which can also be expressed in PLN for gigajoule of chemical energy: *Miscanthus* x *giganteus* 12.65, *Sida hermaphrodita* 12.95, *Spartina pectinata* 12.75, *Panicum virgatum* 13.41. The delivery cost for 100 km transportation distance was assumed to be 20 €.

Table 3

Fuel annual consumption for all energy crops

Quantity	Unit	*Miscanthus* x *giganteus*	*Sida hermaphrodita*	*Spartina pectinata*	*Panicum virgatum*
Syngas annual consumption	[m^3]	7,725,000	10,014,000	9,474,000	10,264,000
Biomass annual consumption	[Mg]	2,435	2,493	2,456	2,581

Table 3 shows the biomass annual consumption, Table 4 shows selected assumptions for economic analysis of all types of studied biomass.

Table 4

Selected assumptions for the economic analysis

Specification	Unit	Value
Annual working time	[h]	6,000
Exploitation time	[years]	15
Construction time	[years]	1
Share of own resources	[%]	35
Share of commercial credit	[%]	65
Commercial credit rate	[%]	6
Payback time of the commercial credit	[years]	7
Income tax rate	[%]	19
Discount rate "*r*"	[%]	5
Depreciation rate	[%]	6.67
Investment cost	[PLN]	5,776,000
Gasification system	[€/kW_{bio}]	436
CHP system	[€/kW_{el}]	903
Exchange rate	[PLN/€]	4.1
Number of employees	[pers.]	2
Monthly salary including related cost	[PLN/pers./m]	4,000
Cost of using the CHP system (% of the investment cost)	[%]	1
Unit cost of repair (% of the investment cost)	[%]	2
Unit cost of water	[PLN/GJ]	0.13
Unit cost of sewage treatment	[PLN/GJ]	0.02
Unit price of the sale of useful heat	[PLN/GJ]	30
Unit price of the sale of electricity	[PLN/MWh]	160
Green certificate price	[PLN/MWh]	114
Yellow certificate price	[PLN/MWh]	115

Results of economic efficiency analysis

According to methodology described earlier the economic analysis of the CHP system with gas piston engine integrated with biomass gasification was made. Figure 6 shows the values of the Net Present Value for all systems fuelled with all types of produced gas which did not reach positive values. Given the assumptions, the smallest loss after fifteen years of operation was achieved for the installation fuelled with *Spartina pectinata*. However, there is an important element which may strongly influence these calculations. In this work, the gas cleaning unit was considered as a part of the gasification system and the investment cost was calculated with the unit cost method. Systems have different annual gas consumptions which may strongly influence the investment and operating costs of the gas purification installation.

Results of the Break Even Point calculations are presented in Tables 5 and 6. Break even price of electricity represents the minimum price of the product that prevents the investment from being unprofitable (which relates also to the break even price of biomass as the maximum price of fuel).

The economic viability of such systems is strongly influenced by economic and legal environment. The sensitivity analysis of selected parameters on the break even price of

electricity was carried out. The following parameters were selected for the analysis: annual operating time of the system (τ), price of the fuel (K_{bio}), price of the green certificates (K_{cert}). The parameters varied in the range of –20 to +20% relative to the values assumed in previous calculations. Results of the sensitivity analysis are presented in Figure 7. Figure 7 was drawn for *Spartina pectinata* but the same dependencies were noticed for the remaining energy crops.

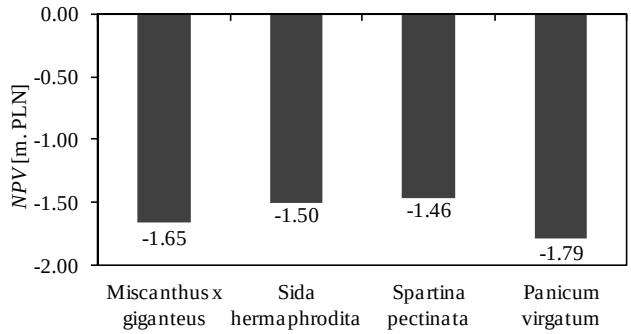

Fig. 6. The values of the *NPV* indicator for studied cases

Table 5

Break even price of electricity

Quantity	Unit	*Miscanthus* x *giganteus*	*Sida hermaphrodita*	*Spartina pectinata*	*Panicum virgatum*
k_{el}^{BE}	[PLN/MWh]	221.82	216.22	214.83	226.88

Table 6

Break even cost of biomass

Quantity	Unit	*Miscanthus* x *giganteus*	*Sida hermaphrodita*	*Spartina pectinata*	*Panicum virgatum*
k_{bio}^{BE}	[PLN/GJ]	9.12	9.74	9.63	9.59

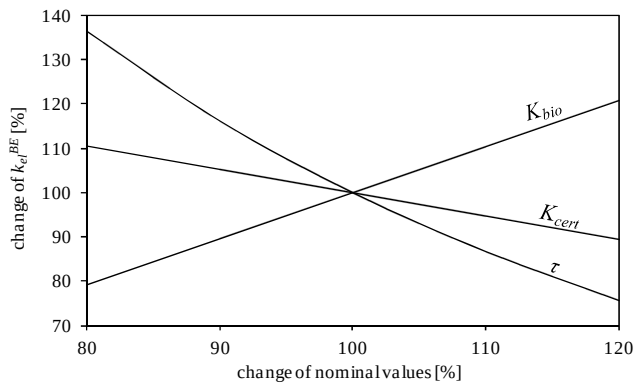

Fig. 7. Results of the sensitivity analysis for the CHP unit fueled with the *Spartina pectinata* syngas

The analysis shows that the most influential factor is annual working time. It was assumed that the installation operates 6,000 hours a year because of the limited availability of an innovative technology. Break even price of electricity decreased by 24.4 percentage points when the operating time was extended to 7,200 hours. Change of the price the biomass influenced the change of k_{el}^{BE} in the range of ±20.8%. Change of the price of the green certificates caused the change of k_{el}^{BE} in the range of ±10.6%.

Conclusions

Utilization of energy crops gasification gas as a fuel for CHP system with gas piston engine analysis was carried out. The influence of air excess ratio on the lower heating value was investigated. The results shows there are optimal conditions of the gasification process - in this case the amount of the gasification agent. For all types of biomass, the maximum value of the *LHV* was achieved for λ = 0.18. The theoretical part of the work consists of the energetic effectiveness indices calculations of the CHP unit and its economic analysis. The thermodynamic calculations were focused on determining the streams of electricity and useful heat produced in the system and the annual consumption of the biomass. These quantities allow to carry out the economic analysis. None of the presented system reach the positive value of the *NPV*. However, it was assumed that the systems operate 6,000 hours per year as the CHP unit integrated with biomass gasification is an innovative technology and it is not validated in many real facilities. The sensitivity analysis shows that annual operating time is very important factor of changing the values of economic indices. The advantage of the energy crops utilization is the phytoremediation process. The environmental aspects of such technology may provide support mechanisms that will have strong impact on the economic effectiveness.

References

[1] Lopez-Bellido L, Wery J, Lopez-Bellido R. Europ J Agron. 2014;60:1-12. DOI: 10.1016/j.eja.2014.07.001.
[2] Werle S, Bisorca D, Katelbach-Woźniak A, Pogrzeba M, Krzyżak J, Ratman-Kłosińska I, et al. J Energy Inst. 2016 In press. DOI: 10.1016/j.joei.2016.04.002.
[3] Chomiak J, Longwell JP, Sarofim AF. Prog Energy Combust. 1989;15:109-129. DOI: 10.1016/0360-1285(89)90012-9.
[4] Kotowicz J, Sobolewski A, Iluk T. Energy. 2013;52:265-278. DOI: 10.1016/j.energy.2013.02.048.
[5] Kalina J. App Therm Eng. 2011;31:2829-2840. DOI: 10.1016/j.applthermaleng.2011.05.008.
[6] Kalina J. Energy Convers Manage. 2014;86:1050-1057. DOI: 10.1016/j.enconman.2014.06.079.
[7] Skorek-Osikowska A, Bartela Ł, Kotowicz J, Sobolewski A, Iluk T, Remiorz L. Energy. 2014;67:328-340. DOI: 10.1016/j.energy.2014.01.015.
[8] Kotowicz J, Michalski S. Energy. 2015;81:662-673. DOI: 10.1016/j.energy.2015.01.010.

ROŚLINY ENERGETYCZNE JAKO LOKALNY NOŚNIK ENERGII

[1] Instytut Maszyn i Urządzeń Energetycznych, Politechnika Śląska, Gliwice
[2] Instytut Techniki Cieplnej, Politechnika Śląska, Gliwice

Abstrakt: Przeprowadzono badania eksperymentalne wieloletnich roślin energetycznych (miskanta olbrzymiego, ślazowca pensylwańskiego, spartyny preriowej, prosa rózgowatego) oraz określono wpływ stosunku nadmiaru powietrza w reaktorze na wartość opałową gazu palnego. Wykorzystano reaktor dolnociągowy ze złożem stałym. Najwyższą wartość opałową gazu uzyskano dla λ = 0,18 niezależnie od rodzaju biomasy. Składy otrzymanych gazów posłużyły do obliczeń termodynamicznych i ekonomicznych układu kogeneracyjnego z gazowym silnikiem tłokowym. Wyznaczono wskaźniki efektywności energetycznej układu CHP oraz szereg danych wejściowych do analizy ekonomicznej. Rachunek ekonomiczny przeprowadzono w oparciu o metodę wartości zaktualizowanej netto. Dla założeń przyjętych w obliczeniach dla układów zasilanych wieloletnimi roślinami energetycznymi nie uzyskano dodatnich wartości wskaźnika *NPV*. Wyznaczono graniczne ceny sprzedaży energii elektrycznej oraz graniczne ceny pozyskania biomasy z warunku *NPV* = 0. Efektywność ekonomiczna instalacji zasilanych biomasą silnie zależy od otoczenia ekonomiczno-prawnego, dlatego przeprowadzono analizy wrażliwości granicznej ceny sprzedaży energii elektrycznej ze względu na czas pracy instalacji, koszt pozyskania paliwa oraz cenę zielonych certyfikatów.

Słowa kluczowe: biomasa, zgazowanie, kogeneracja, rośliny energetyczne, gazowy silnik tłokowy